Nuclear Superfluidity and Field Theory of Elementary Excitations (*).

D. R. BÉS

Comision Nacional de Energia Atomica - Buenos Aires, Argentina

R. A. BROGLIA

The Niels Bohr Institute, University of Copenhagen - DK-2100 Copenhagen Ø, Denmark (**)
State University of New York, Physics Department - Stony Brook, L. I., N. Y. 11794

Introduction.

In these lectures (***) we discuss the properties of the elementary modes of excitation associated with the dynamical breaking of the number-of-particle symmetry, and the field-theoretical methods which allow for a systematic study of the coupling between the different nuclear degrees of freedom.

I: Pairing modes of excitation in nuclei.

1. – Pairing rotations.

1·1. *The pairing interaction.* – It is well known that a contact interaction in a $(j^2)^I$ configuration strongly depresses the $I = 0$ state [1]. This specificity is able to develop also when several j-shells are present. In this case, the wave function of the two-particle system can be written as

$$|\alpha\rangle = \frac{1}{\sqrt{2}} \sum_j \alpha_j [a_j^\dagger a_j^\dagger]_0^0 |0\rangle \,, \tag{1.1}$$

(*) Partially supported by ERDA contract number AT(11-1)-3001.
(**) Permanent address.
(***) Many of the ideas presented here have originated in discussions with A. BOHR and B. MOTTELSON.

where $|0\rangle$ is the vacuum state and $a_j^\dagger$ creates a particle in the orbital j with time-reversal properties $\tau a_{jm}^\dagger \tau^{-1} = (-1)^{j+m} a_{j-m}^\dagger$. The amplitudes α_j are determined by the secular equation

$$(2\varepsilon_j - E)\alpha_j = \sum_{j'} (j + \tfrac{1}{2})^{\frac{1}{2}} (j' + \tfrac{1}{2})^{\frac{1}{2}} G(j', j', j, j)\, \alpha_{j'}\,, \tag{1.2}$$

where ε_j is the single-particle energy associated with the j-orbital. If we replace all radial integrals (*) $G(j', j', j, j)$ by an average value G, the eigenvalues E are given by the dispersion relation

$$\frac{1}{G} = \sum_j \frac{j + \frac{1}{2}}{2\varepsilon_j - E} = \sum_j \sum_{m>0} \frac{1}{2\varepsilon_j - E} \equiv F(E)\,. \tag{1.3}$$

The nature of the solution is illustrated in fig. 1. When E goes from a value smaller to a value larger than $2\varepsilon_j$, $F(E)$ decreases from ∞ to $-\infty$. As E passes through the origin to negative values, $F(E)$ decreases from ∞ to zero. The eigenvalues E are given by the intersection of $F(E)$ with the line $F(E) = G^{-1}$.

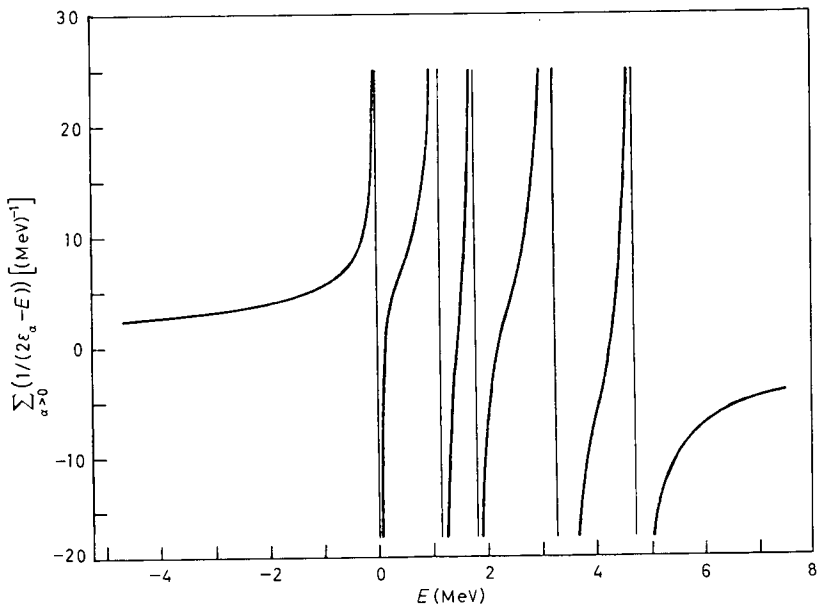

Fig. 1. – Dispersion relation (1.3) for ^{206}Pb. The single-hole states available to the two neutrons are $p_{1/2}(0)$, $f_{5/2}(0.57)$, $p_{3/2}(0.89)$, $i_{13/2}(1.63)$, $f_{7/2}(2.34)$ (from ref. [12]). The label α denotes the quantum numbers (j, m).

(*) For a contact interaction, $G(j', j', j, j) = -(V_0/4\pi)\int u_{j'}^{*2}(r) u_j^2(r)\, r^2\, dr$.

While all other eigenvalues are trapped between the unperturbed energies $2\varepsilon_j$, the ground-state correlation can freely increase as G increases.

If the nucleus was a large box with the states j belonging to a continuum, eq. (1.3) would indicate that there would exist a bound state for an arbitrarily weak coupling, provided that the potential would be attractive near the Fermi surface. This result was first pointed out by COOPER in connection with the problem of electrons moving in a metal at low temperatures [2]. COOPER suggested that the instabihty of the normal phase was due to pairs of electrons entering this type of bound state and giving rise to a condensate. The schematic pairing interaction

$$H_{\mathrm{p}} = -\frac{G}{2}(P^{\dagger}P + PP^{\dagger}), \tag{1.4}$$

where

$$P^{\dagger} = \sum_j P_j^{\dagger} = \sum_j \sum_{m>0} (-1)^{j+m} a_{jm}^{\dagger} a_{j-m}^{\dagger} = -\sum_j \sqrt{j+\tfrac{1}{2}}\, \frac{[a_j^{\dagger} a_j^{\dagger}]_0^0}{\sqrt{2}}, \tag{1.5}$$

gives rise to the type of correlations discussed above, in particular to the phenomenon of condensation. In what follows we discuss in detail the static and dynamic consequences of these correlations in nuclei.

1·2. *Exact many-body solution of the pairing interaction.* – We consider the case of identical particles moving in a degenerate shell and interacting through the monopole pairing interaction. The model is not only appropriate—since it has no other degrees of freedom—but also simply solvable [3, 4]. The operators $P^{\dagger}$, P and

$$H_{\mathrm{op}} = \tfrac{1}{2}(N - \Omega) = \tfrac{1}{2}\Big(\sum_m a_m^{\dagger} a_m - \Omega\Big) \tag{1.6}$$

obey the same SU_2 commutation algebra as, *e.g.*, the angular-momentum components I_+, I_- and I_z, respectively. The Hamiltonian (1.6) is diagonal in the representation characterized by the quantum numbers $I = \frac{1}{2}(\Omega - v)$ and $I_z = \pi$, where v $(= 0, 1, \ldots)$ is the seniority quantum number, and π $(= 0, \pm\frac{1}{2}, \pm 1, \ldots)$ is the number of pairs missing or in excess from the middle of the shell, $\Omega = j + \frac{1}{2}$ being the pair degeneracy of the shell. The eigenvalues of H are, in this representation,

$$E(v, \pi) = -\tfrac{1}{4}G(\Omega - v)(\Omega + 2 - v) + G\pi^2. \tag{1.7a}$$

The spectrum corresponding to $\Omega = 8$ is displayed in fig. 2.

The matrix element of the two-particle transfer operator $P^{\dagger}$ is given by

$$\langle v', \pi' | P^{\dagger} | v, \pi \rangle = \delta(v, v')\,\delta(\pi', \pi + 1) \cdot \cdot \frac{\Omega}{2}\left[1 + \frac{2}{\Omega}(1 - v) + \frac{v}{\Omega^2}(v - 2) - \frac{4\pi}{\Omega^2}(1 + \pi)\right]^{\frac{1}{2}}. \tag{1.7b}$$

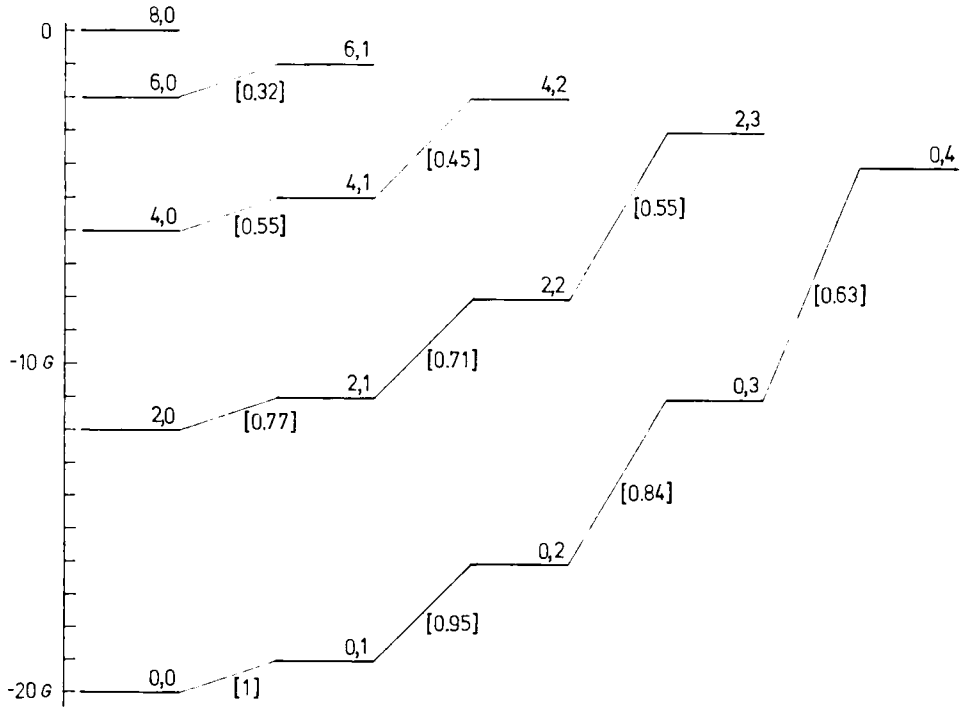

Fig. 2. – The spectrum of a pairing force for even systems with $\pi \geqslant 0$ and degeneracy $\Omega = 8$. Each state is labelled by the quantum numbers (ν, π). The transfer matrix elements are given within square brackets. They are normalized with respect to the matrix element $\langle \nu = 0, \pi = 1 | P^{\dagger} | \nu = 0, \pi = 0 \rangle = 3.7$.

The dependence of the energy and of the transfer matrix element on ν and π allows for a natural grouping of the levels. States of the same seniority and different number of particles can be interpreted as members of a collective band: their energy displays a smooth dependence from π (*i.e.*, they obey a π^2 law) and they are connected by enhanced and fairly constant matrix elements of the two-nucleon transfer operator. States belonging to different bands are widely separated in energy. Furthermore, none of the operators of the group connects levels belonging to different bands. This behaviour becomes more pronounced the smaller the values of ν/Ω and of $|\pi|/\Omega$ become.

1·3. *Empirical evidence on pairing bands.* – Because of the nuclear shell structure, the j-subshells are bunched together within a major shell, and a general tendency towards the degenerate model situation previously discussed is realized in actual nuclei, in particular in single-closed-shell nuclei (*). In what follows we discuss the experimental evidence on pairing rotational bands accumulated on the Sn isotopes.

(*) The problem of pairing between nonidentical nucleons is discussed in sect. 4.

The main term in the nuclear binding energies is linear in the number of particles. Since this term is alien to the pairing degree of freedom, it must be subtracted before a comparison with the pairing rotational energies is made. The experimental binding energies thus corrected are displayed in fig. 3, where they can be seen to follow closely the rotational parabola (*).

The available results on two-neutron transfer cross-sections populating 0^+ states in Sn nuclei are also given in fig. 3. It is apparent that the two impor-

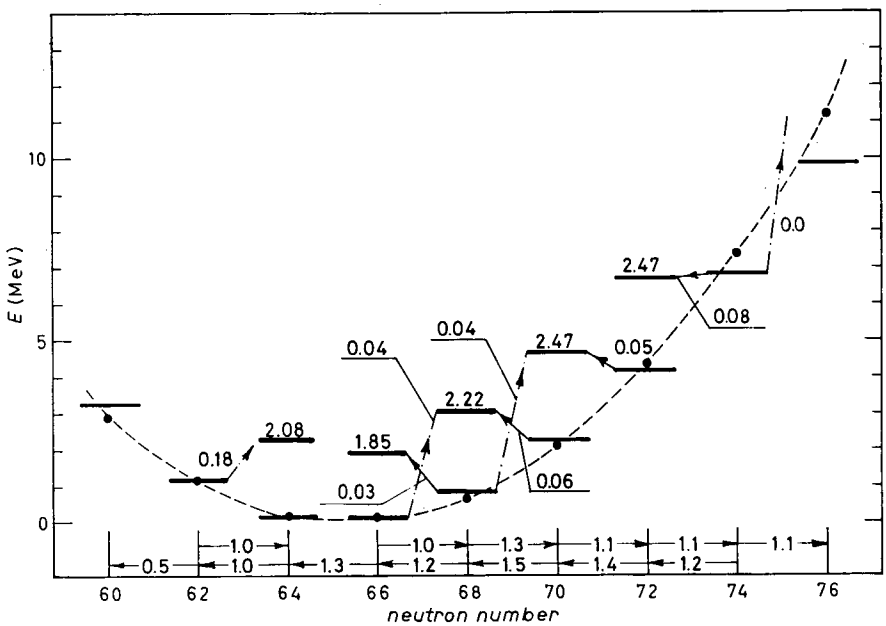

Fig. 3. – Experimental energies of the $J^\pi = 0^+$ states of the even Sn isotopes. The heavy drawn lines represent the values of the expression $E = -B(\mathrm{Sn}) + E_{\mathrm{exc}} + 8.50N + 45.3$ (MeV), where the binding energies $B(A)$ (in MeV) are taken from ref. [13]. The dashed line represents the parabola $0.10(A - 65.4)^2$, which corresponds to a rotational energy parameter $\hbar^2/2\mathscr{I} = 0.040$ MeV. Also displayed is the excited pairing rotational band associated with the pairing vibrational mode. In all cases where more than one $J^\pi = 0^+$ state has been excited below 3 MeV in two-neutron transfer processes, the energy $\sum_i \sigma(0_i)E(0_i^+)/\sum_i \sigma(0_i^+)$ of the centroid is quoted, as well as the corresponding cross-section $\sum_i \sigma(0_i^+)$. The quantity $\sigma(0_i^+)$ is the relative cross-sections with respect to the ground-state cross-sections. The numbers along the abscissa are the ground-state (p, t) and (t, p) cross-sections normalized to the $^{116}\mathrm{Sn} \leftrightarrow {}^{118}\mathrm{Sn(gs)}$ cross-section. The (t, p) and (p, t) data utilized in constructing this figure were taken from ref. [14-16].

(*) However, the existence of other degrees of freedom (*e.g.* of the isospin degree of freedom) which also give rise to a quadratic dependence in the number of particles makes the energy argument an indirect one. Quite generally, the main evidence on the pairing degree of freedom comes from the two-particle transfer cross-sections.

tant features of the band description are well satisfied, namely i) the cross-sections populating the ground states are much stronger than the cross-sections populating excited states and ii) the ground-state cross-sections are fairly constant.

1·4. *Collective interpretation of the pairing bands.* – A deeper understanding of the nature of these collective bands is now called for.

The spectrum corresponding to the second term in (1.7*a*) is characteristic of a two-dimensional rotor with moment of inertia

$$\mathscr{I} = \hbar^2/2G\,. \tag{1.8}$$

The number of pairs of particles $\hbar\Pi_{\text{op}}$ plays here the role of the angular-momentum component I_z. The dynamical variable conjugated to $\hbar\Pi_{\text{op}}$ is an angular variable which plays a similar role as the azimuthal angle, in the case of two-dimensional rotations. It is called the gauge angle and fulfils the commutation relation

$$[\varphi_{\text{op}}, \Pi_{\text{op}}] = i\,. \tag{1.9a}$$

The spectrum (1.7*a*) can be reproduced by a Hamiltonian which is a sum of two terms. The first is the rotational kinetic energy in gauge space. The second is a function of the variables x corresponding to the degrees of freedom which are independent of both the number of pairs and the gauge angle. Thus

$$H = \frac{\hbar^2}{2\mathscr{I}}\Pi_{\text{op}}^2 + H'(x) = -\frac{\hbar^2}{2\mathscr{I}}\frac{\partial^2}{\partial^2\varphi} + H'(x)\,. \tag{1.9b}$$

The eigenfunctions of (1.9*b*) describe a physical system rotating in gauge space with constant angular velocity $\dot{\varphi} = \hbar\pi/\mathscr{I}$. It is therefore convenient (*) to express these wave functions by utilizing a frame of reference which rotates with the same angular velocity $\dot{\varphi}$. The variable φ specifies the orientation of the rotating frame with respect to the laboratory (fixed) frame at each instant of time (**).

We label with a prime all quantities when expressed in the rotating frame, in which case they are scalars with respect to rotations in φ. In particular, the variables x', which describe the intrinsic degrees of freedom of the system.

(*) The formalism concerning the quantal theory of rotations, and the interplay between particle and collective degrees of freedom, can be applied here (cf. ref. [5,6]).

(**) Thus, we assume that it is possible to define an angle which is a function of the degrees of freedom of all the particles, and which is the variable canonically conjugated to the number of pairs of particles. In the present discussion we only make use of the assumption that such an angle exists (for more details cf. ref. [5]).

The results of the exact calculation indicate that the intrinsic spectrum is labelled by the seniority quantum number v. Thus, the eigenfunctions of (1.9*b*) can be written as

$$\psi_{v,\pi}(x', \varphi) = (2\pi)^{-\frac{1}{2}} u_v(x') \exp[i\pi\varphi]. \tag{1.10}$$

The two frames of reference are related by a rotation in gauge space which is generated by the (unitary) transformation

$$G(\varphi) = \exp[i\pi\varphi], \tag{1.11}$$

where φ is the rotation angle.

The operators $P^\dagger$ and P transform according to

$$\begin{cases} P^\dagger = G(\varphi) P'^\dagger G^{-1}(\varphi) = \exp[i\varphi] P'^\dagger, \\ P \;\; = G(\varphi) P' G(\varphi) \quad\; = \exp[-i\varphi] P'. \end{cases} \tag{1.12}$$

Expressing $P^\dagger$ in terms of $P'^\dagger$ and integrating over the gauge angle, one obtains the matrix element corresponding to transitions which do not change seniority

$$\begin{aligned} \langle \psi_{v,\pi'}(x', \varphi) | P^\dagger | \psi_{v,\pi}(x', \varphi) \rangle = \\ = \frac{1}{2\pi} \langle u_v(x') | P'^\dagger | u_v(x') \rangle \int_0^{2\pi} \exp[i(\pi + 1 - \pi')\varphi] \, \mathrm{d}\varphi = \\ = \delta(\pi', \pi + 1) \langle u_v(x') | P'^\dagger | u_v(x') \rangle . \end{aligned} \tag{1.13}$$

Thus, the diagonal matrix element of the transfer operators does not vanish in the rotating frame, implying that $u_v(x')$ is not an eigenstate of the number of particles. This results can be understood by noting that the physical system forms, at all times, a fixed angle φ_0 with the rotating frame of reference, and that the uncertainty in the number of particles is related to that of φ by $\Delta\varphi \, \Delta\pi \geqslant i$. The violation of the conservation law takes place, however, in the intrinsic frame, where no measurement can be carried out. On the other hand, the total wave function (1.10), representing the physical system, is an eigenstate of the number operator in the laboratory frame with eigenvalue 2π.

We define the intrinsic frame of reference as the particular rotating frame in which the expectation value of the two-body transfer operator is real and positive. Thus

$$\langle \psi_{v,\pi+1}(x', \varphi) | P^\dagger | \psi_{v,\pi}(x', \varphi) \rangle = \alpha_v = \text{real}. \tag{1.14}$$

Note that the factorization (1.10) can be only approximate. There are terms coupling the rotation with the other degrees of freedom. In the present case, these terms are responsible for the termination of the band at $\pi = \pm\Omega$, for changes in the matrix elements of $P^\dagger$ as a function of N, etc.

1·5. *The intrinsic wave function of a pairing rotational band.* – The determination of the parameters α_ν and $\mathscr{I}$ of the rotational motion requires the knowledge of the intrinsic wave function $u_\nu(x')$. If we write the operators $P'^\dagger$ as a sum of a diagonal part α_ν and a nondiagonal part $P'^\dagger - \alpha_\nu$, the pairing Hamiltonian can be approximated (*), in the intrinsic system, by

$$H'_{\mathrm{p}} \approx G\alpha_\nu^2 - G\alpha_\nu(P'^\dagger + P') , \tag{1.15}$$

where the term $-G|P'^\dagger - \alpha_\nu|^2$ has been neglected. This approximation implies that the fluctuations in α_ν are much smaller than α_ν itself, *i.e.*

$$|\langle u_\nu(x')|P'^\dagger|u_\omega(x')\rangle|/\alpha_\nu \ll 1 , \tag{1.16}$$

and similarly for P'.

The function

$$|u_0\rangle \equiv |0\rangle = (\tfrac{1}{2})^{\Omega/2} \prod_{m>0} (1 + a_m^\dagger a_{\bar{m}}^\dagger)|\mathrm{sm}\rangle , \tag{1.17}$$

where $|\mathrm{sm}\rangle$ is the shell model vacuum, is an eigenfunction (**) of (1.15). The diagonal matrix element of $P^\dagger$ in the state (1.17) has the value

$$\alpha_0 = \langle 0|P'^\dagger|0\rangle = \tfrac{1}{2} \sum_{m>0} = \tfrac{1}{2}\Omega . \tag{1.18}$$

The functions corresponding to the lowest excited states of H'_{p} are equal to

$$|m, \bar{m}\rangle = (\tfrac{1}{2})^{\Omega/2}(1 - a_m'^\dagger a_{\bar{m}}'^\dagger) \prod_{\substack{m' \neq m \\ m'>0}} (1 + a_{m'}'^\dagger a_{\bar{m}'}'^\dagger)|\mathrm{sm}\rangle . \tag{1.19}$$

(*) The advantage of the definition (1.14) of the intrinsic system becomes here obvious, since (1.15) depends on a single parameter α_ν instead of the two (Re α_ν, Im α_ν) which would appear in any other rotating frame.

(**) It would not be surprising that the student, not familiar with the phenomenon of superfluidity, gets somewhat restless by the apparent ease and lack of plausibility arguments with which we have introduced (1.17). In fact, the step has been taken deliberately. We think that one of the basic intellectual experiences that the theory of many-body problems offers is to be exposed to the quantum jump of insight which BARDEEN, COOPER and SCHRIEFFER [7] displayed in giving a microscopic solution to the problem of superconductivity.

The excitation energy of the state $|m, \overline{m}\rangle$ is given by

$$E_2 - E_0 = -G\alpha_2^2 + G\alpha_0^2 = G\Omega\left(1 - \frac{1}{\Omega}\right). \tag{1.20}$$

In the limit $\Omega \gg 1$ this energy coincides with the excitation energy of the seniority-two states (cf. (1.7*a*)), obtained in the exact treatment of the pairing Hamiltonian (*).

The ratio between the matrix elements $\langle m, \overline{m}|P'|0\rangle$ and α_0 gives

$$\left|\langle 0|P'|m, \overline{m}\rangle\right|/\alpha_0 = \Omega^{-1} \ll 1 . \tag{1.16'}$$

This relation justifies the approximation (1.15) and shows that the system becomes very stiff against fluctuations in α_0 for large values of Ω. We now generalize the previous calculation to the case in which the differences between the single-particle energies cannot be completely neglected as compared to the pairing potential.

If we take into account the single-particle kinetic energy, the generalized single-particle Hamiltonian (1.15) can be written as

$$H'_{\mathrm{p}} \approx \sum_{\nu} (\varepsilon(\nu) - \lambda) a'^{\dagger}(\nu) a'(\nu) - G\alpha_0(P'^{\dagger} + P') + G\alpha_0^2 , \tag{1.15'}$$

where we measure all single-particle energies from the Fermi surface λ.

An eigenstate of (1.15') is (**)

$$|0\rangle = \prod_{\nu>0} (V_\nu)^{-1} \alpha(\nu)\alpha(\tilde{\nu})|\mathrm{sm}\rangle = \prod_{\nu>0} [U(\nu) + V(\nu) a'^{\dagger}(\nu) a'^{\dagger}(\tilde{\nu})]|\mathrm{sm}\rangle , \tag{1.17'a}$$

where

$$\alpha(\nu) = U(\nu) a'(\nu) - V(\nu) a'^{\dagger}(\nu) . \tag{1.17'b}$$

We refer to $\alpha^{\dagger}(\nu)$ as the creation operator of a quasi-particle. The transformation from the particle to the quasi-particle operator corresponds to a canonical transformation [8, 9] imposing

$$U^2(\nu) + V^2(\nu) = 1 . \tag{1.21}$$

(*) Following a similar procedure, we obtain the states corresponding to an arbitrary seniority ν.

(**) Note that the difference between this wave function and (1.17) is due to the coupling between the intrinsic motion and the rotation in gauge space: because of the presence of the (Coriolis) term $-\lambda N_{\mathrm{op}}$ in (1.15'), the intrinsic state (1.17'*a*) depends on N_0 (or π_0).

The state $|0\rangle$ is the vacuum state for quasi-particles. The space spanned by $|0\rangle$ and by all states which are obtained by successive applications of the operators $\alpha^{\dagger}(\nu)$ on $|0\rangle$ constitutes a complete set of states.

Using the transformation inverse to (1.17′b) one can express H_{p}' in terms of quasi-particles as

$$H_{\mathrm{p}}' = H_{00} + H_{11} + H_{20}\,. \tag{1.22}$$

The third term, H_{20}, creates and destroys two quasi-particles. The states with a definite number of quasi-particles are eigenfunctions of H_{p}' provided $H_{20} = 0$. This condition yields the relations

$$\begin{cases} U(\nu) = \dfrac{1}{\sqrt{2}}\left[1 + \dfrac{\varepsilon(\nu) - \lambda}{E(\nu)}\right]^{\frac{1}{2}}, \\ V(\nu) = \dfrac{1}{\sqrt{2}}\left[1 - \dfrac{\varepsilon(\nu) - \lambda}{E(\nu)}\right]^{\frac{1}{2}}, \end{cases} \tag{1.23}$$

where

$$E(\nu) = \left[(\varepsilon(\nu) - \lambda)^2 + G\alpha_0^2\right]^{\frac{1}{2}}. \tag{1.24}$$

The term H_{11} describes the independent motion of quasi-particles and is given by

$$H_{11} = \sum_{\nu} E(\nu)\,\alpha^{\dagger}(\nu)\alpha(\nu)\,. \tag{1.25}$$

The above solution of H_{p}' holds for arbitrary values of α_0 and λ. The self-consistent value of these parameters is determined from the requirements

$$\begin{cases} \alpha_0 = \langle 0|P'|0\rangle\,, \\ N_0 = \langle 0|N_{\mathrm{op}}'|0\rangle\,. \end{cases} \tag{1.26}$$

These two equations yield

$$\begin{cases} \dfrac{2}{G} = \sum\limits_{\nu>0} \dfrac{1}{E(\nu)}\,, \\ N_0 = 2\sum\limits_{\nu>0} V^2(\nu)\,, \end{cases} \tag{1.27}$$

which are known as the gap and the number equation, respectively, in the BCS theory. Together they determine the value of the Fermi energy λ and the gap parameter $\Delta = G\alpha_0$. The total wave function is still given by eq. (1.10), the number of quasi-particles playing here the role of the seniority ν.

The dependence of the solution (1.17′a) on π_0 may be used to give a physical interpretation of the Lagrange multiplier λ and to obtain the moment of inertia.

For this purpose the intrinsic energy is expanded in powers of $\pi - \pi_0$, *i.e.*

$$U(\pi) = H_{00} + \lambda N = U(\pi_0) + 2\lambda(\pi - \pi_0) + \frac{1}{4}\frac{\partial\lambda}{\partial\pi}\Big|_{\pi=\pi_0}(\pi - \pi_0)^2 + \dots , \tag{1.28}$$

where the relation (*) $\partial H_{00}/\partial\lambda = -N$ was utilized. The Lagrange parameter fixes the frequency of rotation of the system. In fact, equating the relations

$$\left[i\hbar\frac{\partial}{\partial t}, \varphi\right]|\psi\rangle = i\hbar\frac{\partial}{\partial t}\varphi|\psi\rangle - i\hbar\varphi\frac{\partial}{\partial t}|\psi\rangle = i\hbar\dot{\varphi}|\psi\rangle \tag{1.29}$$

and

$$2\left[H'_{\mathrm{p}}, i\frac{\partial}{\partial N}\right]|\psi\rangle = 2iH'_{\mathrm{p}}\frac{\partial}{\partial N}|\psi\rangle - 2i\frac{\partial}{\partial N}H'_{\mathrm{p}}|\psi\rangle = -2i\frac{\partial H'_{\mathrm{p}}}{\partial N}|\psi\rangle \tag{1.30}$$

yields

$$2\langle 0|\frac{\partial H'_{\mathrm{p}}}{\partial N}|0\rangle = \frac{2\partial U(N)}{\partial N} = -\hbar\langle 0|\dot{\varphi}|0\rangle = -\hbar\dot{\varphi} . \tag{1.31}$$

Utihzing $\lambda = \partial U(N)/\partial N$, we obtain an interpretation of λ in terms of the angular velocity $\dot{\varphi}$, *i.e.*

$$\lambda = -\frac{\hbar}{2}\dot{\varphi} . \tag{1.32}$$

The energy needed to change this frequency is determined by

$$\frac{\partial\lambda}{\partial N} = \frac{\hbar^2}{4\mathscr{I}} . \tag{1.33}$$

Working ont the derivatives of the gap and number equations with respect to the number of particles, *i.e.*

$$\frac{\partial}{\partial N} = \frac{\partial\lambda}{\partial N}\frac{\partial}{\partial\lambda} + \frac{\partial\Delta}{\partial N}\frac{\partial}{\partial\Delta} , \tag{1.34}$$

(*) The quantity H_{00} is the lowest eigenvalue of H'_{p} (*i.e.* $H'_{\mathrm{p}}|0\rangle = H_{00}|0\rangle$), and thus it is stationary with respect to changes in all of the parameters in which the minimization was carried out. Thus, in changing N or λ, H_{00} can change only if the operator is changed. Consequently,

$$\frac{\partial U}{\partial N} = \frac{\partial\lambda}{\partial N}\frac{\partial H_{00}}{\partial\lambda} + N\frac{\partial\lambda}{\partial N} + \lambda = -N\frac{\partial\lambda}{\partial N} + N\frac{\partial\lambda}{\partial N} + \lambda = \lambda .$$

we obtain the set of two coupled equations

$$\begin{cases} \dfrac{\partial\lambda}{\partial N}\,\Delta^2 \sum\limits_{\nu>0} \dfrac{1}{(E(\nu))^3} + \dfrac{\partial\Delta}{\partial N}\,\Delta \sum\limits_{\nu>0} \dfrac{\varepsilon(\nu)-\lambda}{(E(\nu))^3} = 1\,, \\ \dfrac{\partial\lambda}{\partial N} \sum\limits_{\nu>0} \dfrac{\varepsilon(\nu)-\lambda}{(E(\nu))^3} - \Delta\,\dfrac{\partial\Delta}{\partial N} \sum\limits_{\nu>0} \left(\dfrac{1}{E(\nu)}\right)^3 = 0\,. \end{cases} \tag{1.35}$$

Solving for $\partial\lambda/\partial N$ and inserting in (1.33), we obtain the moment of inertia

$$\mathscr{I} = \frac{\hbar^2}{4}\,\frac{\Delta^2\Big(\sum\limits_{\nu>0} 1/E^3(\nu)\Big)^2 + \Big(\sum\limits_{\nu>0} (\varepsilon(\nu)-\lambda)/E^3(\nu)\Big)^2}{\sum\limits_{\nu=0} 1/E^3(\nu)}\,. \tag{1.36}$$

For a half-filled j-shell $\varepsilon(\nu) = \lambda = 0$ and $E(\nu) = \Delta = \frac{1}{2}G\Omega$. In this limit, the above expression reduces to the value (1.8).

As discussed previously, the other quantities which characterize the band structure generated by strong pairing correlations are the matrix elements of $P'^{\dagger}$ and P'. They are equal to (*)

$$_{\pi+1}\langle 0|P'|0\rangle_{\pi} \approx \sum_{\nu>0} U(\nu)\,V(\nu) = \frac{\Delta}{2G}\,. \tag{1.37}$$

The complete coherence of the contributions corresponding to the single-particle pairs ν and $\tilde{\nu}$ is apparent. Quite generally, the existence of such a coherence is a necessary condition for an appropriate description of the system in terms of a collective variable.

The two-particle transfer amplitude corresponding to the transition between the ground state and a state of two quasi-particles is given by

$$|\langle\beta^{\dagger}(\nu)\beta^{\dagger}(\tilde{\nu})|P'|0\rangle| = V^2(\nu) \leqslant 1\,. \tag{1.38}$$

The matrix element $\langle 0|P'|0\rangle$ should be much larger than this estimate for the collective model to be valid and thus requires

$$\Delta \gg 2G\,. \tag{1.39}$$

If the relative distances $|\varepsilon(\nu) - \lambda|$ become large, Δ decreases in order to satisfy the gap equation. Therefore, the BCS solution (and thus the descrip-

(*) Here we have utilized the same intrinsic eigenfunction to describe the initial and the final state. Alternatively one may solve the BCS number and gap equations for every value of N_0, in which case one takes into account in some approximate way the Coriolis coupling.

tion of the pairing collective motion in terms of rotations) loses its validity if the density of single-particle levels becomes low (*).

The static properties of the strong-coupling solution, *i.e.* the consequences of the BCS solution concerning the description of the intrinsic system, are usually negative (absence of levels in the neighbourhood of the ground state, decrease in the static quadrupole value, decrease in the moment of inertia of quadrupole-deformed nuclei, etc.). Historically, these properties were the first to be studied. Reviews of these properties can be found, for instance, in [10, 11].

An application of the present strong-coupling solution to the transfer of two neutrons is carried out in subsect. 3·2.

2. – Pairing vibrations.

In this section some of the physical consequences of fluctuations in the pairing gap [6, 17, 18] are discussed. A quantal description of the corresponding elementary modes of excitation is presented. The existence of an alternative description in terms of a classical model is pointed out.

2·1. *Two-level model.* – The simplest model which displays fluctuations of the pairing gap contains two j-shells [19, 20] which may have the same or different degeneracy, and which are separated by a distance D. Pairs of particles are scattered in these orbitals by a pairing force with constant matrix elements.

The model Hamiltonian can be written as

$$H = \frac{D}{2}(N_{j_2} - N_{j_1}) - \frac{1}{4}G(P^\dagger_{j_1} + P^\dagger_{j_2})(P_{j_1} + P_{j_2}) , \tag{2.1}$$

where

$$\begin{cases} P^\dagger_j = \sum_{m>0} (-1)^{j+m} a^\dagger_{jm} a^\dagger_{j-m} = -\sqrt{j+\tfrac{1}{2}}\,[a^\dagger_j a^\dagger_j]^0_0 , \\ N_j = \sum_m a^\dagger_{jm} a_{jm} \qquad (j = j_1, j_2) . \end{cases} \tag{2.2}$$

The two-level model has not an analytic solution, although it allows for a rather simple numerical solution in the orthonormal basis

$$|m, n-m\rangle = M_m^{-1}(P^\dagger_{j_1})^m (P^\dagger_{j_2})^{n-m}|0\rangle , \tag{2.3}$$

(*) This may occur for closed-shell nuclei or for low-A nuclei.

n being the total number of pairs of particles in the system. The matrix element of the Hamiltonian (2.1) in this basis is

$$\begin{aligned}(2.4)\quad &\langle m', n-m'|H|m, n-m\rangle = \\ &= \delta(m, m')[(n-2m)D - G(m(\Omega_1+1-m)) + (n-m)(\Omega_2+1-n+m)]^{\frac{1}{2}} - \\ &- \delta(m', (m-1))\, G[m(\Omega_1+1-m)(n-m+1)(\Omega_2-n+m)]^{\frac{1}{2}} - \\ &- \delta(m', (m+1))\, G[(m+1)(\Omega_1-m)(n-m)(\Omega_2+1-n+m)]^{\frac{1}{2}}.\end{aligned}$$

To obtain the solutions of the model one has thus to diagonalize a co-diagonal matrix.

As discussed in the previous section, two-particle transfer processes are the specific tools to study the pairing degrees of freedom, in particular pairing vibrations. The model operator which induces such processes is defined as

$$(2.5)\qquad T = P_1^\dagger + P_2^\dagger .$$

In the basis (2.3) the T operator has the following matrix elements

$$\begin{aligned}(2.6)\quad &\langle m', n+1-m'|T|m, n-m\rangle = \\ &= \delta(m', m)[(n-m+1)(\Omega_2-n+m)]^{\frac{1}{2}} + \delta(m', (m+1))[(m+1)(\Omega_1-m)]^{\frac{1}{2}}.\end{aligned}$$

The two-particle transfer cross-section can be shown to be proportional to the square of the matrix element (2.6) (cf., *e.g.*, [26]).

From the commutation relation $[N_i, P_j^\dagger] = 2\delta(i, j)P_i^\dagger$ one can calculate the occupation number of the two orbits

$$(2.7)\qquad \begin{cases} \langle\alpha|N_1|\alpha\rangle = 2\sum_m m|c_{n,m}|^2, \\ \langle\alpha|N_2|\alpha\rangle = 2\sum_m (n-m)|c_{n,m}|^2, \end{cases}$$

where the eigenfunction of the total Hamiltonian is

$$(2.8)\qquad |\alpha\rangle = \sum_m c_{n,m}|m, n-m\rangle .$$

For $\Omega_1 = \Omega_2 = \Omega$ there are two dimensionless parameters in the model. The first is chosen to be Ω and it gives a measure of the phase space which the particles have at their disposal to correlate. The second is

$$(2.9)\qquad x = 2G\Omega/D$$

and measures the interplay between the pairing strength and the shell effects.

In fig. 4 we display the energies, cross-sections and occupation amplitudes associated with a system $\Omega_1 = \Omega_2 = \Omega = 20$ for $x = 0.5$ and $x = 2.0$ as a function of the number of pairs $n = \pi$ $(18 \leqslant n \leqslant 22)$.

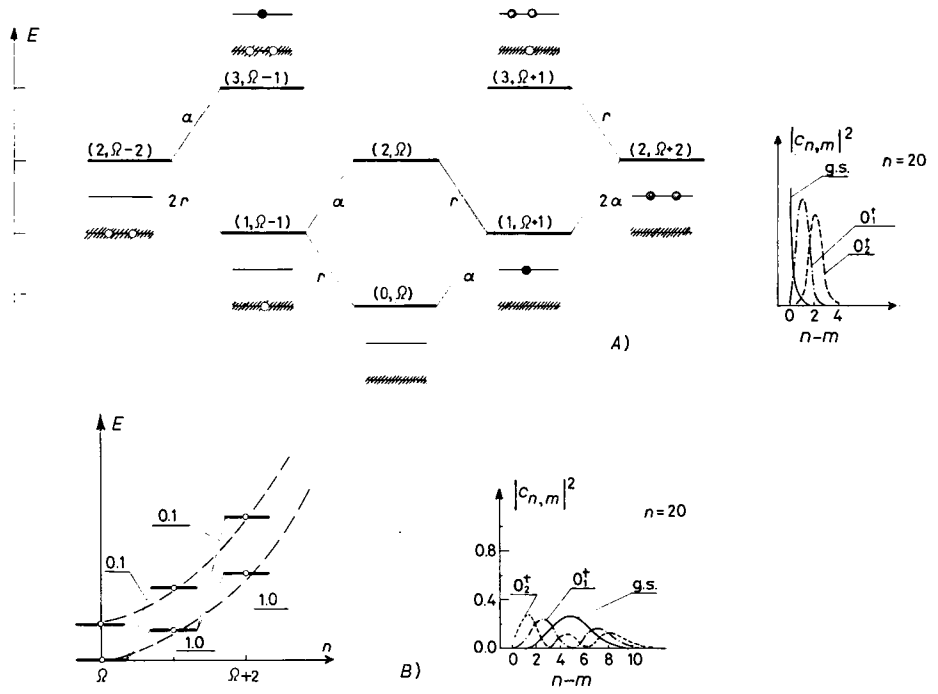

Fig. 4. – Schematic representation of the solution of the two-level model for $\Omega_1 = \Omega_2 = 20$ and for different values of x and n. In A) the results for $x = 0.5$ are displayed. Because of the particular degeneracy of the model, the energy of the ground state of the systems with $n = \Omega \pm 1$ pairs of particles is the same when measured with respect to the closed-shell system. All two-particle transition probabilities are measured in terms of $a = \sigma(\mathrm{gs}(\Omega_1) \to \mathrm{gs}(\Omega_1 + 1))$ and of $r = \sigma(\mathrm{gs}(\Omega_1) \to \mathrm{gs}(\Omega_1 - 1))$. Because of the particular symmetry of the model $a = r$. For each level of the spectrum, which is identified by the quantum numbers (N, n), a schematic representation of the main component of the wave function is shown. The corresponding square amplitudes $|c_{n,m}|^2$ (cf. eqs. (2.7) and (2.8)) associated with the ground state and low excited states of the $n = \Omega_1$ system are also shown. In B) the energies and two-particle cross-sections for $x = 2.0$ associated with the ground and the first excited state of the systems with $n \geqslant \Omega_1$ are displayed. The quantities $|c_{n,m}|^2$ corresponding to the ground state and two lowest excited states are also displayed.

In the case of $x = 0.5$ there is one characteristic energy. Any level lies at approximately an integer number of times this energy with respect to the ground state. The two-nucleon transfer cross-section associated with transitions between ground states is proportional to $|n - \Omega|$, *i.e.* to the absolute

value of the number of pairs missing from or in excess in the closed shell. All the first-excited-state stripping cross-sections for $n - \Omega < 0$ are equal and their common value is close to $|\langle \mathrm{gs}(n = 20)|T|\mathrm{gs}(n = 19)\rangle|^2$. On the other hand, none of the lowest excited states with $n - \Omega \geqslant 0$ is populated in such reactions. This is also true for the second and higher excited states for $n - \Omega \leqslant 0$. A similar pattern is observed for two-nucleon pickup processes.

For the case of $x = 2$ the energy of the states follows a parabolic distribution (pairing rotational band) as a function of the number of particles. There are two characteristic energies, corresponding to interband and intraband spacing. The situation is very similar to the one encountered in the case of a j-shell (*). In this case, however, there is a finite cross-section to the excited states, although an order of magnitude smaller than between states lying in the same energy parabola.

The situation for $x = 1.2$ is intermediate to the one observed for $x = 0.5$ and $x = 2$.

The probability amplitude $|c_{n,m}|^2$ associated with the ground state of the closed-shell system ($n - \Omega = 0$) is also given in fig. 4 as a function of $n - m$. It is noted that a major change takes place in going from $x = 0.5$ to $x = 2.0$, indicating a change in the coupling scheme of the nucleons correlated through the pairing interaction.

Similar results as those displayed in fig. 4 are obtained for $\Omega_1 \neq \Omega_2$ (cf. ref. [21]). One can, however, distinguish in this case two typical energies and two basic two-particle transfer cross-sections, one associated with the removal of pairs and the other with its addition.

2·2. *Collective treatment of pairing vibrations. Normal systems* ($x < 1$). – The different levels of the pairing spectrum obtained by diagonalizing (2.1) for $x < 1$ and reported in fig. 4*A*) can be labelled by the number of pairs π and by a number N indicating their energy sequence in the spectrum. The lowest state corresponds to a closed-shell system and has ($N = 0$, $\pi = \Omega$). The two lowest excited states have the same energy E and are labelled ($N = 1, \pi = \Omega + 1$) and ($N = 1, \pi = \Omega - 1$), respectively. The next excitation energy is $2E$ and corresponds to a triplet of states comprising the two states ($N = 2$, $\pi = \Omega \pm 2$) and ($N = 2, \pi = \Omega$). This spectrum is characteristic of a two-dimensional harmonic oscillator, where N indicates the number of phonons, while $\hbar\pi$ plays the role of the angular momentum in two dimensions. The values of the transfer cross-sections as well as the selection rules further confirm the harmonic structure of the spectrum. One of the degrees of freedom of the two-dimensional oscillator is associated with the change in the number

(*) For $x \gg 1$, the distance between the levels becomes negligible with respect to the pairing interaction. In this case the diagonalization of the Hamiltonian (2.1) reduces to the group-theoretical solution discussed in the previous section (j-shell model).

of pairs in the shell above the Fermi surface (pair addition mode) and the other with the change in the number of pairs in the shell below the Fermi surface (pair removal mode).

It is thus natural to rewrite the Hamiltonian (2.1) as (*)

$$H = (W_a \Gamma_a^\dagger \Gamma_a + W_r \Gamma_r^\dagger \Gamma_r), \tag{2.10}$$

where $\Gamma_a^\dagger$ and $\Gamma_r^\dagger$ are the creation operators of the pair addition and pair removal modes, which are expressed in terms of the operators $P_j^\dagger$ and P_j as

$$\Gamma_a^\dagger = a_2 P_2^\dagger + a_1 P_1^\dagger \quad \text{and} \quad \Gamma_r^\dagger = r_1 P_1 + r_2 P_2 . \tag{2.11}$$

Assuming the relation (*)

$$[P_j, P_{j'}^\dagger] = (\Omega - N_j)\delta(j, j') \approx \Omega\delta(j, j')[\delta(j, 2) - \delta(j, 1)] \tag{2.12}$$

to be valid for any state of the system under discussion, one obtains

$$a_2 = r_1 = -\frac{2G\sqrt{\Omega}}{(1-x)^{\frac{1}{4}}(2D - W)} \tag{2.13a}$$

and

$$a_1 = r_2 = \frac{2G\sqrt{\Omega}}{(1-x)^{\frac{1}{4}}(2D + W)} , \tag{2.13b}$$

where

$$W = W_a = W_r = 2D(1-x)^{\frac{1}{2}} \tag{2.14}$$

is the common energy of the pairing modes of excitation. The intensity with which the pair addition and pair removal modes are excited is

$$|\langle n_a = 1, n_r | T | n_a = 0, n_r \rangle|^2 = (a_2 - a_1)^2 \Omega^2 = \tag{2.15}$$

$$= |\langle n_a, n_r = 1 | T | n_a, n_r = 0 \rangle|^2 = (r_2 - r_1)^2 \Omega^2 = \Omega(1-x)^{-\frac{1}{2}} .$$

The above results reproduce the main features of the exact calculations for $x < 1$. Acting with $\Gamma_a^\dagger$ and $\Gamma_r^\dagger$ on the vacuum state, one can build the whole pairing spectrum. A general state is given by

$$|n_a, n_r\rangle = \frac{1}{\sqrt{n_a! n_r!}} (\Gamma_a^\dagger)^{n_a} (\Gamma_r^\dagger)^{n_r} |n_a = 0, n_r = 0\rangle . \tag{2.16}$$

(*) Note that this relation is equivalent to the relations $[H, \Gamma_a^\dagger] = W_a \Gamma_a^\dagger$ and $[H, \Gamma_r^\dagger] = W_r \Gamma_r^\dagger$.

The RPA solution is valid for small values of x. As x increases, W decreases and the cross-sections associated with the two modes tend to ∞. The transition between the normal and the superfluid phase takes place for $x = 1$. Similar features as the one discussed above are also observed in the phase transition between spherical and quadrupole deformed nuclei. In this case the electromagnetic-transition probabihty plays the role of the two-nucleon transfer cross-section. The analogy between surface and pairing modes can be carried quite far as discussed in ref. [22].

The theory of pairing vibrations can also be cast in terms of the collective variables α, φ as done in the case of pairing rotations. In fact, in these variables it is possible to formulate the problem of the pairing modes through a Hamiltonian which treats rotations and vibrations on an equal footing (cf. ref. [5]). For $\Delta \sim 0$, the energies associated with fluctuations in α and φ are comparable.

2·3. *Collective treatment of pairing vibrations. Superfluid systems* ($x > 1$). – The main static effects of the pairing correlations for $x > 1$ can be taken into account through the quasi-particle transformation (1.17′*b*) which implies a complete hybridization of particles and holes, and thus an intrinsic system connected with the laboratory system through a rotation in gauge space. As discussed in sect. **1**, the pairing Hamiltonian approximately reduces to the independent quasi-particle Hamiltonian

$$H_{11} = \sum_j E_j [\alpha_j^\dagger \alpha_j]_0^0 , \tag{2.17}$$

E_j being the energy of the intrinsic excitation of the system. In the present section we review the different types of collective modes generated by the residual interaction between the quasi-particles. Some of these modes are the band-heads of the excited rotational bands found in the exact solutions.

We consider the system $n = \Omega_1 = \Omega_2$, in which case $\lambda = 0$. The BCS occupation parameters are in this case

$$U_2^2 = V_1^2 = \frac{1}{2}\left(1 - \frac{1}{x}\right) \tag{2.18}$$

and

$$U_1^2 = V_2^2 = \frac{1}{2}\left(1 + \frac{1}{x}\right), \tag{2.19}$$

while the quasi-particle energy is

$$E = G\Omega . \tag{2.20}$$

The two-level system displays a permanent pairing distortion of magnitude

$$\Delta = G\sqrt{\Omega}\langle 0|T|0\rangle = G\sqrt{\Omega}\,(\sqrt{\Omega}\,U_1 V_1 + \sqrt{\Omega}\,U_2 V_2) = G\Omega\left(1 - \frac{1}{x^2}\right)^{\frac{1}{2}}, \tag{2.21}$$

$|0\rangle$ being the BCS ground state. Note that Δ is a collective deformation receiving contributions from all the pairs of particles, and thus is proportional to Ω. The fluctuations around this equilibrium distortion are induced by the residual interaction among the quasi-particles

$$\begin{cases} H_{\mathrm{R}} \approx H'_{\mathrm{p}} + H''_{\mathrm{p}}, \\ H'_{\mathrm{p}} = -\tfrac{1}{4}G\left(\sum_j \sqrt{\Omega_j} f_j (\Gamma_j^\dagger + \Gamma_j)\right)^2, \\ H''_{\mathrm{p}} = \quad \tfrac{1}{4}G\left(\sum_j \sqrt{\Omega_j} (\Gamma_j^\dagger - \Gamma_j)\right)^2, \end{cases} \tag{2.22}$$

where

$$\Gamma_j^\dagger = \frac{1}{\sqrt{\Omega_j}} \sum_{m>0} (-1)^{j+m} \alpha_{jm}^\dagger \alpha_{j-m}^\dagger \tag{2.23}$$

and

$$f_j = U_j^2 - V_j^2 . \tag{2.24}$$

If we define the collective quasi-boson operator as

$$\Gamma_n^\dagger = \sum_i a_{ni} \Gamma_i^\dagger + \sum_i b_{ni} \Gamma_i , \tag{2.25}$$

the linearization condition

$$[H_{11} + H_{\mathrm{R}}, \Gamma_n^\dagger] = W_n \Gamma_n^\dagger \tag{2.26}$$

gives rise to (cf., *e.g.*, [17] and [23])

$$\begin{vmatrix} (W_n^2 - 4\Delta^2) \sum_i \dfrac{\Omega_i}{2E_i(4E_i^2 - W_n^2)} & W_n \left(\sum_i \dfrac{\Omega_i f_i}{4E_i^2 - W_n^2} \right) \\ W_n \left(\sum_i \dfrac{\Omega_i f_i}{4E_i^2 - W_n^2} \right) & W_n^2 \sum_i \dfrac{\Omega_i}{2E_i(4E_i^2 - W_n^2)} \end{vmatrix} = \tag{2.27}$$

$$= W_n^2 [(W_n^2 - 4\Delta^2) A - B],$$

where

$$A = \left(\sum_i \frac{\Omega_i}{2E_i(4E_i^2 - W_n^2)} \right)^2 \tag{2.28}$$

and

$$B = \left(\sum_i \frac{\Omega_i f_i}{4E_i^2 - W_n^2} \right)^2 . \tag{2.29}$$

The forward-going and backward-going amplitudes are

$$\begin{cases} a_{ni} = \dfrac{\Lambda_{1n} f_i + \Lambda_{2n}\sqrt{\Omega_i}}{2E_i - W_n}, \\ b_{ni} = \dfrac{-\Lambda_{1n} f_i + \Lambda_{2n}\sqrt{\Omega_i}}{2E_i + W_n}, \end{cases} \tag{2.30}$$

while

$$\frac{\Lambda_{2n}}{\Lambda_{1n}} = -\frac{\sum_i \dfrac{\Omega_i f_i}{4E_i^2 - W_n^2}}{W_n \sum_i \dfrac{\Omega_i}{2E_i(4E_i^2 - W_n^2)}} \tag{2.31}$$

and

$$\Lambda_{1n} = \frac{1}{2}\left[W_n \left(\sum_i \frac{f_i^2 2E_i \Omega_i}{(4E_i^2 - W_n^2)^2} \right) + \left(\sum_i \frac{f_i (4E_i^2 + W_n^2)\Omega_i}{(4E_i^2 - W_n^2)^2} \right) \frac{\Lambda_{2n}}{\Lambda_{1n}} + \right. \tag{2.32}$$

$$\left. + W_n \left(\sum_i \frac{2E_i \Omega_i}{(4E_i^2 - \Omega_i)^2} \right) \left(\frac{\Lambda_{2n}}{\Lambda_{1n}} \right)^2 \right]^{-\frac{1}{2}}.$$

The elements a_{11} and a_{22} in the determinant (2.27) correspond to the dispersion relations resulting from the linearization conditions $[H_{11} + H'_p, \Gamma'^{\dagger}_n] = W'_n \Gamma'^{\dagger}_n$ and $[H_{11} + H''_p, \Gamma''^{\dagger}_n] = W''_n \Gamma''^{\dagger}_n$, respectively, the corresponding collective modes being the pairing vibrations and the spurious state associated with the non-conservation of the number of particles (*). Aside from the root at $W_n = 0$, all roots of (2.27) fulfil the condition $W_n \geqslant 2\Delta$. In fact, because A and B are positive quantities, the dispersion relation cannot be zero for $W_n < 2\Delta$. If $W_n = 2\Delta$ is a possible root, then the coupling term between the spurious state and the pairing vibration must be zero. Thus

$$\left. \sum_i \frac{\Omega_i f_i}{4E_i^2 - W_n^2} \right|_{W_n = 2\Delta} = \sum_i \frac{\Omega_i}{4E_i(\varepsilon_i - \lambda)} = 0, \tag{2.33}$$

which implies a symmetric distribution of levels around the Fermi surface. This is the case in the model under discussion. Thus

$$W = 2\Delta \tag{2.34}$$

and

$$\Lambda_{2n}/\Lambda_{1n} = 0. \tag{2.35}$$

(*) This phenomenon is equivalent to the phenomenon of spontaneously broken symmetry (violation of particle number conservation) and the spurious state is the corresponding Goldstone boson. For further discussion on the physical interpretation of the spurious mode cf. ref. [24].

Utilizing the fact that $f_1 = -f_2 = -\varepsilon/G\Omega$, (2.20), (2.21) and (2.34), we obtain

$$\Delta_{1n} = \left[\frac{W_n}{2}\left(\sum_i \frac{f_i^2 2E_i\Omega_i}{(4E_i^2 - W_n^2)^2}\right)\right]^{-\frac{1}{2}} = \varepsilon\sqrt{\frac{G}{2\Delta}}. \tag{2.36}$$

Thus

$$a_1 = -\frac{\varepsilon^2}{2(G\Omega - \Delta)}\sqrt{\frac{1}{2\Delta G\Omega}} = -b_1. \tag{2.37}$$

From this result and the expression of the two-body transfer operator

$$T = \sqrt{\Omega_j}\,U_j^2\left(\sum_n a_{ni}\,\Gamma_n^\dagger - \sum_n b_{ni}\,\Gamma_n\right) + \\ + \sqrt{\Omega_j}\,V_j^2\left(\sum_n a_{ni}\Gamma_n - \sum_n b_{ni}\Gamma_n^\dagger\right) + \Omega_j U_j V_j, \tag{2.38}$$

we obtain, in the collective representation,

$$\sigma_{gs} = |\langle \mathrm{gs}\,(\Omega)|T|\mathrm{gs}\,(\Omega-1)\rangle|^2 = \left(\sum_{j=1,2}\sqrt{\Omega_j}\,U_j\,V_j\right)^2 = \left(1 - \frac{1}{x^2}\right)\Omega^2 \tag{2.39}$$

and

$$\sigma_1 = |\langle n = 1(\Omega)|T|\mathrm{gs}\,(\Omega-1)\rangle|^2 = \\ = \left[\sum_j \sqrt{\Omega_j}\,(U_j^2 a_{nj} + V_i^2 b_{nj})\right]^2 = \frac{\Omega}{2x^2(1-1/x^2)^{\frac{1}{2}}} \tag{2.40}$$

for intraband and cross-over two-particle cross-sections, respectively. The main features of the exact calculation discussed in subsect. 2·1 are reproduced by the above results, the agreement becoming quantitative for $x > 1.2$ for (2.39) and $x > 2$ in the case of (2.40).

All pairs of particles participate in the transition between members of the ground-state rotational band and the cross-section is proportional to Ω^2. This transition is very large as compared to the transition to the pairing vibration. The corresponding ratio

$$\frac{\sigma_1}{\sigma_{gs}} \approx \frac{1}{2x^2}\left(1 + \frac{3}{2}\frac{1}{x^2}\right)\frac{1}{\Omega} \tag{2.41}$$

is about 10^{-2} for $x = 2$ and $\Omega \approx 10$, which can be considered typical numbers for superfluid systems.

Thus, the pairing vibration, which can be viewed as a coherent transfer of quasi-particles across the Fermi surface, gives rise to a pairing rotational band weakly connected with the ground-state band.

2·4. *Pairing phase transitions.* – In the case of the quadrupole surface elementary modes of excitation, changes of coupling scheme from the spherical-phonon scheme to the deformed-rotational scheme take place in different regions of the mass table. This change in coupling scheme is usually referred to as a quadrupole phase transition. The pairing order parameter can also be subjected to a « macroscopic » change and the system undergoes a phase transition from the normal (pairing vibrational) to the superconductive (pairing rotational) state. In both cases the polarization effects of particles outside closed shell give rise to a static field which violates, in one case, rotational invariance and, in the other, particle number conservation. The specific probes to study quadrupole phase transitions are Coulomb excitation and inelastic scattering. In a similar way, (t, p) and (p, t) reactions are the specific probes to study the change in the pairing coupling scheme.

The most conspicuous feature associated with a pairing phase transition is the behaviour of the ratio σ_1/σ_{gs} (cf. eqs. (2.39) and (2.40)). For the case of the two-level model this ratio is displayed in fig. 5 as a function of x. For normal systems $\sigma_1/\sigma_{gs} \approx 1$, while for superfluid systems $\sigma_1/\sigma_{gs} \approx 10^{-2}$.

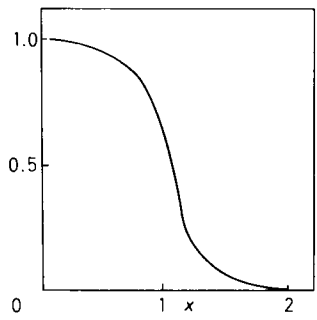

Fig. 5. – Ratio $|\langle n=1(\Omega)|T|\mathrm{gs}(\Omega-1)\rangle|^2/|\langle \mathrm{gs}(\Omega)|T|\mathrm{gs}(\Omega-1)\rangle|^2$ calculated by utilizing the exact wave functions of the two-level model ($\Omega=20$) as a function of x.

The cross-section σ associated with the pair addition mode to the first excited state is also strongly affected by the pairing phase transition (cf. ref. [20]). For $x > 1.4$, the crossing of the closed shell is not felt by σ_a, while there is a sudden drop for $x < 1.0$. This is because, in the superfluid phase, the pairing vibration in the closed-shell system is a two-photon state, whereas, in the superfluid case, it is a one-phonon type of excitation, the closed shell being the state containing no phonons. In both cases, the two-body transfer operator can change the number of phonons in one. The limit $x \approx 1$ is expected to be reached starting from a situation $x > 1$ in the case of high-spin states in deformed nuclei, as discussed in [25]. In this case the angular momentum of rotation plays the role, for the nuclear condensate, which is played by the external electromagnetic field in a superconductor. Around $I = I_c$, the pairing

vibrations are expected to influence the way in which the pairing gap goes to zero. The description of ref. [5] may be used to describe the behaviour of the pairing degree of freedom close to the phase transition, in a similar way as the Ginzburg-Landau theory is used to describe the behaviour of the condensate near the critical temperature.

3. – Applications.

3·1. *Normal systems* (Pb isotopes). – The nucleus ^{208}Pb provides the best example of closed-shell nuclei. There is a neat separation between particles and holes. In fact $D \approx 3$ MeV and $2G\Omega \approx 0.1 \cdot 8 \approx 1.0$ MeV, which results in $x \approx 0.3$.

Systematic (t, p) and (p, t) experiments carried out in this region show a well-developed monopole pairing vibrational band which encompasses states with up to three phonons of the same type (gs(^{202}Pb)) or of different type (excited state in ^{206}Pb) (cf. fig. 6). The identification of 0^+ states excited in either (t, p) or (p, t) reactions is rather simple due to the well-developed diffraction pattern of the associated angular distribution (cf. ref. [26]). Two quantum numbers are needed to classify the different states of this two-dimensional harmonic oscillator. We utilize (n_r, n_a) which indicate the number of pair removal and pair addition modes in each state.

The energy of the (1, 1) state in ^{208}Pb predicted by the pairing vibrational model is

$$W(1,1) = (B(208) - B(206)) - (B(210) - B(208)) = \\ = 14.110 \text{ MeV} - 9.123 \text{ MeV} = 4.987 \text{ MeV}, \tag{3.1}$$

where $B(A)$ is the binding energy of the Pb isotope with mass A.

For pedagogical purposes we require the pair addition and pair subtraction modes to have the same energy. Thus

$$W = W(0,1) = W(1,0) = 2.494 \text{ MeV}. \tag{3.2}$$

The excitation energy of any state of the model can then be written as

$$W(n_r, n_a) = (n_a + n_r)\, 2.494 \text{ MeV}. \tag{3.3}$$

The experimental magnitude to be compared with is

$$E(N) = (B(^{208}\text{Pb}) - B(N)) + 5.808\,(N - 126) \text{ MeV}. \tag{3.4}$$

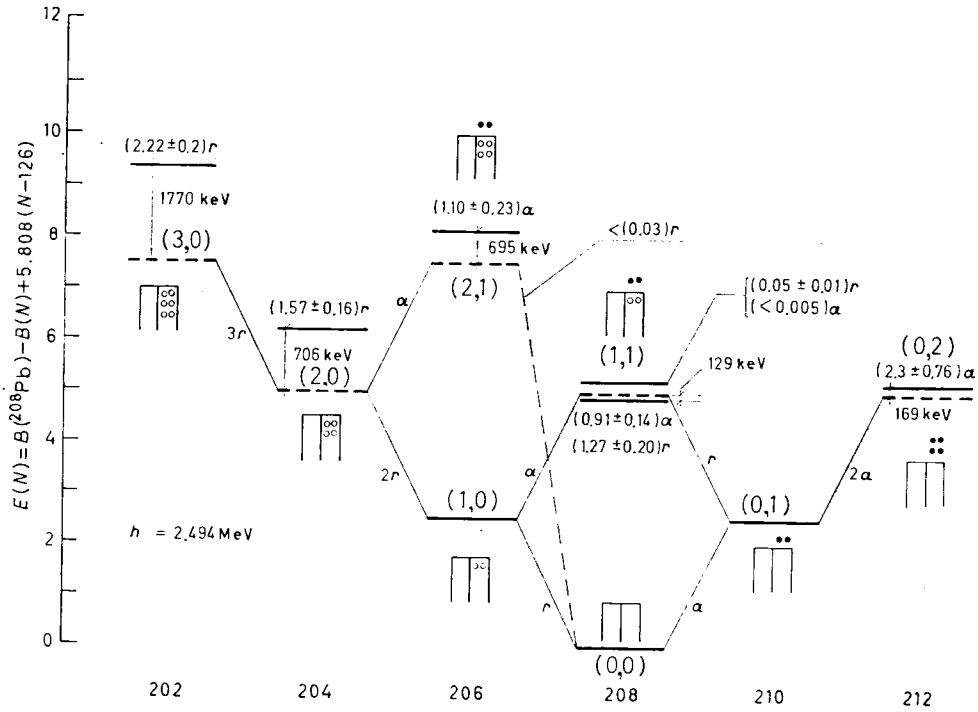

Fig. 6. – The many-phonon pairing spectrum around ^{208}Pb. The energies predicted by the pairing vibrational model are displayed as dashed horizontal lines, while the experimental values are drawn as continuous lines. The harmonic quantum numbers (n_r, n_a) are indicated for each level. A schematic representation of the many-particle many-hole structure of the state is also given. The transitions predicted by the model are indicated in units of r and a (cf. (3.11) and (3.12)). The corresponding experimental numbers are also given together with their errors, above each level. The dashed line between the states (0, 0) and (2, 1) indicates that the ^{208}Pb(p, t)^{206}Pb reaction to the three-phonon state in ^{206}Pb was carried out and an upper limit of $0.03r$ for the corresponding cross-section was determined. The (t, p) data are from ref. [27] and the (p, t) data from ref. [28].

The linear term ensures (*) $E(124) = E(128)$, which corresponds to the condition (3.2). The different transitions associated with these states are given in terms of the basic cross-section

$$a = \sigma(\mathrm{gs}(^{208}\mathrm{Pb}) \to \mathrm{gs}(^{210}\mathrm{Pb})) \quad \text{and} \quad r = \sigma(\mathrm{gs}(^{208}\mathrm{Pb}) \to \mathrm{gs}(^{206}\mathrm{Pb}))\,.$$

A microscopic description of the pair addition and pair subtraction modes is obtained by diagonalizing the pairing Hamiltonian in the RPA. The par-

(*) Note that the pair addition and pair subtraction modes are totally independent of each other. Here $N = 126 + 2(n_a - n_r)$.

TABLE I. – *Forward-going and backward-going amplitude* (3.9) *describing the motion of two particles* (^{210}Pb) *and two holes* (^{206}Pb) *around* ^{208}Pb. A coupling constant $G = 21.4/A$ MeV was utilized to reproduce the extra binding energy (3.6) of ^{210}Pb, while the corresponding quantity (3.5) for ^{206}Pb was reproduced for $G = 21.7/A$ MeV.

Single-particle states		^{206}Pb		^{210}Pb
$0h_{9/2}$	$r_1(\gamma)$	0.11	$a_1(\gamma)$	0.09
$1f_{7/2}$		0.14		0.10
$0i_{13/2}$		0.27		0.16
$2p_{3/2}$		0.24		0.10
$1f_{5/2}$		0.41		0.14
$2p_{1/2}$		0.84		−0.10
$1g_{9/2}$	$r_1(\omega)$	0.13	$a_1(\omega)$	0.82
$0i_{11/2}$		0.11		0.44
$0j_{15/2}$		0.11		0.35
$2d_{5/2}$		0.06		0.20
$3s_{1/2}$		0.03		0.09
$1g_{7/2}$		0.06		0.17
$2d_{3/2}$		0.04		0.11

ticles and holes are allowed to move in the six levels below and the seven levels above the Fermi surface which are experimentally known (cf. table I). The strength of the coupling constant is determined by fitting the extra binding energy

$$\Delta E(206) = 2[B(208) - B(207)] - [B(208) - B(206)] = \tag{3.5}$$

$$= 14.750 - 14.110 = 640 \text{ keV}$$

and

$$\Delta E(210) = [B(210) - B(208)] - [B(209) - B(208)] = \tag{3.6}$$

$$= 9123 - 7886 = 1237 \text{ keV}.$$

The pair addition and pair removal creation operators can be written as

$$\Gamma_n^\dagger(\alpha = 2) = \sum_\omega a_n(\omega)\Gamma^\dagger(\omega) + \sum_\gamma a_n(\gamma)\Gamma(\gamma) \tag{3.7a}$$

and

$$\Gamma_n^\dagger(\alpha = -2) = \sum_\gamma r_n(\gamma)\Gamma^\dagger(\gamma) + \sum_\omega r_n(\omega)\Gamma(\omega),$$

where

$$\text{(3.7}b\text{)} \qquad \begin{cases} \Gamma^{\dagger}(\omega) \equiv a^{\dagger}(\omega)a^{\dagger}(\bar{\omega}), \\ \Gamma^{\dagger}(\gamma) \equiv a(\bar{\gamma})a(\gamma), \end{cases}$$

and n labels the states according to their energy. The indices ω and γ are the shell model quantum numbers of single-particle orbits above and below the Fermi surface, respectively. The energy W_n obtained by hnearizing the pairing Hamiltonian is the n-th root of the dispersion relation

$$\text{(3.8)} \qquad \frac{1}{G(\pm 2)} = \sum_{\omega} \frac{1}{2\varepsilon(\omega) \mp W_n(\alpha = \pm 2)} + \sum_{\gamma} \frac{1}{2\varepsilon(\gamma) \pm W_n(\alpha = \pm 2)}.$$

The coefficients a_n and r_n are equal to

$$\text{(3.9)} \qquad \begin{cases} a_n(\omega) = \dfrac{\Lambda_n(\alpha = 2)}{2\varepsilon(\omega) - W_n(\alpha = 2)}, & a_n(\gamma) = -\dfrac{\Lambda_n(\alpha = 2)}{2\varepsilon(\gamma) + W_n(\alpha = 2)}, \\ r_n(\omega) = -\dfrac{\Lambda_n(\alpha = -2)}{2\varepsilon(\omega) + W_n(\alpha = -2)}, & r_n(\gamma) = \dfrac{\Lambda_n(\alpha = -2)}{2\varepsilon(\gamma) - W_n(\alpha = -2)}, \end{cases}$$

where

$$\text{(3.10)} \qquad \langle 0|\Gamma_n^{\dagger}(\alpha = \pm 2) H_p a^{\dagger}(j)a^{\dagger}(\bar{j})|0\rangle = \Lambda_n(\alpha = \pm 2) =$$
$$= \left[\pm \sum_{\omega} [2\varepsilon(\omega) \mp W_n(\alpha = \pm 2)]^{-2} \mp \sum_{\gamma} [2\varepsilon(\gamma) \pm W_n(\alpha = \pm 2)]^{-2}\right]^{-\frac{1}{2}}$$

is the normalization constant as well as the strength with which a pair of particles in time-reversed states couples to the pairing mode.

Note that the amplitudes (3.9) are obtained by dividing the matrix element (3.10) by the corresponding energy denominators (cf. fig. 7). This is a common feature of separable forces. The central role played by $\Lambda_n(\alpha)$ in the study of the interplay between the different modes of excitation will become apparent in the following sections.

In the 0s approximation (cf. [26]), the cross-section associated with the transfer of two particles starting from the $N_0 - 2$ ground-state system and leading to the closed-shell (N_0) ground state is

$$\text{(3.11)} \qquad r \equiv \sigma^{(0s)}((1, 0) \to (0, 0)) \propto \Lambda_1^2(\alpha = -2).$$

For the cross-section leading to the pair addition mode one obtains

$$\text{(3.12)} \qquad a \equiv \sigma^{(0s)}((0, 0) \to (0, 1)) \propto \Lambda_1^2(\alpha = 2).$$

The values of the pairing strengths obtained by fitting the energy of the 206 and 210 ground states are $G(2) = 0.10$ MeV and $G(-2) = 0.14$ MeV. The

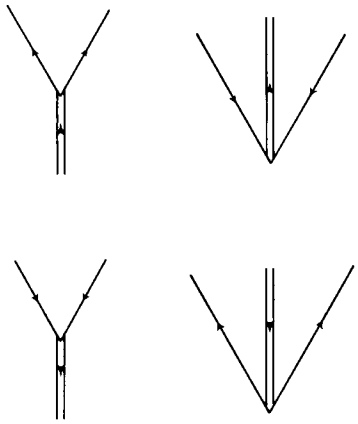

Fig. 7. – Graphical representation of the forward-going and backward-going amplitudes (3.9) of the pairing modes. The vertex strength is equal to $\Delta_n(\alpha = \pm 2)$ (cf. (3.10)). The pairing boson is represented by a double arrowed line, while a single arrowed line represents a fermion.

resulting absolute cross-sections are reproduced within a factor of two for a normalization factor $D_0 = 30 \cdot 10^4\,(\mathrm{MeV})^2\,\mathrm{fm}^3$ (cf. ref. [26] and [29] for details on the calculation of two-particle transfer cross-sections).

By utilizing the microscopic results it is possible to give a measure of the collectivity of the pair addition and pair removal modes by expressing the corresponding cross-sections in terms of absolute two-particle units (cf. [26]). Typical enhancements

$$\varepsilon = \sigma_{\mathrm{exp}}/\sigma_{2\mathrm{p}} \tag{3.13}$$

of order 12 are obtained. This number can be compared with the value of 10 B_{sp} which is typical of the $B(E2)$ transition rate connecting the lowest 2^+ with the ground state of spherical nuclei.

Note that the contributions of all the different two-particle and two-hole components of the microscopic wave function are constructively coherent.

3·2. *Superfluid systems* (Sn isotopes). – The Sn isotopes provide the best example of spherical nuclei with a large number of particles outside closed shell (≈ 16 neutrons) and a large value of the pairing gap parameter Δ.

The (t, p) and (p, t) data are displayed in fig. 3 and 8. Although the ground-state transition dominates the spectrum, the interband-to-intraband ratio can become as large as 0.18, the behaviour of the (t, p) and (p, t) intensities being rather asymmetric, indicating a competition between pairing and shell effects, as shown below.

We discuss first the reaction $^{118}\mathrm{Sn(t, p)}^{120}\mathrm{Sn}$. The Hamiltonian $H = H_{11} + H'_{\mathrm{p}} + H''_{\mathrm{p}}$ (cf. eq. (2.22)) was diagonalized in the RPA. A coupling

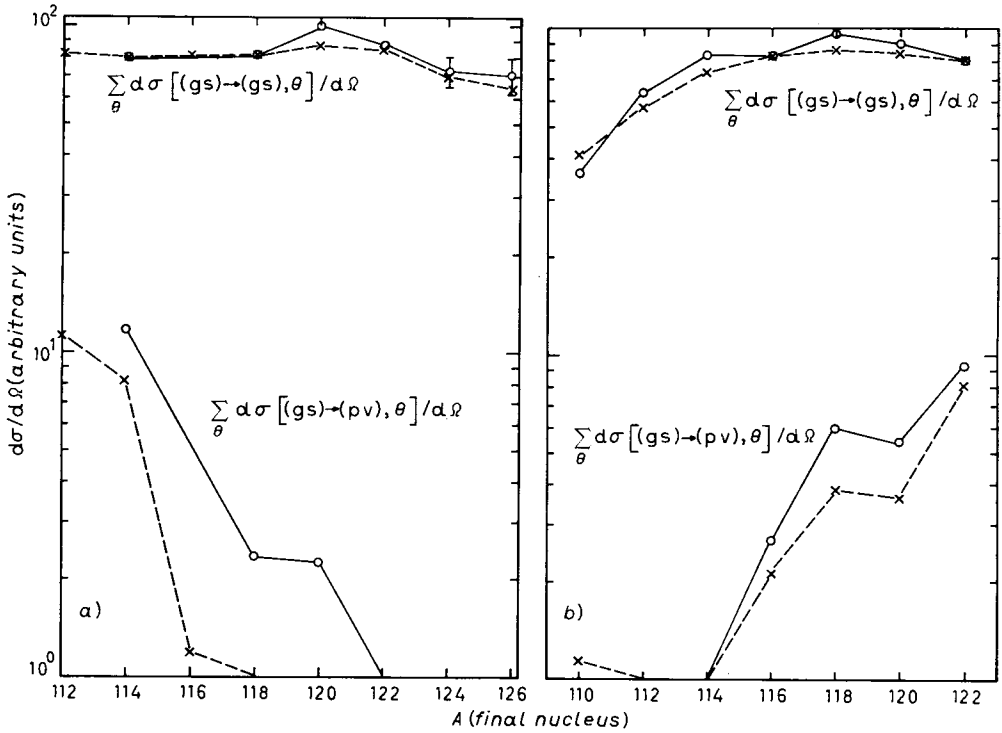

Fig. 8. – Experimental [14-16] (·····o———) and theoretical (— — —×— — —) cross-sections corresponding to the $J^\pi = 0^+$ states below 3 MeV excited in the reactions *a*) $^{A+2}$Sn(p, t) and *b*) $^{A-2}$Sn(t, p). When more than one excited state was observed, the numbers reported are the centroid energy and the summed cross-section. The normalization between theory and experiment was done in both cases to the ^{118}Sn $\leftrightarrow$ ^{120}Sn reactions.

constant $G = 23/A$ was utilized, determined by fitting the ^{118}Sn pairing gap ($\Delta_n = 1.39$ MeV). This procedure yields the occupation parameters, energies and wave functions displayed in table II (cf. also [30]).

TABLE II. – *Wave functions (cf. eq. (2.30)) and energies associated with the lowest states of* ^{118}Sn. The valence particles were allowed to move in the five single-particle states displayed. The corresponding BCS occupation parameters U are also given.

		$2d_{5/2}$	$1g_{7/2}$	$3s_{1/2}$	$2h_{11/2}$	$2d_{3/2}$
U		0.2449	0.3489	0.4438	0.7861	0.8494
0_1^+	*a*	−0.0143	−0.0278	−0.0212	0.4340	0.9003
$W = 2.61$ MeV	*b*	0.0122	0.0155	0.0075	−0.0034	−0.0005
0_2^+	*a*	−0.1903	−0.4773	−0.7384	−0.4128	0.1638
$W = 2.73$ MeV	*b*	0.0163	0.0160	0.0039	0.0629	−0.0450
0_3^+	*a*	−0.1768	−0.7429	0.6243	−0.1605	0.0666
$W = 3.24$ MeV	*b*	0.0050	0.0029	−0.0013	0.0458	−0.0313

Utilizing these wave functions and the normalization factor

$$D_0^2 = 20\ (\mathrm{MeV})^2\ \mathrm{fm}^3\,,$$

we obtain the following enhancement factors:

$$\varepsilon = \begin{cases} 220 & \mathrm{gs}\,, \\ 4 & 0_1^+\,, \\ 4 & 0_2^+\,. \end{cases} \tag{3.14}$$

The square root of the value associated with the ground state gives a measure of the number of twofold degenerate levels contributing to the static pairing distortion Δ. This number is ≈ 15. Thus, all the levels considered in solving the BCS equation contribute to the ground-state transition $\left(\text{in fact } \sum_j (j + \frac{1}{2}) = 18\right)$. The enhancement factor $\varepsilon(\mathrm{gs}) = 220$ associated with an interband transition should be compared with the enhancement factors obtained for the $E2$ decay of the 2^+ member of the ground-state rotational band in quadrupole deformed nuclei. Typical numbers are $200\ B_{\mathrm{sp}}$ implying that about $\sqrt{200} \approx 14$ twofold degenerate levels contribute to the quadrupole static deformation Q_0.

The systematic comparison between the intensities predicted by the pairing vibrational model and the experimental data is carried out in fig. 8. A rather considerable change of the order parameter $\Delta/\langle\delta\varepsilon\rangle$ takes place through Sn isotopes. The quantity $\langle\delta\varepsilon\rangle$ is the average distance between the levels around the Fermi surface. Thus $\Delta/\langle\delta\varepsilon\rangle$ plays a similar role as played by x in the case of the two-level model (cf. sect. **2**), and it may be approximated by the number $n_\Delta(A)$ of double degenerate single-particle levels in the interval $\Delta(A)$ around $\lambda(A)$. We obtain

$$\begin{cases} n_\Delta(^{112}\mathrm{Sn}) = 8\,, \\ n_\Delta(^{116}\mathrm{Sn}) = 3 \end{cases} \tag{3.15}$$

and

$$n_\Delta(^{120}\mathrm{Sn}) = 8\,. \tag{3.16}$$

These changes in $\Delta/\langle\delta\varepsilon\rangle$ give rise to a partial distinction between particles and holes and, consequently, to two collective transitions similar to the case of normal systems, in particular for the case of ^{114}Sn. For more details see ref. [31].

3·3. *Multipole pairing vibrations.* – In the previous sections we have concentrated our attention in the monopole pairing modes. Thus, we have re-

stricted the distortions and vibrations of the Fermi surface to be isotropic. The condensation in p-wave observed in the case of ^{3}He gives an example, in the macroscopic scale, of nonisotropic distortions of the Fermi surface, produced by a pairing interaction acting in a $l = 1$ state of relative motion. In fact, the three superfluid phases corresponding to $\uparrow\uparrow$, $\downarrow\downarrow$ and $\uparrow\downarrow$ ($m = \pm 1, 0$) have been observed (cf. ref. [32] and [33]). In nuclei the only component of the short-range part of the residual interaction which gives rise to a condensate is the monopole pairing force. It is, however, expected that multipole vibrations, which change the number of particles in two, can play an important role in the dynamics of the nuclear spectrum.

In fact, there is specific evidence for the existence of multipole pairing vibrations provided by the strong $L = 2$, 4 and 6 cross-sections associated with (t, p) and (p, t) transitions in the Pb isotopes. In fig. 9 we display the energy and the two-nucleon transfer cross-sections associated with the $\lambda = 0$ and $\lambda = 2$ pair addition and pair subtraction modes. A microscopic descrip-

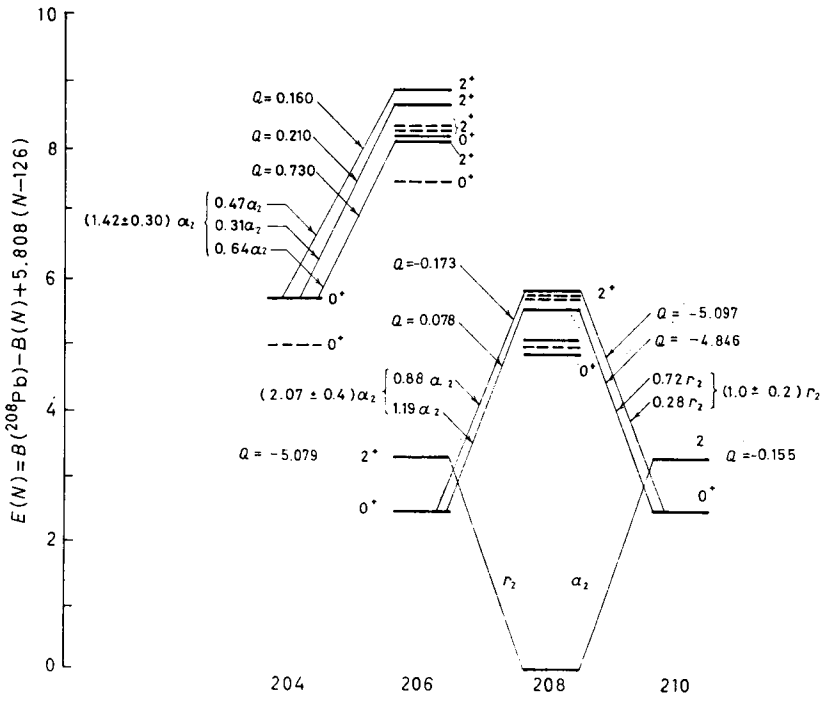

Fig. 9. – Theoretical predictions of the pairing vibrational model for the $J^\pi = 0^+$ and 2^+ excited states of ^{206}Pb and ^{208}Pb, expected to display the same Q-value, angular distributions and intensities in the ^{206,204}Pb(t, p) reactions as the ground state and the lowest 2^+ state of ^{210}Pb excited in the ^{208}Pb(t, p)^{210}Pb reaction. These levels are depicted as dashed lines. The corresponding cross-sections and Q-values associated with each state are also quoted. The experimental energies (solid lines) and (t, p) and (p, t) cross-sections are also given [27, 28, 34, 35].

tion of these modes can be obtained, as in the case of the monopole pairing vibration, in the framework of the random-phase approximation, allowing the particles to correlate through the schematic interaction [36]

$$H(2\lambda) = -\frac{\pi G_\lambda}{2\lambda+1}\sum_\mu P^\dagger_{\lambda\mu} P_{\lambda\mu}\,, \tag{3.17}$$

where

$$P^\dagger_{\lambda\mu} = \sum_{j_1 j_2} \langle j_1 \| Y_\lambda \| j_2 \rangle [a^\dagger_{j_1} a^\dagger_{j_2}]^\lambda_\mu\,. \tag{3.18}$$

The coupling constant G_λ can be determined through the dispersion relations (3.8), by fitting the binding energy of the two-particle and two-hole system, respectively. The resulting values corresponding to the multipolarities $\lambda = 0, 2, 4$ and 6 and to both ^{206}Pb (pair removal modes) and ^{210}Pb (pair addition modes) are very similar to each other and equal to (cf. ref. [37])

$$G_\lambda \approx 27/A \text{ MeV}\,. \tag{3.19}$$

Utilizing the corresponding wave functions one obtains the (t, p) and (p, t) cross-sections displayed in table III. The absolute cross-sections are reproduced within a factor of 2, by utilizing the empirical normalization value $D_0^2 = 22 \cdot 10^4$ (MeV)^2 fm^3.

TABLE III. – *Ratio of experimental* [27, 28, 34, 35] *and theoretical* [37] *cross-sections associated with the reactions* ^{208}Pb(t, p)^{210}Pb *and* ^{208}Pb(p, t)^{206}Pb *leading to the lowest states of each spin and parity.*

J^π	^{208}Pb(p, t)^{206}Pb (J^π)		^{208}Pb(t, p)^{210}Pb (J^π)	
	E (MeV)	$\frac{[d\sigma(J^\pi)/d\Omega]_{exp}}{[d\sigma(J^\pi)/d\Omega]_{th}}$	E (MeV)	$\frac{[d\sigma(J^\pi)/d\Omega]_{exp}}{[d\sigma(J^\pi)/d\Omega]_{th}}$
0^+	0.00	0.94	0.00	1.47
2^+	0.803	0.75	0.795	0.78
4^+	1.684	0.88	1.094	1.21
6^+	3.253	0.49	1.193	0.77

The quadrupole transition probability between the lowest 2^+ and the ground state of ^{210}Pb is given in the present model by

$$B(E2;\, 0 \to 2^+) = (e_{\text{eff}})^2 \left\{ 2 \sum_{j_1 j_2} a(j_1 j_2;\, 2^+)\, a(j_1^2;\, \text{gs}) \frac{\langle j_2 \| r^2 Y_2 \| j_1 \rangle}{\sqrt{2j_1+1}} \right\}^2 . \tag{3.20}$$

Utilizing the calculated amplitudes and the experimental data ($B(E2)_{206} =$

$= 7B_{sp} = 0.5\,B(E2)_{210}$), one obtains for the effective charges

$$e_{eff}(^{206}\mathrm{Pb}) = 0.98\,, \qquad e_{eff}(^{210}\mathrm{Pb}) = 1.03\,. \tag{3.21}$$

These values are consistent with the effective charges obtained from transitions among single-particle states in ^{207}Pb and ^{209}Pb. This result provides further support to the description of the 2_1^+ of ^{210}Pb as a pairing vibration of ^{208}Pb.

The existence of a $\mu = 0$ quadrupole pairing force of strength approximately equal to (3.19) has been shown [38] (cf. also subsect. 3·5) to play a basic role in the 0^+ spectrum of the actinide nuclei. As discussed in [39], the $\mu = 1$ component of the quadrupole pairing force plays an important role in determining the value of the moment of inertia of deformed nuclei.

3·4. *Alternative description of* ^{206}Pb. – Although the pairing spectrum of ^{206}Pb fits smoothly into the pairing vibrational scheme of normal systems, one can also utilize a description in terms of quasi-particles.

Because of the many-body aspects of the quasi-particle wave functions describing the excited states of ^{206}Pb, they can describe both (2h) and (4h-2p)-like states. Such a treatment is thus able to treat in a simple, albeit approximate way, the interaction between the different elementary modes of excitation.

We can divide the resulting spectrum in two parts. The first is a low-energy region ($\leqslant 4$ MeV), which is basically controlled by the magnitude of the static pairing gap. In this region the wave functions have large components on single-hole levels up to and including the $2p_{\frac{1}{2}}$ orbital, *i.e.* levels for which $\varepsilon_j - \lambda \leqslant 2\Delta$, where λ is the Fermi energy. Because of the presence of the condensate, the ground state collects most of the 0^+ two-nucleon transfer sum rule associated with the valence hole levels. The second region is expected at excitation energies E, where $5 \leqslant E \leqslant 10$ MeV, and consists of two–quasi-particle states built out of single-particle levels with $\varepsilon_j - \lambda \gg 2\Delta$. Two–quasi-particle states of this type are excited, for example, in the ^{204}Pb(t, p)^{206}Pb reaction by transferring the two neutrons into the orbitals above the $N = 126$ shell closure, *i.e.* into single-particle states that are practically empty.

The corresponding results for $\lambda = 0$ and 2 are collected in fig. 10.

3·5. *Pairing isomers.* – As discussed above, in normal spherical nuclei the Hamiltonian (3.17) generates the $\alpha = \pm 2$ modes, but has no systematic effect on the particle-hole states, *i.e.* states with $\alpha = 0$. The part of the nuclear interaction which generates isoscalar surface vibrations can be written schematically as

$$H(0\lambda) = -\frac{K_\lambda}{2} \sum_\mu Q^\dagger_{\lambda\mu} Q_{\lambda\mu}\,, \tag{3.22}$$

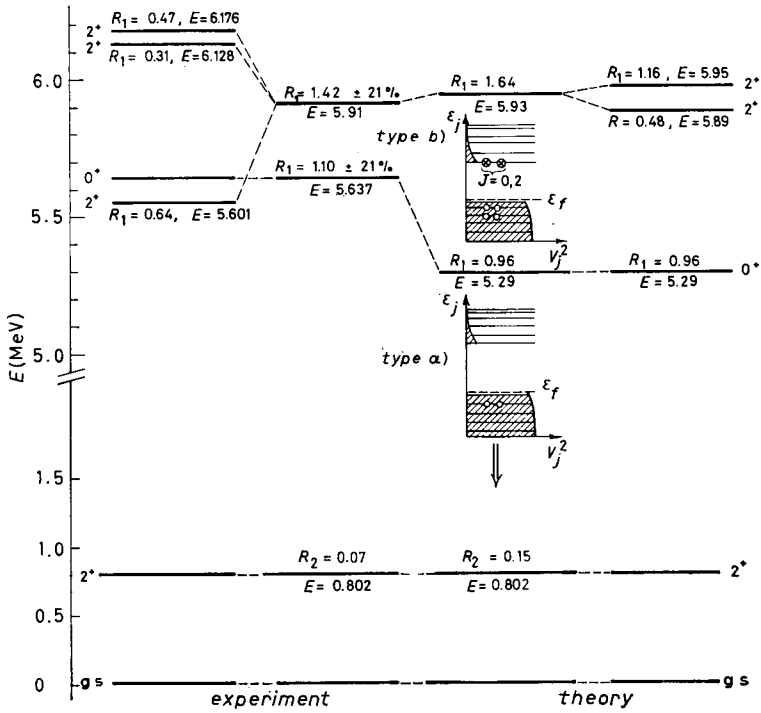

Fig. 10. – States containing one and three pairing vibrational phonons, excited in the ^{204}Pb(t, p)^{206}Pb reaction. In the first and second columns the experimental levels [35] and the corresponding centroids are plotted. In the last two columns the corresponding theoretical results are displayed [40]. The two lowest states (*i.e.* g.s. and lowest 2^+) are examples of one-phonon pairing states (*i.e.* type-*a*) states) and their structure in terms of the occnpation parameters V_j^2 is schematically illustrated in the third column. The relative cross-section $R_2 = \mathrm{d}\sigma(2^+;\, \theta = 35°)/\mathrm{d}\sigma(\mathrm{gs};\, \theta = 25°)$ of the 2_1^+ with respect to the ground state is reported. The higher part of the spectrum ($E > 5$ MeV) shows the three pairing phonon states whose main structure is $|0^+\rangle = |\mathrm{gs}(^{206}\mathrm{Pb}) \otimes \mathrm{gs}(^{206}\mathrm{Pb}) \otimes \mathrm{gs}(^{210}\mathrm{Pb})\rangle$ and $|2^+\rangle = |\mathrm{gs}(^{206}\mathrm{Pb}) \otimes \mathrm{gs}(^{206}\mathrm{Pb}) \otimes 2^+(^{210}\mathrm{Pb})\rangle$ (type-*b*) states). In this case the relative cross-section

$$R_1 = \frac{\mathrm{d}\sigma(\mathrm{gs}(^{204}\mathrm{Pb}) \to J^\pi(^{206}\mathrm{Pb}))}{\mathrm{d}\sigma(\mathrm{gs}(^{208}\mathrm{Pb}) \to J_1^\pi(^{210}\mathrm{Pb}))}$$

is reported.

where

$$Q_{\lambda\mu} = -\frac{1}{\sqrt{2\lambda+1}} \sum_{a_1 a_2} \langle a_1 \| r^\lambda Y_\lambda \| a_2 \rangle [a_{a_1}^\dagger a_{a_2}]_\mu^\lambda \,. \tag{3.23}$$

In superfluid nuclei, because the distinction between particles and holes is

lost, the two–quasi-particle states $(\lambda, \pi = (-1)^{\lambda})$ are correlated by both the multipole pairing and the particle-hole interaction (*).

However, because of the conservation of angular momentum, the BCS pairing gap, which can be related to the odd-even mass difference, is determined by the monopole pairing interaction. This is also true, as discussed above, for the fluctuations of the gap giving rise to two quasi-particle 0^+ pairing vibrational states.

For deformed nuclei this restriction is not vahd any longer. The pairing gap is now state dependent. It receives contributions from different pairing multipoles, *i.e.*

$$\Delta_i = \Delta_0 + \sum_{\lambda>0} \Delta_\lambda Q_i^{(\lambda)} , \tag{3.24}$$

where

$$Q_i^{(\lambda)} = \langle i \| Y_\lambda \| i \rangle , \tag{3.25}$$

$$\Delta_0 = G_0 \sum_i U_i V_i \tag{3.25a}$$

is the usual pairing gap and

$$\Delta_\lambda = \sqrt{\frac{\pi}{2\lambda+1}}\, G_\lambda \sum_i \langle i \| Y_\lambda \| i \rangle\, U_i V_i \tag{3.26}$$

measures the multipole distortion (departure from anisotropy) of the Fermi surface. The index i labels Nilsson single-particle levels. Specialized to the case of $\lambda = 2$, the pairing matrix elements are equal to

$$\langle ii | H(2,0) + H(2,2) | jj \rangle = - G_0 - G_2 Q_i Q_j , \tag{3.27}$$

where we have used $Q_i = Q_i^{(2)}$. The violation of both the angular momentum and the particle number conservation brings new dimensions to the role of the multipole pairing correlations.

In particular, the gap (3.24) can become very small for certain levels (**) as well as the matrix element (3.27). We can distinguish two different types of pairing matrix elements: i) those that are related with the scattering of particles between pairs of single particles having the same sign of the quadru-

(*) While the correlations generated by (3.17) specifically enhance two-nucleon transfer reactions, (3.22) enhances inelastic scattering and Coulomb excitation processes.

(**) This phenomenon is analogous to the phenomenon of gapless superconductivity in solid-state physics. There, an impurity traps a magnetic field which is larger than $\mathscr{H}_{cr}$ and thus gives rise to some quasi-particles for which $\Delta \approx 0$. In nuclei, it is the shell structure which acts as impurity.

pole moment, *i.e.*

$$G_{oo} = \langle i_o \bar{i}_o | H(20) + H(22) | i'_o \bar{i}'_o \rangle = - G_o - G_2 | Q_{i_o} Q_{i'_o} | , \tag{3.28}$$

$$G_{op} = \langle i_p \bar{i}_p | H(20) + H(22) | i'_p \bar{i}'_p \rangle = - G_o - G_2 | Q_{i_p} Q_{i'_p} | , \tag{3.29}$$

and ii) those between pairs of orbitals with opposite sign of the quadrupole moment, *i.e.*

$$G_{op} = \langle i_p \bar{i}_p | H(20) + H(22) | i'_o \bar{i}'_o \rangle = - G_o + G_2 | Q_{i_p} Q_{i'_o} | . \tag{3.30}$$

The label o denotes oblate orbitals having a negative sign of the quadrupole moment and p stands for prolate orbitals corresponding to a positive sign.

In general

$$|G_{oo}| \approx |G_{pp}| \gg |G_{op}| . \tag{3.31}$$

In this case we can distinguish, as in the case of closed-shell systems, between two groups of single-particle levels which are uncoupled from each other.

In the closed-shell system $\langle i \bar{i} | H(20) | i' \bar{i}' \rangle$ has similar values for the scattering of any pair of particles. However, if $i > i_F$ and $i' < i_F$, the scattering amplitude $G_o/\Delta\varepsilon$ becomes very small (*), $\Delta\varepsilon$ being twice the single energy gap. There is thus a static decoupling between the single-particle levels.

In the case of deformed nuclei, on the other hand, $\Delta\varepsilon$ is of the order of G, the single-particle levels being closely spaced (cf. fig. 11). (Note that the average spacing of the ten single-particle levels displayed is 360 keV.) However, because of (3.31), the scattering amplitude between oblate and prolate single-particle orbitals can become very small. In this case there is a decoupling between the single-particle levels due to the correlations among the particles.

Let us consider the effect of the monopole plus quadrupole pairing force acting on a system of particles moving in the single-particle levels of fig. 11. Around the Fermi surface there is a predominance of prolate levels, while ≈ 0.7 MeV below the Fermi surface there is a group of oblate single-particle levels.

When the residual monopole and quadrupole pairing interactions are switched on, we can construct essentially two ground states. The ground state of nucleus A, based on the levels around the Fermi surface, and the ground state of the $A - 2$ system (pair removal mode), based on the states with negative value of the quadrupole moment. Thus, this latter state has a similar rela-

(*) For Pb, $\Delta\varepsilon \approx 7$ MeV and $G \approx 0.1$ MeV.

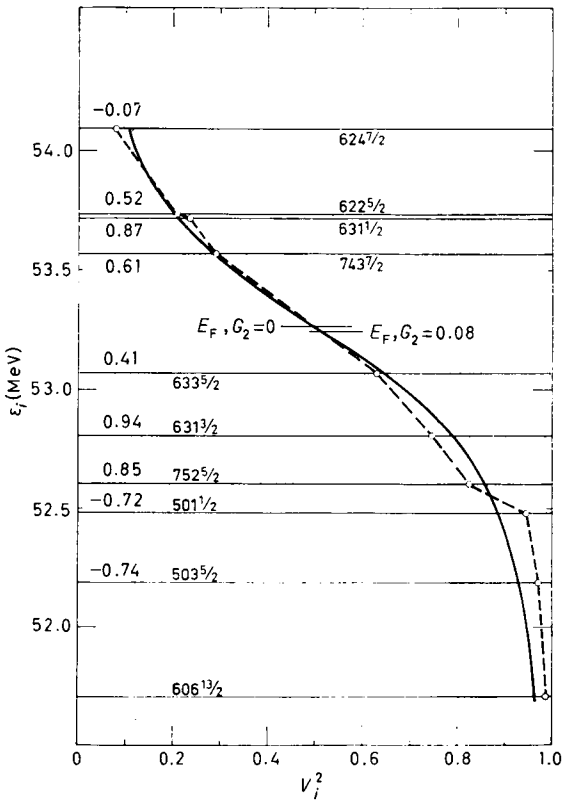

Fig. 11. – The occupation probability V_i^2 for levels around the Fermi surface E_F of ^{234}U for $G_2 = 0$ (solid line) and $G_2 = 0.08$ MeV (dashed line). For each level the asymptotic quantum numbers are given as well as the value of the single-particle quadrupole moment.

tion to its ground state as the $N_0 - 2$ system has to the closed N_0 system ground state (*).

Thus, although the deformed nucleus is superfluid, the quadrupole pairing correlations allow for the existence of real particles ($V_i \approx 1$), almost uncoupled from the superfluid ground state and moving rather close to the Fermi surface. Because of the nonconservation of the number of particles, the states based on the oblate orbitals become an excited state of the A-system, namely an isomeric pairing state with a rather different average value of the gap parameter than the ground state.

(*) Note that all the different terms which contribute to the two-nucleon transfer amplitude of the excited state can produce constructive coherence and still be orthogonal to the ground state, because the two states have components appreciably different from zero on different single-particle orbitals and thus are orthogonal *ab initio*.

The existence of a pairing isomer in a pairing deformed nucleus is evidenced by the unusually large two-nucleon transfer cross-section to an excited 0^+ state, in a similar way that a shape isomer in a quadrupole deformed nucleus displays a very retarded electromagnetic-transition probability.

Giving the same weight to the different configurations, we get, for the ground-state (t, p) and (p, t) cross-sections,

$$\sigma(\mathrm{gs} \to \mathrm{gs}) = \left(\sum_i U_i V_i\right)^2 = (\Delta/G)^2 . \tag{3.32}$$

The corresponding cross-sections to an excited 0^+ state are given by

$$\sigma^{(\mathrm{p,t})}(\mathrm{gs} \to 0^+) \approx \left(2 \sum_i a_i V_i^2\right)^2 \tag{3.33a}$$

and

$$\sigma^{(\mathrm{t,p})}(\mathrm{gs} \to 0^+) \approx \left(2 \sum_i a_i U_i^2\right)^2 , \tag{3.33b}$$

where a_i denotes the two–quasi-particle component (forward-going amplitude) of the single-particle state i.

In the actinide region a typical value for (3.32) is 100, while (3.33) depend strongly on the amplitude a_i. If the first excited state is below the smallest two–quasi-particle energy $2E_i$ and is mainly generated by vibrations of the monopole pairing gap, all the a_i below the Fermi surface have one sign and all those above the opposite sign (cf. fig. 12). This sign change is necessary for the excited state to be orthogonal to the ground state. If $G_2 = 0$, the low-lying excited states will mainly be built out of the states close to the Fermi surface (with $U_i \approx V_i \approx 0.5$), which means that (3.33a) and (3.33b) will be about equal and of the order of unity because of cancellations from states below and above the Fermi surface.

The pairing isomer ($G_2 \approx 0.1$), on the other hand, is mainly built out of the oblate levels below the Fermi surface (cf. fig. 12) and is, from the start, orthogonal to the ground state which has very small components on these single-particle levels. For these oblate levels, $V_i^2 \approx 1$ ($\varepsilon_i < \varepsilon_\mathrm{F}$) and the different contributions to (3.33a) add with the same sign resulting in a large (p, t) cross-section.

In a schematic model where the 0^+ state has equal amplitudes on configurations built out of the five oblate orbitals, we find

$$\sigma^{(\mathrm{p,t})}(\mathrm{gs} \to 0^+) \approx \left(2 \sum_{i=1}^{5} \sqrt{\frac{1}{5}}\right)^2 = 20 . \tag{3.34}$$

The (p, t) cross-section of this state relative to the ground state is then 20 %, while the (t, p) cross-section is essentially zero ($U_i^2 \approx 0$) ($\varepsilon_i < \varepsilon_\mathrm{F}$). Moreover,

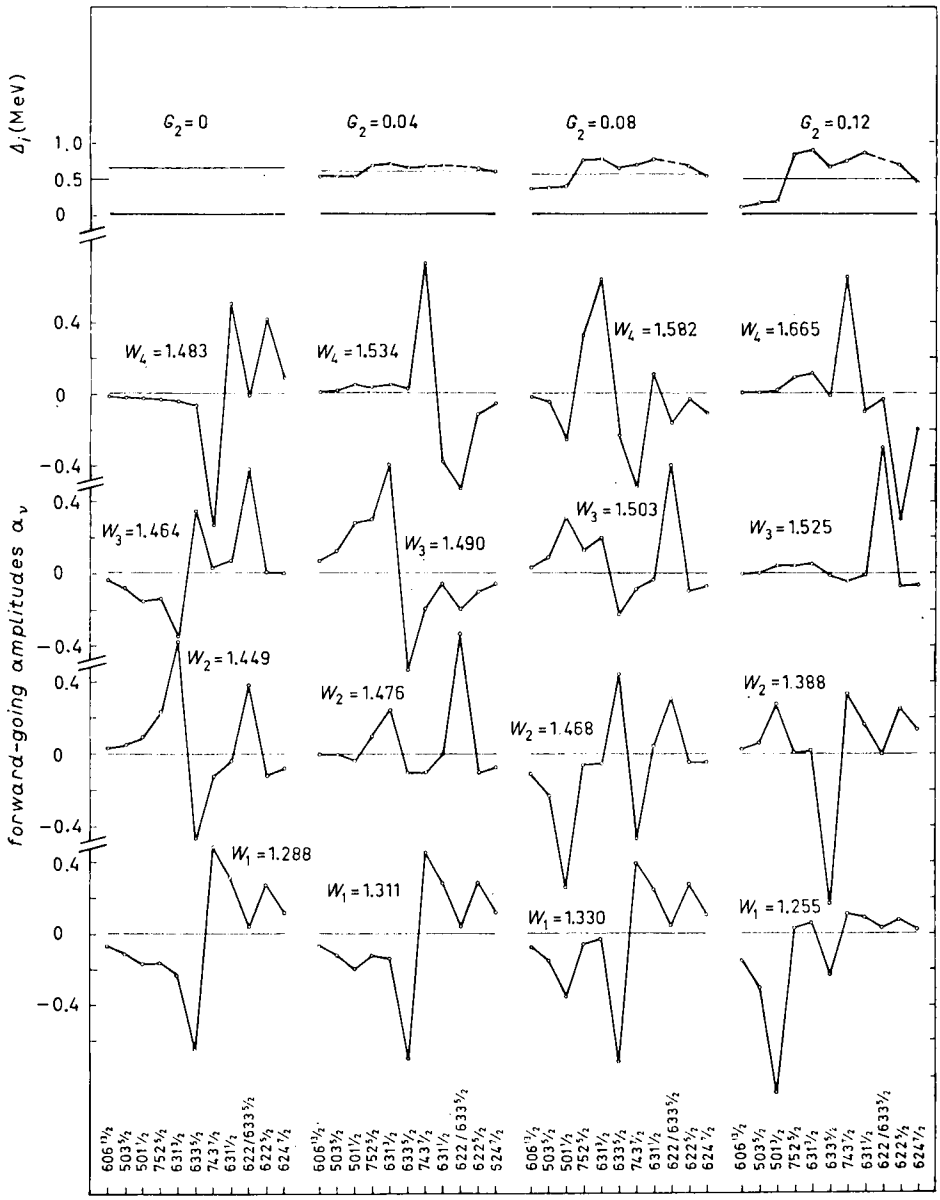

Fig. 12.. – Forward-going amplitudes for the four lowest 0^+ states of ^{234}U and for different values of G_2. They were obtained through a RPA diagonalization, *i.e.* diagonalization $[H_{sp} + H_{02} + H_{22}, \Gamma_n^\dagger] = W_n \Gamma_n^\dagger$. The value $G_2 = 0.08$ MeV corresponds to $G_2 \approx G_0$. The asymptotic quantum numbers $(Nn_z\Lambda\Omega)$ corresponding to the most important two-quasi-particle configurations are displayed. In the upper part of the figure the pairing gap Δ_i associated with each two-particle configuration i is also reported.

as the oblate single-particle levels have a small average value of Δ, the quasiparticle energies $E_i = \sqrt{(\varepsilon_i - \lambda)^2 + \Delta^2}$ will be relatively small implying that the pairing isomer will be found at a low excitation energy.

In fig. 13 we display the change of the different physical magnitudes (W, σ(t, p), σ(p, t), Δ_0 and Δ_2) as a function of G_2. According to the discussion of subsect. 3·3, one should choose $G_2 \approx G_0$. For this value of G_2 we

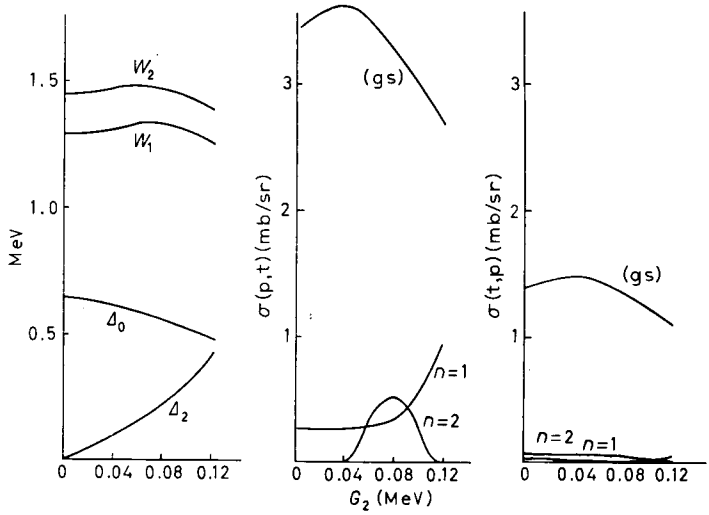

Fig. 13. – Dependence of the different parameters associated with the monopole and quadrupole pairing degree of freedom as a function of G_2, and for the nucleus ^{234}U. The labels $n = 1$ and $n = 2$ indicate the first and the second 0^+ excited state, respectively.

display in table IV the results of the model for nuclei in the actinide region, in comparison with the experimental data (cf. also ref. [38]). Note, in the present situation, the fact that the orbital [501] $\frac{1}{2}$ carries a very large intrinsic cross-section and contributes 50 % of the total cross-section of the excited state.

3·6. *α-vibrations.* – There is experimental evidence that the $\tau = 1$ and $\tau = 0$ components of the nuclear residual interaction have similar strength. However, the correlations induced by the two types of forces are very different. The spectrum of ^{42}Sc offers a conspicuous example. In fact, the ground state is the only $T = 1$ state which displays a large (≈ 2 MeV) correlation energy. On the other hand, the different $T = 0$ states (*i.e.* 1^+, 3^+, 5^+ and 7^+) are depressed from the unperturbed energy by about the same amount.

In the case of a four-particle system this result implies that, although the $\tau = 0$ component of the force can be of importance for the energy of the $(2\pi, 2\nu)$ system, its coupling scheme is determined by the $\tau = 1$ residual interaction. Thus, the four-particle system can be viewed as the product of a

TABLE IV. – *The experimental* [41] *excitation energies, relative* (p, t) *cross-sections and* $X = \varrho^2 e^2 R_0^4 / B(E2; 2 \to 0)$ *values associated with the low-lying* 0^+ *states are compared with the theoretical calculations* [38] *for the actinide region.*

Nucleus	Excitation energy (keV)		$\frac{\sigma(\text{excited } 0^+)}{\sigma(\text{g.s. } 0^+)}$		X	
	Experimental	Theoretical	Experimental	Theoretical	Experimental	Theoretical
^{228}Th	830		18		(0.83)	
		930		13.4		0.33
^{230}Th	636		18		0.22 ± 0.10	
	1590		3			
		1040		16.8		0.35
		1270		4.4		0.39
^{232}U	695		13		0.17 ± 0.04	
		930		8.5		0.37
^{234}U	812		13		0.50 ± 0.08	
		1020		16.5		0.41
		1250		2.0		0.46
^{236}U	920		13			
		950		11.7		0.39
		1220		2.1		0.35
		1760		1.6		0.97
^{240}Pu	862		15		0.05 ± 0.01	
	1091		10			
		1070		6.0		0.41
		1260		1.5		0.40
		1450		2.6		
^{242}Pu	956		24			
		1100		9.0		0.39
		1210		13.7		0.24
		1610		5.9		
^{246}Cm	1176		11			
		1180		4.8		0.42
		1300		5.2		0.24
		1610		11.1		

proton pairing vibration and a neutron pairing vibration and we refer to it as an α-vibration [42].

In ^{208}Pb this state is expected at an energy

$$(3.35) \qquad W_\alpha = [B(^{208}\mathrm{Pb}) - B(^{204}\mathrm{Hg})] - [B(^{212}\mathrm{Po}) - B(^{208}\mathrm{Pb})] = 8.440 \text{ MeV},$$

and it should be excited in, *e.g.*, the reaction ^{204}Hg(^{6}Li, d)^{208}Pb, with the same cross-section and Q-value as that associated with the ^{208}Pb(^{6}Li, d)^{212}Po(gs) process. Also the $J^\pi = 0^+$ states which are selectively excited in the $(N-2, Z) \to (N, Z)$ and $(N, Z-2) \to (N, Z)$ reactions should be selectively excited in the $(N-2, Z-2) \to (N, Z)$ reaction.

Recently both the ^{208}Pb(^{16}O, ^{14}C) and ^{204}Hg(^{16}O, ^{14}C) reactions were carried out. The ground state of ^{212}Po was excited with a peak cross-section of (0.75 ± 0.16) μb/sr (cf. ref. [43]), while an upper limit of ≈ 0.20 μb/sr was set for the cross-sections associated with levels within $(7 \div 8)$ MeV excited in the reaction ^{204}Hg(^{16}O, ^{12}C)^{208}Pb [44]. Further experiments are needed to determine whether the predicted state is present in the spectrum or whether its strength is distributed over several states.

Viewing the α-transfer as a simultaneous transfer of a neutron and a proton pair addition or pair subtraction modes, one expects to observe large α-transfer cross-sections, in the different regions (around closed shell) where the pairing vibrations are strongly excited.

Recent (^{6}Li, d) reactions carried out at Los Alamos in the Ni region seem to indicate that the main predictions of the model are borne out by the experiment [45, 46].

4. – Isospin structure of the pairing modes (*).

An important nuclear symmetry property manifests itself in the conservation of isospin: a nuclear state is characterized by the total isospin quantum number as well as by the total angular momentum, the number of pairs of particles, etc. The existence of the isospin symmetry requires that the Hamiltonian describing the nuclear system should be invariant under rotations in isospace, exception made of the Coulomb term, which is small relatively to the nuclear interaction. The isospin symmetry is violated by a pairing interaction acting only between identical nucleons, as was the case considered in the previous sections. Thus, an invariant pairing force must, in addition to the nn and pp terms, contain pn components.

One may distinguish between an isoscalar ($\tau = 0$) and an isovector ($\tau = 1$)

(*) The content of the present section is largely based on [47].

pairing interaction, according to whether the associated pair addition and pair removal modes carry isospin $\tau = 0$ or $\tau = 1$, respectively.

In previous sections we have been confronted with strong evidence on the existence of pairing correlations acting between identical particles. This evidence, combined with the condition of isospin invariance, requires the existence of an isovector pairing interaction (cf. also 3·6).

In what follows the elementary pairing modes of excitation generated by an isovector pairing force are studied.

4·1. *Exact solutions and their collective interpretation.* – As in the case of the pairing force acting only between identical particles, we first discuss the solutions corresponding to the degenerate case.

The group-theoretical methods which have been used in the case of identical particles may be generalized in order to account for the isospin degree of freedom [48]. The role of the seniority v is now played by two quantum numbers, namely the seniority itself and the reduced isospin t (which is the isospin of the pairs moving in time-reversed states). Within each representation (v, t), the states are labelled by the total number of pairs π, the total isospin T and its z-component T_z. The energy eigenvalues are given by

$$E(v, t; \pi, T) = \tfrac{1}{2}G[\pi^2 + T(T+1)] - \tfrac{1}{2}G[\Omega^2 + \Omega(3-v) - \tfrac{1}{4}v(6-v) + t(t+1)]\,. \tag{4.1}$$

If $v = 0$, there are only even (odd) values of T, if π is even (odd).

As in (1.7), there are two characteristic frequencies which are present in the spectrum: i) the one associated with the rotational motion in both gauge and isospace (note that both rotational bands have the same moment of inertia $\mathscr{I} = \hbar^2/G$), ii) the one which is responsible of the sphtting between states with $\Delta v = 2$ and the same value of π, T, this splitting being of order $G\Omega$.

The three operators $P^\dagger_{\tau_z} = \sum_{m>0} [a^\dagger_m a^\dagger_{\bar{m}}]^{\tau=1}_{\tau_z}$ $(\tau_z = 0, \pm 1)$ add two particles coupled to angular momentum zero, isospin one and isospin projection τ_z. These operators do not connect states with different seniority or reduced isospin. In the case $v = t = 0$, the corresponding reduced matrix elements between members of rotational bands are

$$\langle \pi + 1, T \pm 1 \| P^\dagger \| \pi, T\rangle = [\tfrac{1}{2}(\Omega \pm T + \pi + \tfrac{5}{2} \pm \tfrac{1}{2})(\Omega \mp T - \pi + \tfrac{1}{2} \mp \tfrac{1}{2})(T + \tfrac{1}{2} \pm \tfrac{1}{2})]^{\frac{1}{2}} \approx \approx \tfrac{1}{2}\Omega(2T + 1 \pm 1)^{\frac{1}{2}}\,. \tag{4.2}$$

These matrix elements are enhanced by a factor Ω, as in (1.7*b*), with respect to typical pure two-particle matrix elements.

The solution for the case of two levels separated by an energy D is similar to the one developed in sect. 2 (cf. also [49]). Again, if $x = 2G\Omega/\varepsilon \gg 1$, the spectrum corresponding to the degenerate case is reproduced. For $x \ll 1$, all energies are integer multiples of a single energy $\hbar\omega$, and only matrix elements between states which differ by $\hbar\omega$ are different from zero. Thus, a vibrational spectrum is obtained, where the building blocks are the pair addition and pair removal quanta. They carry transfer quantum number $\alpha = \pm 2$, spin $J = 0$, positive parity, isospin $\tau = 1$ and projection $\tau_z = 1$ or 0.

Similar to the systems discussed above, the present model displays a simple structure in both rotational (*i.e.* rotation in gauge and isospin space) and vibrational limits. Since the available experimental evidence strongly supports the second limit, we discuss only the harmonic model.

4·2. *The harmonic model, level spectrum.* – The basic idea underlying the harmonic model is that the six isospin pairing modes behave as independent phonons, which retain their identity in the presence of other degrees of freedom. Thus, any level of the vibrational band is obtained by superimposing a certain number of phonons. A possible coupling scheme for these states is given by [50]

$$|n_r t_r, n_a t_a; TT_z\rangle = M[[(\Gamma_r^\dagger)^{n_r}]_{t_r}[(\Gamma_a^\dagger)^{n_a}]_{t_a}]_{TT_z}|0\rangle\,, \tag{4.3}$$

here n_r and n_a denote the number of pair removal ($\alpha = -2$) and pair addition ($\alpha = 2$) phonons, respectively, while t_r and t_a are the isospin to which the corresponding phonons are coupled. The quantum numbers T and T_z are the total isospin and its z-projection.

We denote by $\Gamma_a^\dagger(\tau_z) \equiv \Gamma^\dagger(\alpha = 2, \tau = 1, \tau_z)$ the creation operator of a pair addition mode and by $\Gamma_r^\dagger(\tau_z) = \Gamma^\dagger(\alpha = -2, \tau = 1, \tau_z)$ the corresponding operator associated with the pair removal mode. The square brackets represent the vector coupling of the boson operators to the intermediate and total isospin. The state $|0\rangle$ is the vacuum of the pairing quanta.

The counting of the states generated by coupling phonons of the same type is mathematically equivalent to the counting of states in a three-dimensional harmonic oscillator, where n plays the role of the principal quantum number and t that of the angular momentum. Therefore

$$t_r = n_r\,,\ n_r - 2\,,\ \ldots\,,\ 1 \text{ or } 0 \tag{4.4}$$

and similarly for t_a.

In the following, we consider the spectrum with $\pi < 0$, where π is the number of pairs added to the closed shell $A_0 = 56$, and it is defined by the relation

$$\pi = n_a - n_r\,. \tag{4.5}$$

The closed-shell system ^{56}Ni has the same number $\frac{1}{2}A_0 = 28$ of protons

and neutrons and $\pi = 0$. Its ground state, which is the boson vacuum, has $T = 0 = \pi$, and is labelled by $(n_r t_r, n_a t_a; TT_z) = (00, 00; 00)$.

We consider two types of states. The first contains only pair removal modes. The second contains one pair addition mode and several pair removal quanta (*). In the following we discuss the properties of states with $T = T_z$. The corresponding properties associated with states with $T \neq T_z$ are related to those of the $T = T_z$ states in a model-independent way.

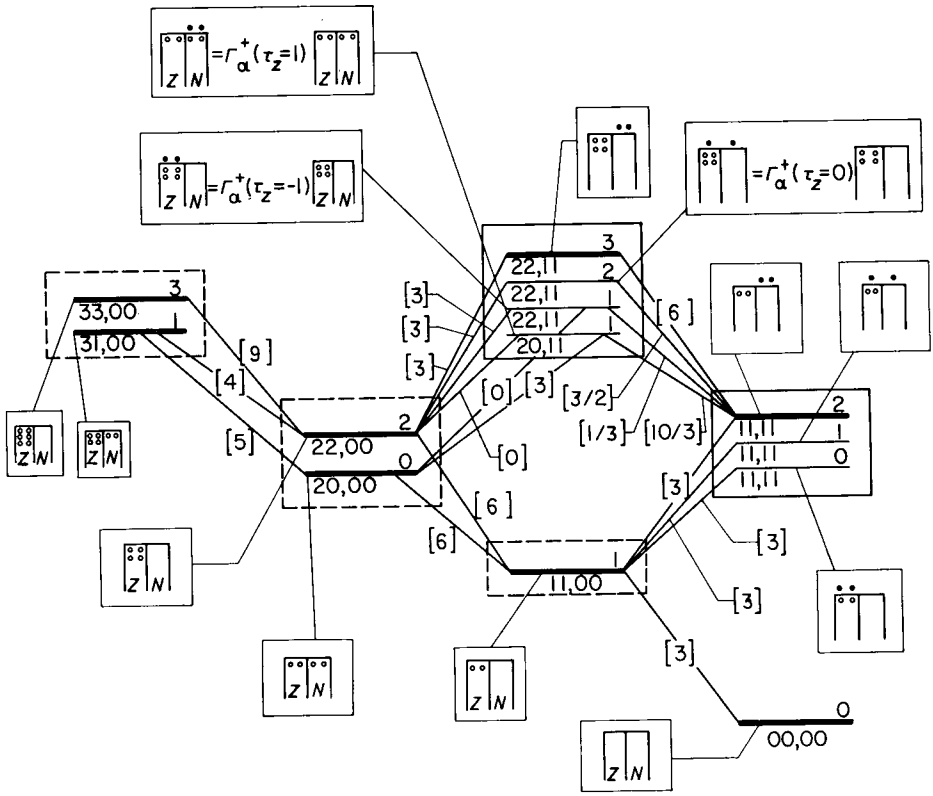

Fig. 14. – Energy levels and reduced two-particle transfer matrix elements corresponding to the harmonic coupling scheme. The quantum numbers $n_r t_r, n_a t_a$ are indicated below each level, while the total isospin is displayed above it. All states up to and including three phonons and with $\pi \leqslant 0$ are shown. Levels which may correspond to the ground state of an even nucleus are represented by a heavy line. Only those reactions which proceed from these states are displayed. The corresponding isospin-reduced intensities are given in square brackets. It has been assumed that the intrinsic strengths associated with addition and removal phonons are equal. The group of states within each frame are degenerate in the harmonic approximation. The main components of the different states have been displayed in a schematic way in which the active particles are shown.

(*) Only few states not belonging to either groups have been identified.

4·2.1. States with only pair removal mode. For any value of $\pi \leqslant 0$, the lowest states have $n_a = t_a = 0$ and thus $\pi = -n_r$, the total isospin of the system being $T = t_r$. Some of these states are displayed in fig. 14 and are framed with dashed lines.

For $T = |\pi|$ all pairs of particles are aligned in isospace so as to yield the maximum possible value of the isospin (*e.g.* $(22, 00; 22)^{52}$Cr). These states are the ground states of isotones with $N = \frac{1}{2}A_0$, *i.e.* they are ground states of single closed-shell nuclei.

States with the same number of pairs π, but with two units of isospin less ($T = |\pi| - 2$) (*e.g.* $(20, 00; 00)^{52}$Fe) are obtained from the state with $T = |\pi|$ by replacing a pair of proton holes by a pair of neutron holes. They are thus labelled by $\big(\pi(|\pi| - 2), 00; (|\pi| - 2)\ (|\pi| - 2)\big)$ and represent the ground states of isotones with (*) $N = \frac{1}{2}A_0 - 2$.

The set of states $(|\pi|T, 00; TT)$ is identical to the $T_z = T$ set of states which would be obtained for a pairing force acting only between identical particles. They satisfy the selection rule $(-1)^{T+\pi} = 1$ which is characteristic of the ground states of even nuclei.

4·2.2. States with one pair addition and several pair removal modes. For a system with $\pi = -n_r$ pairs, the states with one pair addition quantum and several pair removal quanta are of the form $(n_r + 1\ t_r + 1, 11; TT_z)$ and can be obtained by acting with $\Gamma_a^\dagger \Gamma_r^\dagger$ on the states discussed above. They appear at an energy $\hbar(\omega_a + \omega_r)$ above the states $(n_r t_r, 00; t_r t_r)$. Examples of these states are framed by a continuous line in fig. 14.

The states $(n_r + 1\ n_r + 1, 11; n_r + 2\ n_r + 2)$ (*e.g.* $(22, 11; 33)^{54}$Cr) have two units of isospin more than the single-closed-shell nucleus $(n_r n_r, 00; n_r n_r)$ with the same value of π. They are obtained from this last state (*i.e.* from the $(11, 00; 11)^{54}$Fe) by removing two protons from below the closed shell (thus creating the state $(22, 00; 22)^{52}$Cr) and adding two neutrons above the closed shell. They are also ground states of even nuclei (**).

The addition phonon in the states $(n_r + 1\, t_r, 11; TT_z)$ does not satisfy any symmetry relation with respect to the $n_r + 1$ removal phonons. For example, it may couple with the isospin t_r to the total isospin $T = t_r$, leading to the state $(n_r + 1\, t_r, 11; t_r t_r)$ (*e.g.* the state $(22, 11; 22)$ ^{54}Mn). Because $(-)^{n_r} = (-)^{t_r}$ (as required by the identity of the $n_r + 1$ removal quanta (cf. eq. (4.4)), these states do not fulfil the selection rule $(-)^{\pi+T} = 1$. Thus, the collective spectrum of an isovector pairing force is richer than the corresponding spectrum associated with a $|\tau_z| = 1$ pairing interaction.

(*) Note that for these $n_a = 0$ states the difference $|\pi| - T = n_r - t_r$ is equal to the number of neutrons subtracted from the closed-shell system.

(**) These are the only ground states with $\pi < 0$ that contain one pair addition phonon.

The wave function of the state $(n_r + 1\, t_r, 11; t_r t_r)$ can be written as

$$(4.6)\quad |n_r + 1\, t_r, 11; t_r t_r\rangle = (t_r/(t_r+1))^{\frac{1}{2}} \Gamma_a^\dagger(\tau_z = 0)|n_r + 1\, t_r, 00; t_r t_r\rangle - \\ - (1/(t_r+1))^{\frac{1}{2}} \Gamma_a^\dagger(\tau_z = 1)|n_r + 1\, t_r, 00; t_r t_r - 1\rangle ,$$

showing that the added pair has $\tau_z = 0$ most of the time. The state (4.6) is thus mainly obtained by adding a neutron-proton pair to the ground state $(n_r + 1\, t_r, 00; t_r t_r)$ of the even nucleus with $\pi = -(n_r + 1)$. Because the ground state of odd-odd nuclei in general has $J^\pi \neq 0^+$, (4.6) is an excited state of the $|\pi| = n_r$, $T_z = t_r$ system.

The addition phonon may also be coupled with the $n_r + 1$ removal phonons to produce the state $(n_r + 1\, t_r, 11; t_r - 1\, t_r - 1)$. Within the harmonic model, this state is degenerate with $(n_r + 1\, t_r - 2, 11; t_r - 1\, t_r - 1)$ and both have the same quantum numbers π, T, T_z (*e.g.* the $(22, 11; 11)$ and $(20, 11; 11)$ states in ^{54}Fe).

Combining the different stripping and pickup reactions one can locate both states. For instance, the state $(20, 11; 11)$ is not populated in the two-proton stripping on the $((22, 00; 11)\, ^{52}\mathrm{Cr})$ target while the $(22, 11; 11)$ would not be populated by adding a dineutron on the $((20, 00; 00)^{52}\mathrm{Fe})$ state. Since these selection rules are associated with the model quantum number t_r, these reactions provide a test of the coupling scheme (4.3).

The matrix elements of the phonon creation and annihilation operators in the basis set (4.3) are displayed in fig. 15, 16 and 17 (cf. also [47], [51] and [52]).

4·3. *Comparison with experiments.* – The previous discussion suggests that we may view the pairing spectrum around ^{56}Ni as consisting of proton and neutron vibrational bands similarly to what is done in the Pb region. Most of the transitions predicted by the model can be assigned to either type. This conclusion is reinforced by the relative transition probabilities within each band, which essentially follows the ratios discussed in sect. 2, and are little affected by the presence of the other kind of particles.

The comparison with the experimental material displayed in fig. 15, 16 and 17 and tables V and VI has been carried out through the ratios

$$R^i_{\mathrm{exp}} = \mathrm{d}\sigma_{\mathrm{exp}}/\mathrm{d}\sigma_{\mathrm{DWBA}} .$$

The DWBA cross-sections were calculated by utilizing one form factor for all transitions implying addition modes and another for all those implying removal modes. The theoretical values R^i_{th} $(i = \mathrm{a}, \mathrm{r})$ are obtained by multiplying the square of the matrix elements of the phonon creation and annihilation operators by the intrinsic strength parameters N_r, N_a. These parameters are deter-

mined by averaging R^i_{exp}/R^i_{th} over transitions that connect with the head of each vibrational band, since the Pauli-principle corrections are expected to be small in this case. The experimental results are from the compilation of ref. [47] and include the (t, p) results of Aldermaston and Los Alamos, the (h, p) results of Philadelphia, Argonne and Heidelberg and the (h, n) results of Munich, Rochester and Berlin.

4·3.1. The «proton» pairing vibrational bands. In fig. 15 we display the available evidence concerning the proton pairing degree of freedom for $\pi \leqslant 0$. For the proton bands we obtain $N_a \approx N_r \approx 15$. The experimental intensities are indicated in comparison with the model predictions, for proton removal vibrational bands corresponding to the band heads ^{44}Ti, ^{48}Cr, ^{52}Fe and ^{56}Ni.

It is noted that the ground-state intensities do not increase with t_r at the rate predicted by the model. For instance, the sequence of ground-state intensities ^{48}Ca $\rightarrow$ ^{50}Ti $\rightarrow$ ^{52}Cr $\rightarrow$ ^{54}Fe $\rightarrow$ ^{56}Ni is in the ratio 1:1.2:1.4:1 instead of the ratios 4:3:2:1 predicted by the harmonic description. This deviation was to be expected, since the Pauli principle limits the validity of the harmonic description as proton pairs are removed from the (f, p) shell.

Transitions involving proton addition phonons and leading to states with the same isospin as the ground state are also given in fig. 15. Two strong states have been observed in some nuclei. One of these states is the proton pairing vibration, while the other state is viewed as arising from shape deformation degrees of freedom. Intensity arguments and energy considerations may serve to identify the intruder state. We assume that all the excited states having the same isospin as the ground state derive their two-proton transfer strength by admixing with the pairing vibration. Thus the ratio R associated with the excited states is worked out by utilizing the pair addition form factor.

The intensity and energy of the single excited state reported in fig. 15 is equal to the sum of the intensities and the corresponding centroid energy. For example, in the ^{52}Cr(h, n)^{54}Fe ($T = 1$) reaction, the experimental values of R are 16 (gs), 1.0 (4.29 MeV) and 1.7 (6.50 MeV). The state at 4.29 is considered to be an intruder state. The total intensity (*) to the excited state is thus 2.7 ± 1.5 ($\approx [3\,\underline{2}]$) and the intensity-weighted energy 5.68 MeV.

The intensity of the transitions corresponding to addition phonons, in the presence of either one or more removal phonons, is smaller than the value predicted by the harmonic model, but for the ^{54}Fe(^{3}He, n)^{56}Ni reaction. However, the fact that these transitions still have an intensity of the same order of magnitude as the intensity with which the ground state of the same nucleus is

(*) Typical errors of 15% are assigned to (t, p) and (h, p) cross-sections, 30% to (h, n) ground-state transitions and 60% to (h, n) reactions populating excited states. The assignment of these errors is discussed in [47].

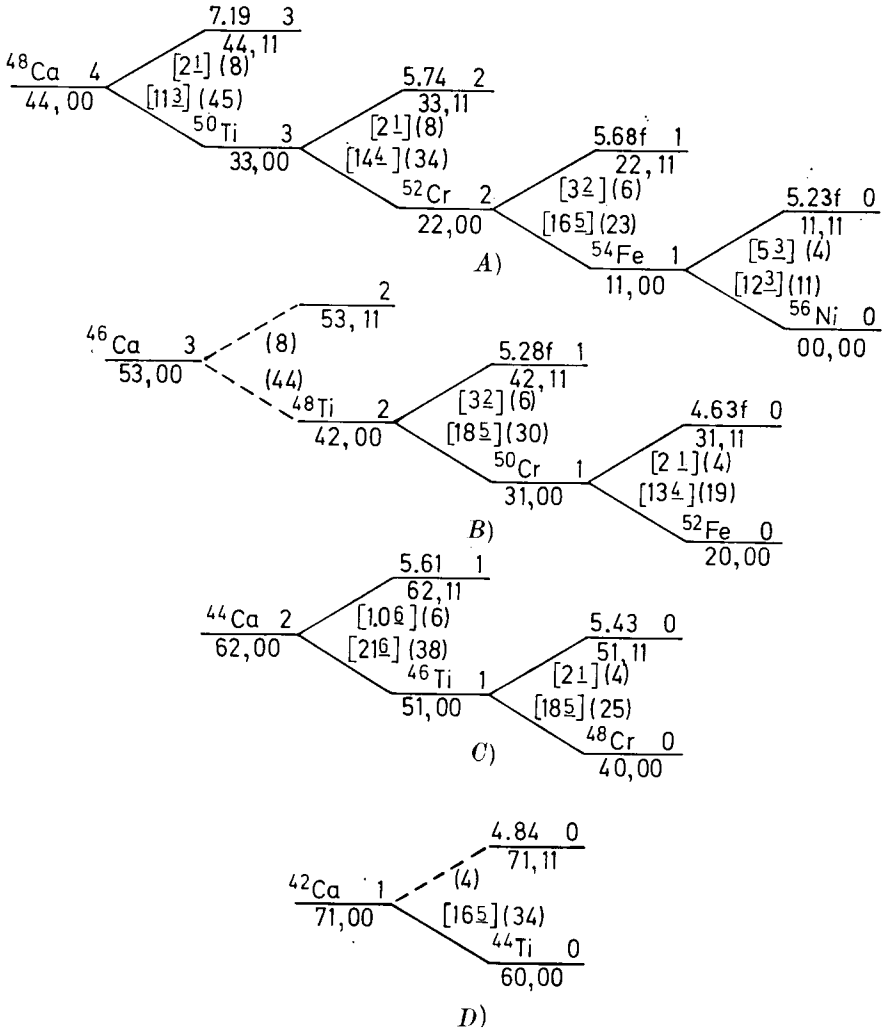

Fig. 15. – The proton vibrational bands for $\pi < 0$. Each state is labelled by the quantum numbers $(n_r t_r, n_a t_a)$ and the total isospin. The nucleus corresponding to these quantum numbers and with $T_z = T$ is also given when they correspond to ground states. For the excited states the energies are also displayed. The numbers in brackets are the experimental values of $\langle R \rangle$ taken from [47] and corresponding errors. The values in parentheses are the theoretical predictions. The label *f* indicates that the associated intensity is fragmented into several states. In these cases the sum of the intensities is shown as well as the centroid energy. For more details cf. [47].

populated gives support to the vibrational picture (*). Model calculations indicate that the different anharmonicities will transfer intensity from the excited state to the ground state, as observed.

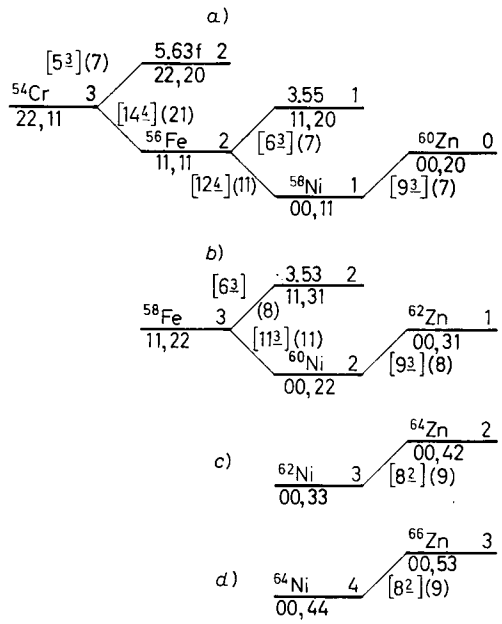

Fig. 16. – The proton vibrational bands for $\pi > 0$. The labelling of the states and the experimental and theoretical predictions are displayed in similar fashion as in fig. 15.

Figure 16 shows the experimental and theoretical intensities for $\pi \geqslant 0$. Four vibrational bands have been identified. The ratio of the cross-sections associated with the reactions ^{54}Cr(h, n)^{56}Fe(gs) and ^{56}Fe(h, n)^{58}Ni(gs) provides the only test of the n_r dependence of the intensities. While the theory predicts a factor of two for the rate of increase, the observed intensities are equal within experimental errors.

The intensities of the transitions involving an addition phonon agree with the model predictions for the seven cases shown in fig. 16. This is true regardless of whether removal phonons are present (*i.e.* ^{54}Cr $\rightarrow$ ^{56}Fe(5.63 MeV), ^{56}Fe $\rightarrow$ ^{58}Ni(3.55 MeV) and ^{58}Fe $\rightarrow$ ^{60}Ni(3.53 MeV)) or not (*i.e.* ^{4}Ni $\rightarrow$ $^{4+2}$Zn(gs)).

(*) The empirical evidence for two-nucleon transfer reactions on systems further away from closed shells is consistent with the ground state being excited two orders of magnitude stronger than any other $J^{\pi} = 0^{+}$ state (cf. fig. 3). This fact is viewed as a manifestation of the superfluid character of these nuclei. In such cases, the collective vibrational description of the pairing motion has to be replaced by a description based on the rotational degree of freedom.

4·3.2. The «neutron» pairing vibrational bands. Figure 17 shows the available evidence concerning the neutron pairing vibrational bands. Since the information obtained from the different two-particle transfer processes is independent of the T_z of the final state, only the (t, p) experimental results are given in this figure. According to the same prescription as for the proton pairing bands, the values $N_a = 32$ and $N_r = 45$ were obtained in the present case.

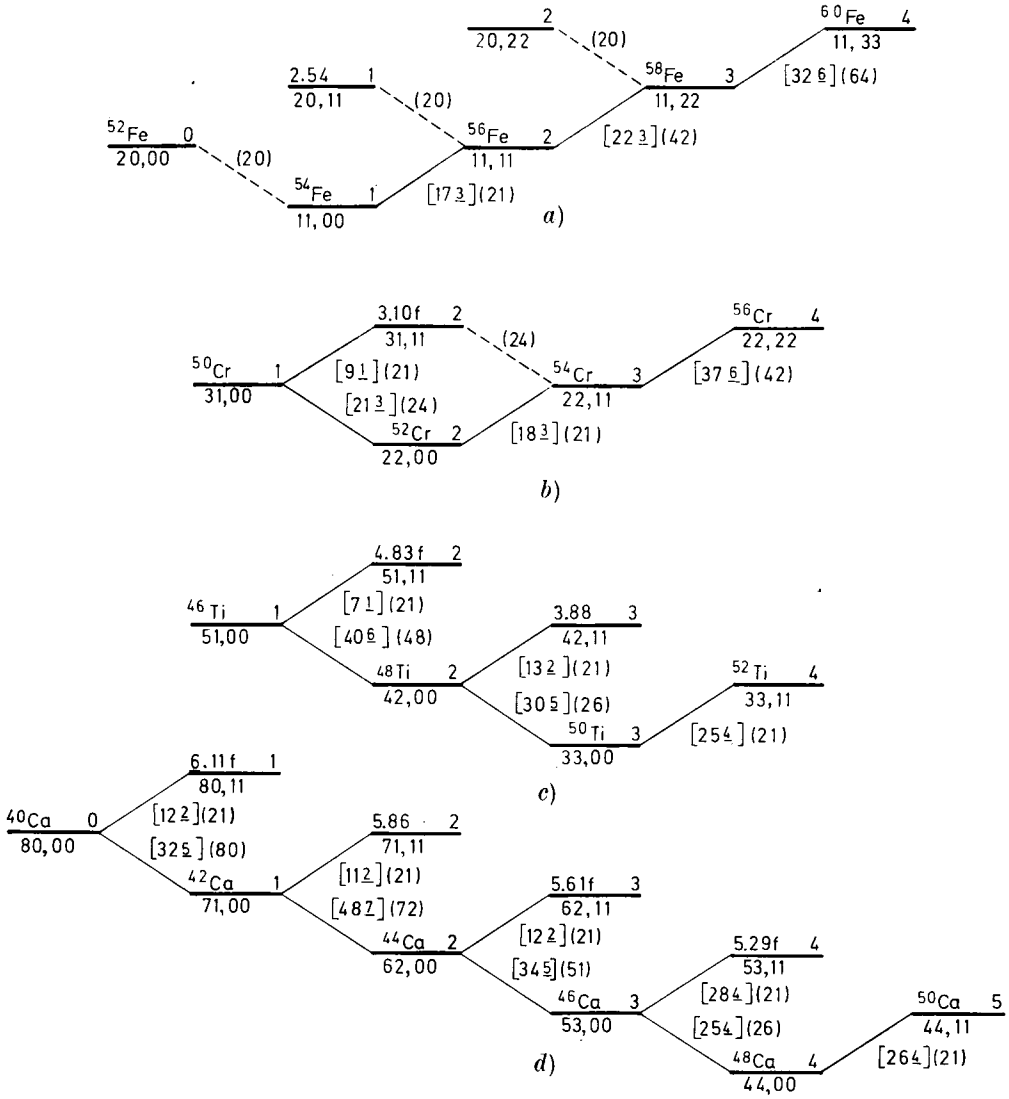

Fig. 17. – The neutron vibrational bands. Only the (t, p) data are shown. For more datails see caption to fig. 15.

The main features observed for the neutron bands are similar to those encountered in the case of proton pairing bands. In particular, the predicted rate of increase in intensity when neutron phonons are added is larger than experimentally observed. For instance, the experimental ground-state intensities associated with the Ca pair removal band (^{A}Ca $\rightarrow$ $^{A+2}$Ca(gs); $A = 40, 42, 44$ and 46) are in the ratio 1.3:1.9:1.4:1.0, while the harmonic ratio is 3.0:2.7:1.9:1.0. For the Fe pair addition band (^{A}Fe $\rightarrow$ $^{A+2}$Fe(gs); $A = 54, 56$ and 58) the experimental ratios are 1:1.3:1.9, while the theoretical ratios are 1:2:3. The Cr pair addition band intensity ratio on the other hand is 1:2, which agrees with the model prediction.

All the intensities associated with transitions implying a change in the number of addition phonons in the presence of one or more removal phonons are smaller than predicted by the model. The only exception to this systematics is provided by the ^{46}Ca $\rightarrow$ ^{48}Ca(4.28 + 5.46 MeV) transition which has, within experimental errors, the same intensity as the ^{48}Ca $\rightarrow$ ^{50}Ca(gs) transition.

4·3.3. Neutron-proton states. Table V contains the analysis of the $\Delta T = 0$ transitions, *i.e.* transitions leading to states with the same isospin as the target isospin. Only (h, p) data were utilized in this analysis.

Unlike the transitions discussed above, the $\Delta T = 0$ transitions are characteristic of the isovector pairing vibrational model. Note, however, that a $\Delta T = 0$ vibrational band cannot be experimentally followed up, since the corresponding members are never ground states. A measure of the adequacy of the model is

TABLE V. – *Intensity of the proton-neutron transitions.* Columns one and two indicate the target and the excitation energy (MeV) of the final nuclear state. They are identified with the vibrational-scheme quantum numbers in columns three and four. In column five we give the (h, p) intensities taken from the compilation of ref. [47]. In column six we show the relative theoretical intensities. The ratio between the theoretical and experimental values are given in column seven.

Transitions	E_x (MeV)	Initial state	Final state	R_{exp}	$R_{th}^{(a)}/N_a$	N_a
^{56}Fe $\rightarrow$ ^{58}Co	1.82	11, 11; 22	11, 22; 22	1.0	0.11	9
^{54}Fe $\rightarrow$ ^{56}Co	1.45	11, 00; 11	11, 11; 11	1.8	0.17	11
^{52}Cr $\rightarrow$ ^{54}Mn	2.12	22, 00; 22	22, 11; 22	2.5	0.22	11
^{50}Cr $\rightarrow$ ^{52}Mn	2.47	31, 00; 11	31, 11; 11	1.4	0.17	8
^{50}Ti $\rightarrow$ ^{52}V	2.40	33, 00; 33	33, 11; 33	0.9	0.25	4
^{48}Ti $\rightarrow$ ^{50}V	3.57	42, 00; 22	42, 11; 22	0.9	0.22	4
^{48}Ca $\rightarrow$ ^{50}Sc	3.09	44, 00; 44	44, 11; 44	1.3	0.27	5
^{54}Cr $\rightarrow$ ^{56}Mn	2.48	22, 11; 33	22, 22; 33	0.4	0.17	2
						$N_a = 7$

provided by the mean square deviation of the values of N_a derived from each transition, which is larger than the experimental uncertainties.

An independent source of information on $\Delta T = 0$ transitions is provided by (h, n) reactions to analogue states. The corresponding information is collected in table VI. The seven N_a values agree, within experimental errors,

TABLE VI. – *Intensity of the* $\Delta T = 0$ (*proton-neutron*) *transitions associated with* (h, n) *reactions populating analogue states.* For more details see caption to table V. Column eight was obtained by utilizing $N_a = 14$.

Transitions	E_x (MeV)	Initial state	Final state	R_{exp}	$\frac{R_{th}^{(a)}}{N_a}$	N_a	Theoretical prediction ($N_a = 14$)
$^{56}Fe \rightarrow {}^{58}Ni$	10.59	11, 11; 22	11, 22; 21	3.5 $\underline{21}$	0.11	32	1.5
$^{54}Fe \rightarrow {}^{56}Ni$	7.94	11, 00; 11	11, 11; 10	5.4 $\underline{32}$	0.33	16	4.6
$^{52}Cr \rightarrow {}^{54}Fe$	10.70	22, 00; 22	22, 11; 21	2.1 $\underline{13}$	0.22	10	3.1
$^{50}Cr \rightarrow {}^{52}Fe$	8.05	31, 00; 11	31, 11; 10	3.0 $\underline{18}$	0.33	9	4.6
$^{50}Ti \rightarrow {}^{52}Cr$	13.52	33, 00; 33	33, 11; 32	1.5 $\underline{12}$	0.17	9	2.4
$^{48}Ti \rightarrow {}^{50}Cr$	11.95	42, 00; 22	42, 11; 21	1.4 $\underline{17}$	0.22	6	3.1
$^{48}Ca \rightarrow {}^{50}Ti$	16.58	44, 00; 44	44, 11; 43	1.7 $\underline{10}$	0.13	13	1.8
						$N_a = 14$	

with the average value of 14. Note, however, the larger magnitude of the experimental uncertainties.

From the above discussion it is concluded that the $L = 0$, $\Delta T = 1$ two-particle transfer data associated with $J^\pi = 0^+$ states in the Ca-Ni region can be systematized through the concept of independent isovector pairing vibrations which behave like phonons. More than sixty members of this many-phonon vibrational band have been identified. This band can be decomposed rather accurately into bands corresponding to pairing vibrational phonons generated by correlations between identical particles. Thus, all the states excited in two-nucleon transfer reactions (excepting those implying $\Delta T = 0$ transitions) and having maximum isospin projection give rise to proton and neutron vibrational bands.

The isovector property of the pairing phonons manifests itself in the $\Delta T = 1$ transitions to the analogue states and in the $\Delta T = 0$ transitions to the $T = T_z$, $J^\pi = 0^+$ states in odd-odd nuclei.

Some systematic deviations from the harmonic-model predictions (anharmonicities) are found in the different bands. Thus, the rate of increase of the two-particle transfer intensity with the number of phonons is slower than predicted. This anharmonicity has its origin in the Pauli principle.

The excited states with the same isospin as the ground state, even if strongly

populated in two-nucleon transfer processes, are weaker than predicted by the harmonic model. The residual pairing interactions tend to produce a condensation of the boson, namely a superconducting state. This tendency drains strength from the excited into the ground state.

II: Field theory of elementary excitations in nuclei.

In the first part of these lectures the concept of elementary modes of excitation was discussed in terms of simple schematic models. The usefulness of such a concept to describe the nuclear structure was demonstrated in the discussion of selected examples involving pairing modes.

Because all the nuclear degrees of freedom are exhausted by the protons and the neutrons, it is an essential feature of descriptions based on elementary modes of excitation to violate the Pauli principle and to require the use of an over-complete basis.

In the second part of these lectures we develop a field theory, in which the nuclear elementary modes of excitation are the fermionic and bosonic free fields, and where their mutual interweaving takes place through the particle-vibration coupling and the bare model four-point vertex interaction.

5. – The concept of elementary modes of excitation.

The Hamiltonian of a many-body system of noninteracting particles, bosons or fermions, can be written as

$$H = \sum_i H_i \,, \tag{5.1}$$

where the summation is over all the particles of the system and where each H_i depends only on the variables of the i-th particle. The single-particle Schrödinger equation is

$$H_i \psi_k(\boldsymbol{r}_i) = \varepsilon_k \psi_k(\boldsymbol{r}_i) \,, \tag{5.2}$$

where ε_k is the single-particle energy eigenvalue and

$$\psi_k(\boldsymbol{r}_i) \equiv \langle \boldsymbol{r}_i | a_k^\dagger | 0 \rangle \tag{5.3}$$

is the corresponding wave function. The operator $a_k^\dagger$ creates a particle in the state k when acting in the vacuum state $|0\rangle$. The energy levels of the system

are then given by the equation

$$E_n = \sum_k n_k \varepsilon_k \,, \tag{5.4}$$

the corresponding eigenstates being

$$|n\rangle = \prod_k \frac{(a_k^\dagger)^{n_k}}{\sqrt{n_k!}} |0\rangle \,, \tag{5.5}$$

where $n_k = 0$ or 1 in the case of fermions and $n_k = 0, 1, 2, \ldots$ in the case of bosons.

Now we consider a system of interacting particles. The Hamiltonian will in this case be

$$H = \sum_i H_i + \tfrac{1}{2} \sum_{i,j} H_{ij} \,, \tag{5.6}$$

where i, j label the co-ordinates of the i-th and j-th particle.

In some cases it is possible to recast the two-body Hamiltonian in the form

$$H = \sum_\tau H'_\tau \,, \tag{5.7}$$

with the associated Schrödinger equation

$$H'_\tau \psi_\tau(\zeta) = \varepsilon_\tau \psi_\tau(\zeta) \,, \tag{5.8}$$

ζ representing a generalized variable (*e.g.* the single-particle co-ordinate, the gap parameter, the shape of the nucleus, etc.). The wave function $\psi_\tau(\zeta)$ is the ζ–co-ordinate representation of the eigenstate $\alpha_\tau^\dagger|\tilde{0}\rangle$. The operator $\alpha_\tau^\dagger$ creates an excitation with quantum number τ when acting in the state $|\tilde{0}\rangle$, the vacuum of all the excitations τ.

The energy of the levels of the system, or at any rate of the most important ones to determine the physical response of it to external probles, can be written in the form

$$E_m = \sum_\tau n_\tau \varepsilon_\tau \,. \tag{5.9}$$

The corresponding eigenstate can be written in the same way as before, *i.e.*

$$|n\rangle = \prod_\tau \frac{(\alpha_\tau^\dagger)^{n_\tau}}{\sqrt{n_\tau!}} |\tilde{0}\rangle \,. \tag{5.10}$$

Additivity features similar to (5.9) hold for other physical quantities, *i.e.*

$$\langle n|\mathcal{O}|m\rangle = \sum_{\tau} A_\tau \sqrt{n_\tau}\,\delta(n_\tau, m_\tau + 1)\,, \tag{5.11}$$

where

$$\mathcal{O} = \sum_{\tau} A_\tau \alpha_\tau^\dagger \tag{5.12}$$

is the operator which specifically excites the eigenstates described by $\psi_\tau(\zeta)$. Because the excitation energies E_m and observables $|\langle m'|\mathcal{O}|m\rangle|^2$ (*e.g.* two-particle transfer cross-section, electromagnetic-transition probabilities, etc.) are linear combinations of ε_τ and A_τ, respectively, the eigenstates with energy ε_τ and associated observable A_τ are called the *elementary excitations of the system.*

There lie thus two ideas behind the concept of elementary excitations (*). First, there is the idea that the total binding energy does not have much to do with the behaviour of the physical system. Thus, the state $|\tilde{0}\rangle$ is assumed to exist but to act only as a background whose detailed intrinsic structure one does not need to know to describe the behaviour of the system. What is important is the behaviour of the lower excited states relative to the ground state.

The second idea is that the low-lying states often are of a particular simple character, and are amenable to a simple and rigorous mathematical treatment.

With the help of experimental probes which couple weakly to the nucleus, *i.e.* in such a way that the system can be expressed in terms of the properties of the excitation in the absence of probes, it has been possible to identify the following elementary excitations in systems around closed shells (**):

a) single particle and holes,

b) shape vibrations,

c) spin and isospin vibrations and charge exchange modes,

d) pairing vibrations.

Different probes have been utilized in the process of identification of the different modes. In particular two-neutron transfer reactions induced by tritons and protons have played a central role in unraveling the basic features of the pairing modes. This subject has been discussed in detail in part I of these lectures.

(*) This concept was first introduced by LANDAU [53] to describe the spectrum of He II. It was subsequently utilized in nuclear physics by BOHR and MOTTELSON [6] to obtain a unified description of the nuclear spectrum.

(**) The restriction to closed nuclei is made to simplify the discussion. The concept of elementary modes of excitation applies equally well to open-shell nuclei (cf. [25]).

6. – Nuclear field theory.

A field theory can be formulated in which the nuclear elementary modes of excitation play the role of the free fields and in which their mutual interweaving takes place through the particle-vibration coupling vertices [6, 54, 55]. This theory provides a graphical perturbative approach to obtain the exact solution of the many-body nuclear-structure problem in the product basis $\psi_\tau(\zeta)\psi_\eta(\Delta)\ldots\psi_\gamma(\Gamma)$.

Note that the nuclear bosonic fields are built out by utilizing those degrees of freedom (particles and holes) which already exhaust all the nuclear degrees of freedom. It is thus an essential feature of the product basis to be overcomplete and to violate the Pauli principle. On the other hand, this basis is directly related to observables of the system. The different experiments project out only one or two of its components.

In what follows we state and apply the nuclear-field-theory rules, to calculate the interactions between the nuclear free fields and the reaction processes between the resulting physical states. This is done for a system with one particle outside closed shells and which displays collective vibrations, in the framework of a two-level model.

6·1. *Schematic model.* – The model considered consists of two single-particle levels, each with degeneracy Ω and with a schematic monopole particle-hole interaction coupling the particles in the two levels.

The total Hamiltonian is equal to

$$H = H_{sp} + H_{TB}\,, \tag{6.1}$$

where

$$H_{sp} = \frac{\varepsilon}{2} N_0\,, \qquad N_0 = \sum_{\sigma=\pm 1, m} \sigma a^\dagger_{m,\sigma} a_{m,\sigma}\,, \tag{6.2}$$

and

$$H_{TB} = -\frac{V}{2}(A^\dagger A + AA^\dagger)\,, \qquad A^\dagger = \sum_m a^\dagger_{m,1} a_{m,-1}\,. \tag{6.3}$$

The index σ labels the two levels, while m labels the degenerate states within each level. The strength of the monopole coupling is denoted by V and the energy difference between the two levels is ε.

The matrix element of (6.3) is given by

$$\langle m, 1; m', -1|H_{TB}|m'', 1; m''', -1\rangle = -V\delta(m, m')\delta(m'', m''')\,. \tag{6.3a}$$

6·2. *Field-theoretical solutions.* – The free nuclear and fermion fields are the elementary modes of excitation comprising surface vibrations and single particles, respectively. The boson fields are defined through the random-phase approximation, in terms of particle-hole excitations. The basis utilized to describe the nuclear systems is a product of the different free fields. This basis is, as a rule, over-complete, nonorthogonal and violates the Pauli principle.

The closed-shell system of the schematic model under consideration corresponds to the lowest ($\sigma = -1$) level filled with Ω particles, while the upper ($\sigma = 1$) level remains empty. The basis particle and hole states are obtained by adding or removing a single particle from this closed-shell configuration. The corresponding wave functions and energies, which should include the Hartree-Fock corrections generated by the residual interaction (*), are

$$\begin{cases} |m, 1\rangle = a^{\dagger}_{m,1}|0\rangle\,, & E(m, 1) = \tfrac{1}{2}(\varepsilon + V)\,, \\ |m, -1\rangle = a_{m,-1}|0\rangle\,, & E(m, -1) = \tfrac{1}{2}(\varepsilon + V)\,. \end{cases} \tag{6.4}$$

Thus the unperturbed energy for producing a particle-hole excitation with respect to the ground state is

$$\varepsilon' = E(m, 1) + E(m, -1) = \varepsilon + V\,. \tag{6.5}$$

The contribution V in (6.5) is the Hartree-Fock contribution to the particle-hole excitation.

If we define the creation operator of the normal modes as

$$\beta^{\dagger}_{\nu} = \sum_{m} \lambda^{\nu}_{m} a^{\dagger}_{m,1} a_{m,-1}\,, \tag{6.6}$$

the linearization equation

$$[H, \beta^{\dagger}_{\nu}] = \omega_{\nu}\beta^{\dagger}_{\nu} \tag{6.7}$$

yields

$$\begin{cases} \omega_1 = \varepsilon' - V\Omega\,, \\ \omega_{\nu} = \varepsilon' & (\nu = 2, 3, \ldots, \Omega)\,. \end{cases} \tag{6.8}$$

Utilizing (6.7) and the normalization condition

$$[\beta_{\nu}, \beta^{\dagger}_{\nu'}] = \delta(\nu, \nu')\,, \tag{6.9}$$

(*) The Hartree-Fock energy associated with the Hamiltonian (6.1) can be obtained from the linearization relation $[H, a^{\dagger}_{\sigma,m}] = E(m, \sigma)a^{\dagger}_{\sigma,m}$ acting on the Hartree-Fock vacuum, which in this case coincides with the single-particle vacuum defined by $a^{\dagger}_{m,-1}|0\rangle = a_{m,1}|0\rangle = 0$.

we obtain for the amplitudes λ_m^1 associated with the lowest mode

$$\lambda_m^1 = \frac{1}{\sqrt{\Omega}} . \tag{6.10}$$

One can also write this amplitude as the ratio between a coupling matrix element and an energy denominator, *i.e.*

$$\lambda_m^1 = \frac{\Lambda_1}{\omega_1 - \varepsilon'} . \tag{6.11}$$

From (6.8), (6.10) and (6.11) we obtain

$$\Lambda_1 = - V\sqrt{\Omega} , \tag{6.12}$$

which is the strength with which a particle-hole excitation $(m, 1; m, -1)$ couples to the collective phonon (see fig. 18). This can also be seen by calculating the matrix element of the interaction Hamiltonian (6.3) between the normal modes and the single particle-hole state

$$\Lambda_\nu = \langle n_\nu = 1 | H_{\text{TB}} | m, 1; m', -1 \rangle = - V\sqrt{\Omega}\,\delta(m, m')\delta(\nu, 1) . \tag{6.13}$$

Note that the particle-vibration coupling strengths associated with the other normal modes lying at an energy ε' are equal to zero.

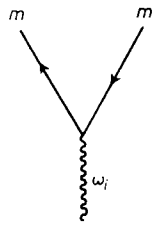

Fig. 18. – Graphical representation of the amplitude of the collective phonon (wavy line) on a given particle-hole excitation $((m, 1), (m, -1))$. This amplitude can be written in terms of the interaction vertex denoted by Λ_i, and the energy denominator $\omega_i - \varepsilon'$. The particles and holes are depicted by arrowed lines.

As shown in ref. [54-55], the exact solution of (6.1) is reproduced by utilizing as the basic degrees of freedom both the vibrations (cf. (6.8)) and the particles (cf. (6.4)) coupled through the interactions (6.3*a*) and (6.13). A significant part of the original interaction has already been included in generating the collective mode (6.8). This implies that the rules for evaluating the effect of the couplings (6.3*a*) and (6.13) between fermions and bosons involve a number

of restrictions as compared with the usual rules of perturbation theory that are to be utilized in evaluating the effect of the original interaction (6.3) acting in a fermion space. They read as follows:

I) In initial and final states, proper diagrams involve collective modes and particle modes, but not any particle configuration that can be replaced by a combination of collective modes. This restriction permits an initial state comprising the configuration $(n_i = 1; m, 1)$, but excludes $(m, 1; m, -1; m', 1)$.

II) The couplings (6.3*a*) and (6.13) are allowed to act in all orders to generate the different diagrams of perturbation theory; the restriction I) does not apply to internal lines of these diagrams.

III) The internal lines of diagrams are, however, restricted by the exclusion of diagrams in which a particle-hole pair is created and subsequently annihilated without having participated in subsequent interactions.

IV) The energies of the uncoupled particle and phonon fields are to be calculated by utilizing the Hartree-Fock approximation (cf. eq. (6.4)) and the RPA (cf. eq. (6.8)), respectively. The contributions of all allowed diagrams are evaluated by the usual rules of perturbation theory.

We note that the external fields acting on the system are allowed to create any state which may generate the different diagrams of perturbation theory. The corresponding matrix elements should be weighted with the amplitude of the component through which the final state is excited.

The above rules are also valid for those situations which cannot be treated in perturbation theory and where a full diagonalization is called for. Thus, *e.g.*, when the system displays a spurious state (cf. sect. 7).

In what follows we discuss the energy of the 2p-1h–like excitations. We distinguish between two types of states, namely

$$(6.14)\qquad |n_i = 1; m, 1\rangle\,, \qquad \begin{cases} \omega_1 = \varepsilon' - V\Omega\,, & \Lambda_1 = -\sqrt{\Omega}\,V \\ & (i = 1;\ m = 1, 2, \ldots, \Omega)\,, \\ \omega_i = \varepsilon'\,, & \Lambda_i = 0 \\ & (i = 2, \ldots, \Omega;\ m = 1, 2, \ldots, \Omega)\,, \end{cases}$$

and (*)

$$(6.15)\qquad |m, 1; m, -1; m', 1\rangle\,, \qquad \varepsilon' \qquad (m, m' = 1, 2, \ldots, \Omega)\,.$$

(*) Since the states (6.15) are restricted to be intermediate states of the perturbation expansion, the configuration $(m, 1; m, -1; m, 1)$ is allowed.

The physical states are to be written as

$$|qm\rangle = \sum_i \xi_{iqm} |n_i = 1;\, m, 1\rangle \,, \tag{6.16}$$

as (6.15) cannot be basis states according to rule I), but only intermediate states. The quantities ξ_{iqm} are the amphtudes of the physical state in the different components of the product basis of elementary excitations.

The model space contains Ω^2 states, while the correct number is $\Omega - 1$. Thus the basis $|n_i = 1;\, m, 1\rangle$ contains Ω spurious states. Its origin can be traced back to the violation of the Pauli principle (cf. also sect. 7).

To obtain the energy of $|qm\rangle$ we have to allow the states $|n_1 = 1;\, m, 1\rangle$ to interact through the vertices (6.3*a*) and (6.13) and generate all the different perturbation theory diagrams (cf. rule II)) except those containing bubbles (cf. rule III)).

The different graphical contributions calculated in the framework of the Brillouin-Wigner perturbation theory are displayed in fig. 19. There is only

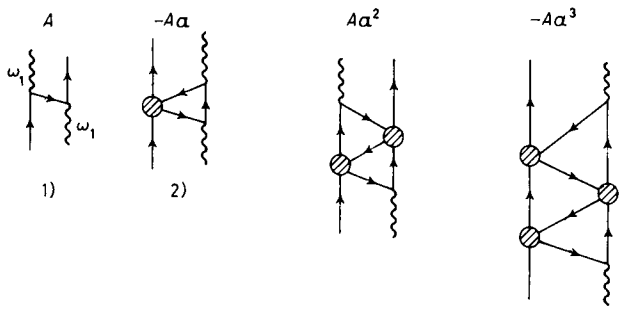

Fig. 19. – Contributions to the interaction of a fermion and a collective boson ω_i to order $1/\Omega^4$. The secular equation $E - E^{(0)} = A \sum_n a^n (-1)^n$ is given in terms of the quantities $A = 4\Omega V^2/(3\varepsilon' - 2E)$ and $a = 2V/(3\varepsilon' - 2E)$.

one (diagonal) matrix element given by a single summation, which can be carried to all orders in the interaction vertices, and can be written as

$$X_{ii'} = A \sum_n (-1)^n a^n \delta(i, i') = \tag{6.17}$$

$$= \frac{A}{1 + a} \delta(i, i') \delta(n, 1) = - K(E) (\sqrt{\Omega}\, V)^2 \delta(i, i') \delta(i, 1) \,,$$

where a and A are defined in the caption to the figure and

$$K(E) = (\tfrac{3}{2}\varepsilon' - E + V)^{-1} \tag{6.18}$$

is the effective coupling strength. The associated secular equation

$$|(\omega_i - E)\delta(i, i') + X_{ii'}| = 0 \tag{6.19}$$

is equivalent to the dispersion relation

$$\frac{1}{K(E)} = \sum_i \frac{(\sqrt{\Omega}\, V)^2}{\omega_i - E}\, \delta(i, 1)\,. \tag{6.20}$$

Thus the energies of the system are determined by the equation

$$E = \omega_1 + \frac{\Omega V^2}{\frac{3}{2}\varepsilon' - E + V}\,. \tag{6.21}$$

It admits the two solutions

$$E_{qm} = \begin{cases} \frac{3}{2}\varepsilon'\,, \\ \frac{1}{2}\varepsilon' + \omega_1 + V = \frac{3}{2}\varepsilon' - \Omega V + V\,, \end{cases} \tag{6.22}$$

and agree with the exact value (*).

Because $\Lambda_i = 0$ for $i \neq 1$, there is no summation in (6.16) and

$$|qm\rangle = N_{qm}|n_1 = 1;\, m, 1\rangle\,,$$

where

$$1 = N_{qm}^2\left(1 - \frac{\partial X_{11}}{\partial E}\right) = N_{qm}^2\left(1 - \frac{\Omega V^2}{(\frac{3}{2}\varepsilon' - E + V)^2}\right). \tag{6.23}$$

For $E_{qm} = \frac{1}{2}\varepsilon' + \omega_1 + V$ we obtain

$$N_{qm}^2 = \frac{\Omega}{\Omega - 1}\,, \tag{6.24}$$

while for $E_{qm} = \frac{3}{2}\varepsilon'$ the state is nonnormalizable as the quantity in parentheses in (6.23) is either negative ($\Omega > 1$) or zero ($\Omega = 1$).

The state defined by

$$|q, m\rangle = \sqrt{\frac{\Omega}{\Omega - 1}}\, |n_1 = 1;\, m, 1\rangle \tag{6.25a}$$

and

$$E_{qm} = \tfrac{1}{2}\varepsilon' + \omega_1 + V = \tfrac{3}{2}\varepsilon' - V(\Omega - 1) \tag{6.25b}$$

(*) The exact solutions can be easily obtained by noting that the operators $A^\dagger$, A and $\frac{1}{2}N_0$ are generators of the SU_2 group.

exhausts the inelastic sum rule in agreement with the exact results. Note that (6.25*a*) is specifically excited in inelastic processes, as can be seen by direct inspection.

The external inelastic field can act in two ways, exciting either a particle-hole pair or a phonon, with amplitudes

$$\langle m, 1; m', -1|A_1^\dagger|0\rangle = \delta(m, m') \tag{6.26}$$

and

$$\langle n_i = 1|A_1^\dagger|0\rangle = \sqrt{\Omega}\,\delta(i, 1)\,, \tag{6.27}$$

respectively. The different graphical contributions to the inelastic-scattering process are displayed in fig. 20, and can again be summed to all orders in the interaction vertices giving

$$\langle n_1 = 1;\, m, 1|A_1^\dagger|m, 1\rangle = \sqrt{\Omega} + \frac{A_1}{\frac{3}{2}\varepsilon' - E_{qm} + V}\,. \tag{6.28}$$

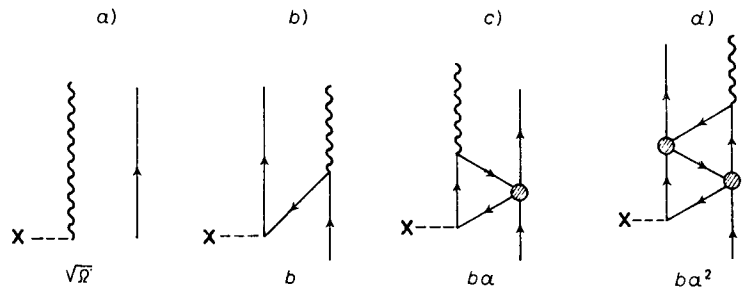

Fig. 20. – Graphical representation of the different terms contributing to the matrix element of the transfer operator $\sqrt{\Omega}A^\dagger$ up to order $1/\Omega^3$. Note that the different contributions *b*), *c*), etc. have a one-to-one correspondence with the different contributions to E (cf. fig. 19). $a = -2V/(3\varepsilon' - 2E)$, $b = 2A_1/(3\varepsilon' - 2E)$.

For $E_{qm} = \frac{3}{2}\varepsilon'$ this quantity is equal to zero. Thus, the corresponding states do not carry any inelastic strength, a feature which is closely related to the fact that they cannot be normalized and that they do not display any correlation energy (*).

(*) Note that, even if $N(E_{qm} = \varepsilon_m) \to \infty$, the matrix elements associated with the different transitions tend to zero more rapidly and the final result converges and is equal to zero as expected.

On the other hand, the matrix element associated with (6.25*a*) is

$$\langle qm|A^{\dagger}|m,1\rangle = \sqrt{\frac{\Omega}{\Omega-1}}\,\frac{\Omega-1}{\sqrt{\Omega}} = \sqrt{\Omega-1}\,, \tag{6.29}$$

which agrees with the exact answer.

The results (6.25*b*) and (6.29) can be traced down to Pauli-principle corrections. In fact, the state $|n_i = 1;\ m,1\rangle$ has a nonvanishing matrix element, implying a single particle-vibration coupling vertex, with the state $|m,1;\ m,-1;\ m,1\rangle$. This component, which is spurious, is removed by the different graphs displayed in fig. 19 and 20. The presence of the odd particle $(m,1)$ blocks the particle-hole excitation $(m,1;\ m,-1)$ which was present in the uncoupled system. Thus the system increases its energy by a quantity V. The reduction of the inelastic amplitude from $\sqrt{\Omega}$ to $\sqrt{\Omega-1}$ also indicates that there is one less particle-hole excitation responding to the external probe.

7. – Spurious states.

While the model space product of elementary modes of excitation discussed in the last section contains Ω^2 states, only $\Omega(\Omega-1)$ are physically possible, the number of spurious states being Ω. On the other hand, the agreement between the exact and the nuclear-field-theoretical results shows that the effects of those spurious states are eliminated from all the matrix elements associated with physical observables.

In what follows we show that, in fact, the spurious states are isolated in an explicit way in the nuclear field theory [55]. Their energy coincides with the initial unperturbed energy, while all physical operators have zero off-diagonal matrix elements between any physical state and a spurious state, in particular the unit operator, which measures the overlap of the two types of states.

For this purpose we use again a schematic model consisting in a number, Ω, of single-particle levels in which particles interact by means of a « monopole » force

$$H = H_{\rm sp} + H_{\rm int}\,, \tag{7.1}$$

where

$$H_{\rm sp} = \tfrac{1}{2}\sum_{m=1}^{\Omega}\varepsilon_m(a^{\dagger}_{m,1}a_{m,1} - a^{\dagger}_{m,-1}a_{m,-1}) \tag{7.2}$$

and

$$H_{\rm int} = -\,VA^{\dagger}A \tag{7.3}$$

with

$$A^{\dagger} = \sum_{m=1}^{\Omega} a^{\dagger}_{m,1} a_{m,-1} \,. \tag{7.4}$$

The energy of the i-th phonon is determined by the RPA dispersion relation (cf. rule IV))

$$\sum_{m=1}^{\Omega} \frac{1}{\varepsilon_m - \omega_i} = \frac{1}{V} \qquad (i = 1, 2, \ldots, \Omega) \,. \tag{7.5}$$

The eigenfunction corresponding to the different modes is

$$|n_i = 1\rangle = \sum_m \frac{\Lambda_i}{\varepsilon_m - \omega_i} a^{\dagger}_{m,1} a_{m,-1} |0\rangle \,. \tag{7.6}$$

The particle-vibration coupling constant is given by

$$\Lambda_i = -\langle n_i = 1 | H_{\text{int}} | m, 1; m', -1\rangle = \left[\sum_m \frac{1}{(\varepsilon_m - \omega_i)^2}\right]^{-\frac{1}{2}} \delta(n, n') \,, \tag{7.7}$$

where $|n_i = 1\rangle$ denotes a state containing one phonon, while $|m, 1; m, -1\rangle$ is the eigenstate associated with particle-hole excitation.

The other interaction to be included (rule II)) is the four-point vertex which has the value

$$\langle m, 1; m', -1 | H_{\text{int}} | m'', 1; m''', -1\rangle = -V\delta(m, m')\delta(m'', m''') \,. \tag{7.8}$$

The single-particle energies to be used in calculating the different graphs are $\frac{1}{2}\varepsilon_m$, as the Hartree-Fock contribution (cf. rule IV)) of H_{int} is zero.

Similarly to H_{int}, the « inelastic operator » has two different matrix elements, namely

$$\langle n_i = 1 | a^{\dagger}_{m',1} a_{m',-1} | 0\rangle = \frac{\Lambda_i}{\varepsilon_{m'} - \omega_i} \tag{7.9}$$

and

$$\langle m', 1; m'', -1 | a^{\dagger}_{m,1} a_{m,-1} | 0\rangle = \delta(m, m')\delta(m', m'') \,. \tag{7.10}$$

In what follows we discuss again the system comprising an odd particle, in the orbit $(m, 1)$, in addition to a single phonon excitation of the vacuum.

According to rule I) initial and final states may involve both collective mode and particle modes, but not any particle configuration that can be replaced by a combination of collective modes. The exclusion of the states $|m, 1; m', 1; m', -1\rangle$ eliminates most of the double counting of two-particle, one-hole states. The Ω « proper » states of the form $|n_i = 1; m, 1\rangle$ are allowed. However,

there are only $\Omega - 1$ (two-particle, one-hole) states in which the odd particle is in the state $(m, 1)$. Therefore, a spurious state remains in the spectrum of the elementary modes of excitation.

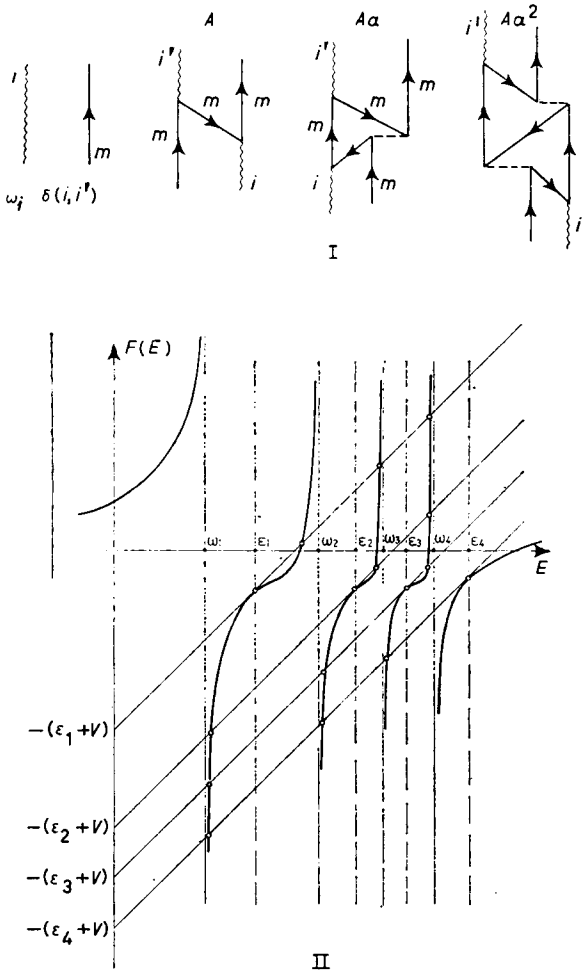

Fig. 21. – I) Lower-order contributions to the energy matrix element between the basis states $|n_i = 1; m, 1\rangle$. The dashed line stands for the model bare interaction (cf. eq. (7.8)). The quantity $X_{ii'}(E) = A \sum_n a^n = -\Lambda_i \Lambda_{i'}/(E - \varepsilon_m - V)$, where $A = -\Lambda_i \Lambda_{i'}/(E - \varepsilon_m)$ and $a = V/(E - \varepsilon_m)$, is the matrix element iterated to all orders in $1/\Omega$. The secular equation of the problem is $|(\omega_i - E)\delta(i, i') + X_{ii'}| = 0$, and is equivalent to the dispersion relation (7.15). II) Graphical solution of the dispersion relation (7.15), for the case $\Omega = 4$. The function $F(E) = \sum_i \Lambda_i^2/(\omega_i - E)$ is displayed as a continuous thick line, while the parallel lines $E - \varepsilon_m - V$ have been drawn as thin continuous lines intersecting the ordinate axis at $-(\varepsilon_m + V)$. The intersections between the two functions give the eigenvalues of the secular equation. For each value of ε_m there are $\Omega + 1$ roots, the root at $E = \varepsilon_m$ being double.

If we displace the zero-point energy of the odd system to $\frac{1}{2}\varepsilon_m$, the unperturbed energy of the basis state $|n_i = 1; m, 1\rangle$ is ω_i.

The lower-order corrections to this energy which do not contain bubbles are drawn in fig. 21. Iterating these processes to infinite order we obtain the secular equation

$$|(\omega_i - E)\delta(i, i') + X_{ii'}(E)| = 0\,, \tag{7.11}$$

where

$$X_{ii'} = -\frac{\Lambda_i \Lambda_{i'}}{E - \varepsilon_m - V}\,. \tag{7.12}$$

The different contributions calculated in the framework of the Brillouin-Wigner perturbation theory are energy dependent, and take into account renormalization effects of the states not explicitly included in the calculations.

If we utilize the following correspondence

$$\sqrt{j + \tfrac{1}{2}} \leftrightarrow \Lambda_i \tag{7.13}$$

and

$$G \leftrightarrow (E - \varepsilon_m - V)^{-1}\,, \tag{7.14}$$

the result (1.3) can be directly utilized. Thus

$$E - \varepsilon_m - V = \sum_{i=1}^{\Omega} \frac{\Lambda_i^2}{\omega_i - E} = F(E) \tag{7.15}$$

is the dispersion relation fixing the energies E_{qm} of the physical states. There is one equation for each single-particle level because the monopole force cannot change the m-state of the odd particle. The relation (7.15) can be solved graphically as shown in fig. 21 II. The energy $E = \varepsilon_m$ is always a root of (7.15), in fact a double root since

$$\left[\frac{\mathrm{d}F(E)}{\mathrm{d}E}\right]_{E=\varepsilon_m} = \sum_i \frac{\Lambda_i^2}{(\omega_i - \varepsilon_m)^2} = 1 \tag{7.16}$$

and the line $E - \varepsilon_m - V$ is at 45°. The remaining intersections of this line and the function $F(E)$ give rise to $\Omega - 1$ additional roots denoted by (qm), whose energy E_{qm} agrees with the physical eigenvalues obtained from the exact solution of the model.

The eigenvectors associated with the physical states (qm) are

$$|qm\rangle_F = \sum_i \xi_{iqm} |i; m, 1\rangle\,, \tag{7.17}$$

where

$$\xi_{iqm} = -N_{qm}\frac{\Lambda_i}{\omega_i - E_{qm}} = \langle i;\, m, 1|qm\rangle_F\,. \tag{7.18}$$

The normalization condition which determines N_{qm} is (cf. [56])

$$\begin{aligned} {}_F\langle qm|qm\rangle_F = 1 = \sum_{i,i'}\left(\delta(i,i') - \frac{\partial X_{ii'}}{\partial E}\right)\xi^*_{iqm}\xi_{i'qm} = \\ = N^2_{qm}\left[\sum_i \frac{\Lambda_i^2}{(\omega_i - E_{qm})^2} - \frac{1}{(E_{qm} - \varepsilon_m - V)^2}\sum_{i,i'}\frac{\Lambda_i^2\Lambda_{i'}^2}{(\omega_i - E_{qm})(\omega_{i'} - E_{qm})}\right] = \\ = N^2_{qm}\left[\sum_i \frac{\Lambda_i^2}{(\omega_i - E_{qm})^2} - 1\right], \end{aligned} \tag{7.19}$$

where the dispersion relation (7.15) has been utilized, and where $X_{ii'}$ is the matrix element appearing in (7.11). For $E_{qm} = \varepsilon_m$ the factor multiplying N^2_{qm} is zero (cf. eq. (7.16)). Thus, there are only $\Omega - 1$ states which can be normalized when solving the Hamiltonian (7.1) in the framework of the nuclear field theory. The full spuriosity of the elementary-mode product basis is concentrated in a single state (*).

The subscript F has been utilized in (7.17) to indicate that we are deahng with the nuclear-field solution of the Hamiltonian (7.1). Note that these eigenvectors are expressed in terms of only the allowed initial or final states (cf. rule I))

$$|i;\, m, 1\rangle \equiv a^\dagger_{m,1}|i\rangle\,, \tag{7.20}$$

which are assumed to form an orthonormal basis, in particular in deriving the relation (7.19). This is equivalent to the basic assumption of the nuclear field theory of the independence of the different modes of excitation, *i.e.*, in the present case,

$$[\Gamma_i, a^\dagger_{m,1}] = 0\,. \tag{7.21}$$

Rules I)-IV) discussed in the last section give the proper mathematical framework to this ansatz, which has played a basic role in developing a unified theory of nuclear structure (cf. [6]).

The above discussion can be illuminated by utilizing a conventional treatment of the residual interaction (cf. also [62]). Expanding the states $|n_i = 1;$

(*) Note that the mathematical relation $N^2 f(E) = 1$, N^2 being the norm of the state with energy E, implies that such state is spurious if $f(E) = 0$ or $f(E) < 0$ (cf. eq. (6.23) and subsequent discussion).

$m, 1\rangle$ in terms of particle and hole state, we can write, with the help of (7.6),

$$a^{\dagger}_{m,1}|n_i = 1\rangle = a^{\dagger}_{m,1} \sum_{m' \neq m} \frac{\Lambda_i}{\varepsilon_{m'} - \omega_i} a^{\dagger}_{m',1} a_{m',-1}|0\rangle \,. \tag{7.22}$$

The overlap between the states $|n_i = 1;\, m, 1\rangle$ is thus given by

$$\begin{aligned} Z(i, i') = \langle i'|a_{m,1} a^{\dagger}_{m,1}|i\rangle = \\ = \sum_{m' \neq m} \frac{\Lambda_i \Lambda_{i'}}{(\varepsilon_{m'} - \omega_i)(\varepsilon_{m'} - \omega_{i'})} = \delta(i, i') - \frac{\Lambda_i \Lambda_{i'}}{(\varepsilon_m - \omega_i)(\varepsilon_m - \omega_{i'})} \,, \end{aligned} \tag{7.23}$$

where the orthogonality relation

$$\sum_{m'} \frac{\Lambda_i \Lambda_{i'}}{(\varepsilon_{m'} - \omega_i)(\varepsilon_{m'} - \omega_{i'})} = \delta(i, i') \tag{7.24}$$

of the RPA solutions in the even system has been utilized. Because of the nonorthogonality of the basis, the eigenvalues of the system are determined by the relation

$$|Z(E)(H - E)| = 0 \,. \tag{7.25}$$

This is fulfilled for

$$|H - E| = 0 \,,$$

which yields the $\Omega - 1$ physical roots, as well as for

$$|Z(E)| = 0 \,. \tag{7.26}$$

This solution corresponds to the spurious root $E_{qm} = \varepsilon_m$. In fact,

$$\begin{aligned} \lim_{\delta \to 0} \sum_i \xi_{iqm}(E_{qm} = \varepsilon_m + \delta) Z_{ii'} = \lim_{\delta \to 0} N_{qm}(E_{qm} = \varepsilon_m + \delta) \cdot \\ \cdot \sum_i \frac{\Lambda_i}{\omega_i - (\varepsilon_m + \delta)} \sum_{m \neq m'} \frac{\Lambda_i \Lambda_{i'}}{(\varepsilon_{m'} - \omega_i)(\varepsilon_{m'} - \omega_{i'})} = 0 \,, \end{aligned} \tag{7.27}$$

since

$$\sum_i \frac{\Lambda_i^2}{(\omega_i - \varepsilon_m)(\omega_i - \varepsilon_{m'})} = \delta(m, m') \,. \tag{7.28}$$

Note that this solution in terms of the overlap Z gives the exact answer in the present case, because of the simphcity of the model. In a general case which includes ground-state correlations this may not be true any longer.

We now calculate the one-particle stripping process leading to the odd system. This calculation illustrates the explicit concentration of the whole spuriosity into a single state which has zero correlation energy (*) and zero amplitude for the different physical processes exciting the $\Omega - 1$ physical states.

One has first to calculate the amplitude for the transition to a basis component $(n_i = 1;\ m, 1)$ including only those graphs in which all intermediate states are excluded from appearing as initial or final states. This exclusion reflects the fact that the diagonalization procedure has included all interaction effects that link these allowed states. The final amplitude for the transition to the state (qm) is obtained by summing the amplitudes to $(n_i = 1;\ m, 1)$ each weighted by the amplitude ξ_{iqm} given by eq. (7.18).

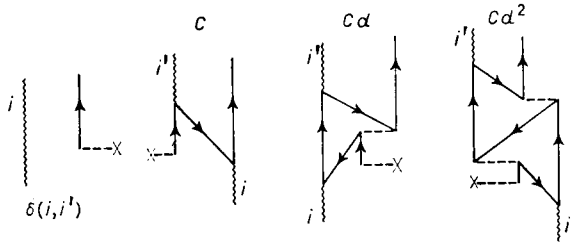

Fig. 22. – Lower-order contributions to the one-particle transfer reaction induced by $a^{\dagger}_{m,1}$. The result of iterating the different contributions to all orders in $1/\Omega$ is equal to $T_{qm}(ii') = C\sum_n d^n = -\Lambda_i\Lambda_{i'}/(\omega_i - \varepsilon_m)(E_{qm} - \varepsilon_m - V)$, $C = -\Lambda_i\Lambda_{i'}/(\omega_i - \varepsilon_m)(E_{qm} - \varepsilon_m)$, $d = V/(E_{qm} - \varepsilon_m)$.

The lower-order contributions to the one-particle transfer amplitude between the state $|n_i = 1\rangle$ and the state $|qm\rangle$ are displayed in fig. 22. They can be summed up to all orders of $1/\Omega$, the result being equal to

$$
\begin{aligned}
(7.29)\qquad \langle qm|a^{\dagger}_{m,1}|n_i = 1\rangle &= \\
&= \sum_{i'} \xi_{i'qm}\left\{\delta(i, i') - \frac{\Lambda_i\Lambda_{i'}}{(\omega_i - \varepsilon_m)(E_{qm} - \varepsilon_m)}\left[\frac{1}{1 - V/(E_{qm} - \varepsilon_m)}\right]\right\} = \\
&= \sum_{i'} \xi_{i'qm}\{\delta(i, i') - T_{qm}(i, i')\} = \\
&= -N_{qm}\left[\frac{\Lambda_i}{\omega_i - E_{qm}} - \frac{\Lambda_i}{(\omega_i - \varepsilon_m)(E_{qm} - \varepsilon_m - V)}\sum_{i'}\frac{\Lambda^2_{i'}}{\omega_{i'} - E_{qm}}\right] = \\
&= \frac{N_{qm}(E_{qm} - \varepsilon_m)\Lambda_i}{(E_{qm} - \omega_i)(\omega_i - \varepsilon_m)}.
\end{aligned}
$$

(*) This is because the spurious state has zero phase space to correlate.

This quantity is zero for the spurious roots (*) (*i.e.* $E_{qm} = \varepsilon_m$) and agrees with the exact result for the $\Omega - 1$ remaining physical roots.

Utilizing the relations

$$\frac{1}{V} = \sum_m \frac{1}{\varepsilon_m - \omega_i} \tag{7.30}$$

and

$$\frac{1}{V} = \sum_{m \neq m'} \frac{1}{\varepsilon_{m'} - E_{qm}}, \tag{7.31}$$

we obtain

$$\sum_{m \neq m'} \frac{1}{(\varepsilon_{m'} - E_{qm})(\varepsilon_{m'} - \omega_i)} = \frac{1}{(E_{qm} - \omega_i)(\varepsilon_m - \omega_i)}. \tag{7.32}$$

Utilizing this relation we can derive the one-particle transfer sum rule. Note that (7.30) is the dispersion relation for the free phonon field. The second relation is, however, ahen to the field theory results. Nevertheless, one can show that the solutions E_{qm} of (7.31) and of the nuclear-field-theory dispersion relation (7.15) are identical, except for the root $E_{qm} = \varepsilon_m$. One can, therefore, utilize (7.31) as a mathematical relation without further justifications in the present context. One obtains

$$\sum_{qm} |\langle qm|a^\dagger_{m,1}|n_i = 1\rangle|^2 = \sum_{qm} \Lambda^2_{qm} \Lambda^2_i \sum_{m \neq m'} \frac{1}{(\varepsilon_{m'} - E_{qm})(\varepsilon_{m'} - \omega_i)} \cdot \sum_{m'' \neq m} \frac{1}{(\varepsilon_{m''} - E_{qm})(\varepsilon_{m''} - \omega_i)}, \tag{7.33}$$

where

$$\Lambda_{qm} = -N_{qm}(E_{qm} - \varepsilon_m) = \left[\sum_{m \neq m'} \frac{1}{(\varepsilon_{m'} - E_{qm})^2}\right]^{-\frac{1}{2}}. \tag{7.34}$$

Thus

$$\sum_{qm} |\langle qm|a^\dagger_{m,1}|n_i = 1\rangle|^2 = \Lambda^2_i \sum_{m' \neq m} \frac{1}{(\varepsilon_{m'} - \omega_i)^2} = 1 - \frac{\Lambda^2_i}{(\varepsilon_m - \omega_i)^2}, \tag{7.35}$$

where use has been made of the orthogonality relation

$$\sum_{qm} \frac{\Lambda^2_{qm}}{(\varepsilon_{m'} - E_{qm})(\varepsilon_{m''} - E_{qm})} = \delta(m', m'') \qquad (m', m'' \neq m). \tag{7.36}$$

(*) In fact

$$\lim_{\delta \to 0} [(E_{qm} - \varepsilon_m) N_{qm}]_{E_{qm} = \varepsilon_m + \delta} = \lim_{\delta \to 0} \left\{ \sqrt{2}\, \delta^{\frac{1}{2}} \Big/ \left[\sum_i \frac{\Lambda_i}{\omega_i - \varepsilon_m}\right]^{\frac{1}{2}} \right\} = 0.$$

The result (7.35) coincides with the exact result. Physically it means that the single-particle orbital $(m, 1)$ is blocked by the amount $\Lambda_i^2/(\varepsilon_m - \omega_i)^2$, which is the probability that the phonon $(n_i = 1)$ is in the particle-hole configuration $(m, 1; m, -1)$, *i.e.* with its particle in the orbital $(m, 1)$.

8. – Applications.

In what follows we discuss some aspects of the low-lying spectrum of the nucleus ^{209}Bi in terms of fermions, surface $(\beta^\dagger(0\lambda))$ and pairing $(\beta^\dagger(2\lambda))$ modes. The application to states containing two or more pairing and surface phonons will be discussed by BORTIGNON [57].

The unperturbed states of the closed-shell-plus-one-particle system can be written in terms of the free fields as

$$|n2\lambda, j; IM\rangle = [\beta_n^\dagger(2\lambda) a_j]_{IM}|0\rangle \tag{8.1}$$

and

$$|n0\lambda, j; IM\rangle = [\beta_n^\dagger(0\lambda) a_j^\dagger]_{IM}|0\rangle . \tag{8.2}$$

This constitutes the basis set of states $\{\alpha_i\}$. All other states give rise to the complementary Hilbert space $\{a_i\}$.

The elementary modes of excitation interact through the particle-vibration and four-point vertices displayed in fig. 23 giving rise to the matrix elements

$$M_1(nj, n'j') \equiv \langle[\beta_n^\dagger(0\lambda) a_{j'}^\dagger]_{IM}|h_{\text{eff}}(E)|[\beta_n^\dagger(0\lambda) a_j^\dagger]_{IM}\rangle , \tag{8.3a}$$

$$M_2(nj, n'j') \equiv \langle[\beta_{n'}^\dagger(2\lambda) a_{j'}]_{IM}|h_{\text{eff}}(E)|[\beta_n^\dagger(2\lambda) a_j]_{IM}\rangle \tag{8.3b}$$

and

$$M_3(nj, n'j') \equiv \langle[\beta_{n'}^\dagger(2\lambda) a_{j'}]_{IM}|h_{\text{eff}}(E)|[\beta_n^\dagger(0\lambda) a_j^\dagger]_{IM}\rangle . \tag{8.3c}$$

They are to be calculated by utilizing the graphical techniques of perturbation theory and the rules discussed in sect. **6**.

There are two parameters on which to expand upon in carrying out a perturbative calculation. The first one is the strength of the interaction vertices measured in terms of the average distance between single-particle levels. The second is $1/\Omega$, where $\Omega = \sum_j (j + \frac{1}{2})$ is the effective degeneracy of the valence shells. These two parameters are in general connected through involved expressions. In the schematic model discussed in sect. **6**, however, their relation is explicit and can be expressed as

$$\varepsilon = \mathcal{O}(1) , \quad \Lambda = \mathcal{O}\left(\frac{1}{\sqrt{\Omega}}\right) \quad \text{and} \quad V = \mathcal{O}\left(\frac{1}{\Omega}\right). \tag{8.4}$$

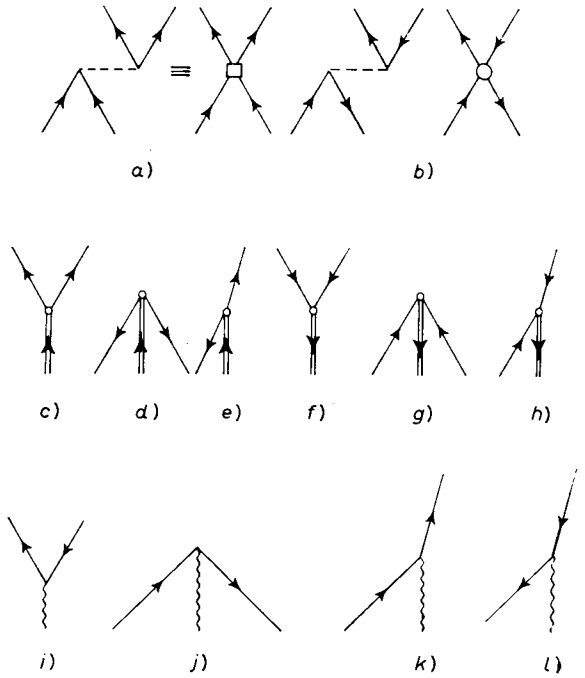

Fig. 23. – Interactions coupling the fermion fields with the pairing and surface vibrations. The different fermion and boson free fields are particle, hole, pairing vibration ($\alpha = 2$), pairing vibration ($\alpha = -2$), surface vibration ($\alpha = 0$). The two possible four-point vertices are given in *a*) and *b*). They correspond to the pairing and particle-hole model bare interactions. In graphs *c*)-*h*) all possible couplings between the fermion fields (arrowed lines) and the pairing vibrational fields (double lines arrowed) are displayed. Graphs *i*)-*l*) are all the coupling vertices between the surface vibrations (wavy line) and the fermion fields. Note that there is no direct coupling between the two boson fields, as the field theory we are dealing with is linear in the different field co-ordinates.

Another feature which determines the family of diagrams to select to a given order of perturbation is the number of internal lines which can be freely summed up. Each of these summations introduces a multiplicative factor Ω.

Because most of the present knowledge on the applicability of the field-theoretical techniques rests upon schematic models, we utilize $1/\Omega$ as the expansion parameter, and assume the relations (8.4) to be valid for more general situations.

The nucleus ^{209}Bi has been investigated by means of high-resolution inelastic scattering [58] and Coulomb excitation [59]. Through these experiments a septuplet of states around 2.6 MeV of excitation was identified, with spins ranging from $\frac{3}{2}^+$ to $\frac{15}{2}^+$.

In zeroth order these states can be interpreted in terms of a proton moving in the $h_{\frac{9}{2}}$ orbital coupled to the lowest octupole vibration of ^{208}Pb. The $\frac{3}{2}^+$ of this multiplet displays also a large parentage based on the proton pair addition and proton hole moving in the $d_{\frac{3}{2}}$ orbital, as revealed by the (t, α) reaction on ^{210}Po [60].

The above results indicate that the (two-particle, one-hole) type of states in ^{209}Bi are amenable to a simple description in term of the basis states

$$|2\lambda, j_1^{-1}; IM\rangle \equiv |j^{-1} \otimes \lambda(^{210}\mathrm{Po}); IM\rangle \qquad (\lambda^\pi = 0^+, 2^+, 4^+) \tag{8.5}$$

and

$$|0\lambda, j_2; IM\rangle \equiv |j_2 \otimes \lambda^\pi(^{208}\mathrm{Pb}); IM\rangle \qquad (\lambda^\pi = 3^-)\,. \tag{8.6}$$

Only the lowest states of each spin and parity λ^π are included in the basis states, while all the RPA solutions are included in the intermediate states. The quadrupole surface vibration modes were allowed only as intermediate states. The single hole and particle states j_1^{-1} and j_2, respectively, correspond to experimentally known levels around the $Z = 82$ shell closure.

In what follows we discuss the different properties of the states generated by the basis spanned by the eigenvectors $|2\lambda, j_1^{-1}; IM\rangle$ and $|0\lambda, j_2; IM\rangle$. We have divided the discussion in two parts.

In the first part the two $\frac{3}{2}^+$ states built out of the $|d_{\frac{3}{2}}^{-1} \otimes \mathrm{gs}(^{210}\mathrm{Po})\rangle$ and $|h_{\frac{9}{2}} \otimes 3^-(^{208}\mathrm{Pb})\rangle$ configurations are studied in this space. This two-state system provides a rich laboratory to study the interplay of surface and pairing modes.

In the second part the properties of the entire multiplet and of those states strongly excited in either the (t, α) or (d, d′) reactions are studied, in the complete configuration space.

a) The $\frac{3}{2}^+$ states.

The two states

$$|1\rangle \equiv |d_{\frac{3}{2}}^{-1} \otimes \mathrm{gs}(^{210}\mathrm{Po}); \tfrac{3}{2}^+\rangle \qquad (2.733\ \mathrm{MeV}) \tag{8.7}$$

and

$$|2\rangle \equiv |h_{\frac{9}{2}} \otimes 3^-(^{208}\mathrm{Pb}); \tfrac{3}{2}\rangle \qquad (2.615\ \mathrm{MeV}) \tag{8.8}$$

are 118 keV apart. They mix strongly through the couplings depicted by the graphs *a*) and *b*) of fig. 24.

Because of the energy dependence of h_{eff} there is a different matrix element for each final state. The diagonalization of the matrices was carried out self-consistently, *i.e.* the energy denominators of the different graphs are to be calculated by utilizing the exact energies (for more details, cf. ref. [61]).

The corresponding graphical contributions to the spectroscopic factor and inelastic cross-sections are also collected in fig. 24. To be noted

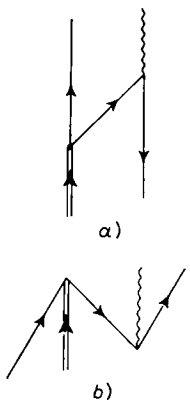

a)

b)

M (keV)	
I	II
319	503
-93	-103
226	400

c)

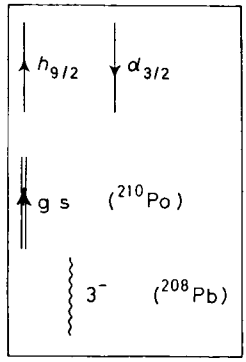

d)

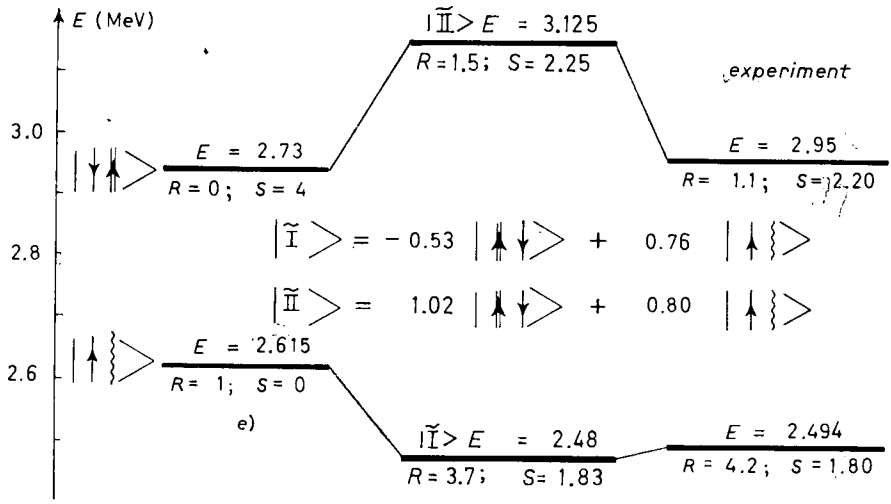

e)

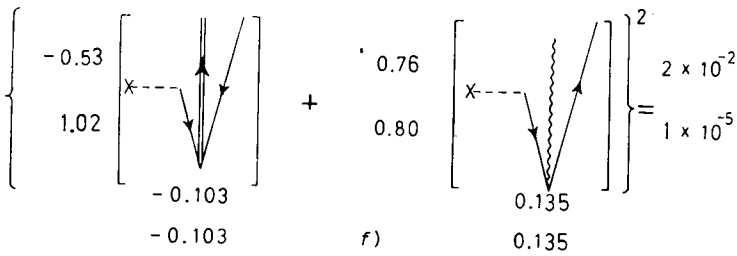
-0.53
1.02
-0.103
-0.103
+
0.76
0.80
0.135
0.135
2
2 x 10^-2
1 x 10^-5
f)

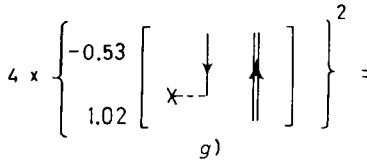
4 x
-0.53
1.02
g)
1.12
4.16

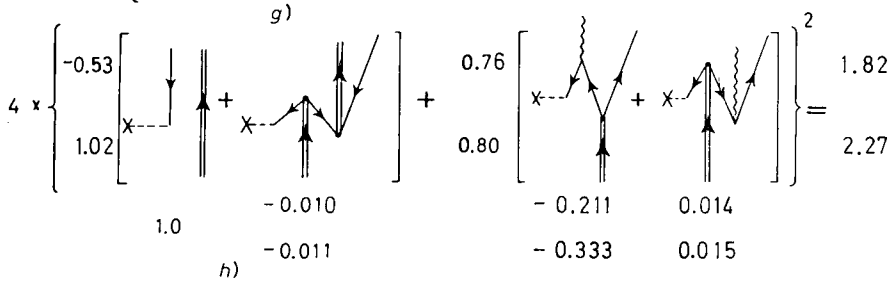
4 x
-0.53
1.02
1.0
-0.010
-0.011
h)
+
0.76
0.80
- 0.211
- 0.333
0.014
0.015
2
1.82
2.27

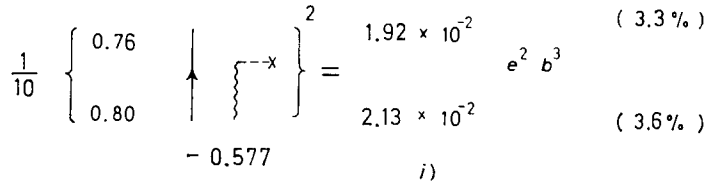
1/10
0.76
0.80
- 0.577
1.92 x 10^-2
2.13 x 10^-2
e^2 b^3
(3.3 %)
(3.6 %)
i)

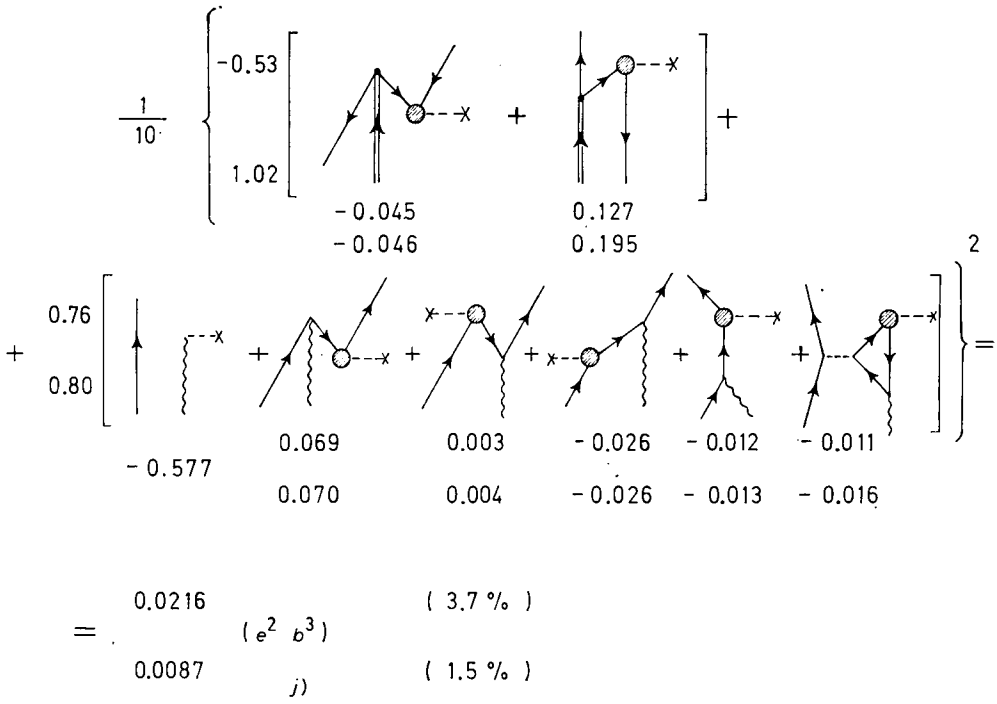

Fig. 24. – In *a*), *b*) and *c*) we give the two contributions to the matrix element $M(E) = \langle d_{3/2}^{-1} \otimes \mathrm{gs}(^{210}\mathrm{Po}) | h_{\mathrm{eff}}(E) | h_{9/2} \otimes 3^-(^{208}\mathrm{Pb}); 3/2 \rangle$ in lowest order in $1/\Omega$. The resulting wave functions $|\tilde{\mathrm{I}}\rangle$ and $|\tilde{\mathrm{II}}\rangle$ are displayed in *e*) normalized according to (7.19). In *e*) we also give the unperturbed, theoretical energies of the levels. The (t, α) spectroscopic factor corresponding to the reaction $^{210}\mathrm{Pi}(\mathrm{t}, \alpha)^{209}\mathrm{Bi}$ is denoted by S, while

$$R = \frac{\mathrm{d}\sigma(h_{9/2} \to J)}{\mathrm{d}\sigma(\mathrm{gs}(^{208}\mathrm{Pb}) \to 3^-(^{208}\mathrm{Pb}))}$$

is the ratio of inelastic cross-sections. In *d*) we display the free fields. The zeroth and order $1/\Omega$ contributions to the electromagnetic excitations are collected in *i*) and *j*). The value $0.58\, e^2 b^3$ is the $B(E3; 0 \to 3)$ value associated with the 2.615 MeV state in ^{208}Pb. In *g*) and *h*) we give the zeroth and order $1/\Omega$ contributions to the spectroscopic factor associated with the $^{210}\mathrm{Po}(\mathrm{t}, \alpha)^{209}\mathrm{Bi}$ reaction. Finally in *f*) we display the lowest contribution to the spectroscopic factor associated with the $^{208}\mathrm{Pb}(^3\mathrm{He}, \mathrm{d})$ reaction, which gives a measure of the ground-state correlations of ^{208}Pb associated with the existence of an octupole and a pairing vibration.

TABLE VII. – *States strongly excited in one or more of the reactions* ^{208}Pb(^{3}He, d)^{209}Bi, ^{210}Po(t, α)^{209}Bi *and* ^{209}Bi(d, d')^{209}Bi (J^{π}). In the first column the spin and parity of the states are given. In the second and third columns we give the experimental and theoretical energy difference $\delta E_j = (E_j - 2615)$ keV of the members of the septuplet measured with respect to the energy of the 3^- state in ^{208}Pb. For the second state $3/2^+$ (2.95 MeV) we give instead the absolute excitation energy. In columns 4 and 5 we collect the experimental and theoretical inelastic excitation cross-section normalized to the 3^- (^{208}Pb) cross-section according to

$$\frac{d\sigma(h_{9/2}(^{209}\mathrm{Bi}) \to J^{\pi}(^{209}\mathrm{Bi}))}{d\sigma(\mathrm{gs}(^{208}\mathrm{Pb}) \to 3^-(^{208}\mathrm{Pb}))} .$$

In columns 6 and 7 the experimental and theoretical values of the (t, α) spectroscopic factor are displayed. In the two final columns we give the spectroscopic factors associated with the (^{3}He, d) reaction.

J	δE_j (keV)		$\frac{d\sigma(h_{9/2}(^{209}\mathrm{Bi}) \to J^{\pi}(^{209}\mathrm{Bi}))}{d\sigma(\mathrm{gs}(^{208}\mathrm{Pb}) \to 3^-(^{208}\mathrm{Pb}))}$ (%)		S(t, α)		S(^{3}He, d)	
	experimental [58]	theoretical	experimental [58]	theoretical	experimental [60]	theoretical	experimental [63]	theoretical
$3/2^+$	−121	−136	4.2 ± 0.3	3.7	1.8 ± 0.3	1.81	< 0.01	0.02
$5/2^+$	3	− 46	9.1 ± 0.5	8.6				—
$7/2^+$	− 30	30	12.3 ± 0.5	11				—
$9/2^+$	− 49	− 90	13.8 ± 0.6	15.8		—		—
$11/2^+$	− 15	− 20	37.4 ± (0.7) (a)	18.5 39.2		—	0.06	0.03
$13/2^+$		− 80		20.7		—		0.01
$15/2^+$	129	190	23.7 ± 0.7	20	< 0.2		< 0.02	0.01
$3/2^+$	2.95 MeV	3.075 MeV	1.1 ± 0.2 (a)	1.3	2.2 ± 0.3	1.96	< 0.01	

(a) Error estimated (not given in original paper).

is the very different ratio of the (d, d′) and (t, α) cross-sections. While $R_1 = B(E3; (\frac{3}{2})_1)/B(E3; (\frac{3}{2})_2)$ is approximately equal to 4, the ratio $R_2 = \sigma((t, \alpha); (\frac{3}{2})_2)/\sigma((t, \alpha); (\frac{3}{2})_1)$ is close to one. Because the component $|2\rangle$ carries the inelastic-scattering strength, while the (t, α) reaction proceeds mainly through the component of type $|1\rangle$, the difference between R_1 and R_2 can be traced back to the over-completeness of the basis which give rise to rather different normalizations of the two physical states (cf. sect. **7**).

b) *The multiplet.*

By utilizing all the states of the basis, and the same techniques discussed above, the states that are strongly excited in at least one of three reactions (d, d′), (t, α) and (^{3}He, d) were calculated. The resulting spectroscopic amplitudes and relative cross-sections are collected in table VII.

The picture of the nuclear states achieved in terms of the elementary modes of excitation displays in a transparent manner the correlation aspects of the nuclear dynamics.

Résumé.

We have shown that the nuclear-field description of the nuclear structure is mathematically correct (cf. sect. **6** and **7**) and that it smoothly joins the ranks of quantum electrodynamics and many-body field theories. We have also shown that its predictions are borne out by the experiment.

One thus achieves a simple picture of the nuclear structure. Each wave function, which is an exact solution of the many-body problem, contains only few components. Each of these components carry a label which reads: « Only to be excited through inelastic scattering » or « Only to be excited in one-particle pickup reactions », *i.e.* each component corresponds to an observable, associated with a concrete experiment one knows how to carry out with the help of accelerators, detectors and targets.

* * *

We want to acknowledge the help of P. F. BORTIGNON, C. H. DASSO, R. LIOTTA and B. S. NILSSON in the preparation of particular subjects contained in the present lectures. Discussions with O. DRAGUN, G. G. DUSSEL, E. MAQUEDA, R. PERAZZO, S. REICH and H. SOFIA are appreciated.

REFERENCES

[1] B. BAYMAN: lectures on *Seniority, quasi-particles, and collective vibrations*, Princeton, N. J., 1960, unpublished.

[2] L. N. COOPER: *Phys. Rev.*, **104**, 1189 (1956).

[3] G. RACAH: *Phys. Rev.*, **63**, 367 (1943).
[4] B. R. MOTTELSON: *Cours de l'Ecole d'Eté de Physique Théorique de Les Houches* (1958).
[5] D. R. BÉS, R. A. BROGLIA, R. J. PERAZZO and K. KUMAR: *Nucl. Phys.*, **143** A, 1 (1970).
[6] A. BOHR and B. R. MOTTELSON: *Nuclear Structure*, Vol. **2** (New York, N. Y., 1975).
[7] J. BARDEEN, L. N. COOPER and J. R. SCHRIEFFER: *Phys. Rev.*, **106**, 162 (1957).
[8] N. N. BOGOLIUBOV: *Nuovo Cimento*, **7**, 794 (1958).
[9] J. G. VALATIN: *Nuovo Cimento*, **7**, 843 (1958).
[10] A. LANE: *Nuclear Theory* (New York, N. Y., 1964).
[11] D. R. BÉS and R. SORENSEN: *Advances in Nuclear Physics*, edited by M. BARANGER and E. VOGT, Vol. **2** (New York, N. Y., 1969), p. 129.
[12] B. BAYMAN: *Nucl. Phys.*, **15**, 33 (1960).
[13] A. H. WAPSTRA and N. B. GOVE: *Nuclear Data Tables*, **9**, 265 (1971).
[14] J. H. BJERREGAARD, O. HANSEN, O. NATHAN, L. VISTISEN, R. CHAPMAN and S. HINDS: *Nucl. Phys.*, **110** A, 1 (1968).
[15] J. H. BJERREGAARD, O. HANSEN, O. NATHAN, R. CHAPMAN and S. HINDS: *Nucl. Phys.*, **131** A, 481 (1969); E. R. FLYNN, J. G. BEERY and A. G. BLAIR: *Nucl. Phys.*, **154** A, 225 (1970).
[16] D. G. FLEMING, M. BLANN, H. W. FULBRIGHT and J. A. ROBBINS: *Nucl. Phys.*, **157** A, 1 (1970).
[17] D. R. BÉS and R. A. BROGLIA: *Nucl. Phys.*, **80**, 289 (1966).
[18] A. BOHR: *Comptes Rendus du Congrès International de Physique Nucléaire, Paris, 1964*, Vol. **1** (Paris, 1964), p. 487.
[19] J. HÖGAASEN-FELDMAN: *Nucl. Phys.*, **28**, 258 (1961).
[20] R. A. BROGLIA, C. RIEDEL and B. SØRENSEN: *Nucl. Phys.*, **107**, 1 (1968).
[21] R. A. BROGLIA and B. SØRENSEN: *Nucl. Phys.*, **110** A, 241 (1968).
[22] R. A. BROGLIA: *Ann. of Phys.*, **80**, 60 (1972).
[23] R. A. BROGLIA: in *Proceedings of the Eleventh Summer Meeting of Nuclear Physicists*, edited by L. SIPS, Vol. **1** (Herceg Novi, 1966), p. 201.
[24] R. A. BROGLIA, A. MOLINARI and T. REGGE: *On the hydrodynamics of Fermi superfluids* (to be published).
[25] A. BOHR: this volume, p. 3.
[26] R. A. BROGLIA, O. HANSEN and C. RIEDEL: *Advances in Nuclear Physics*, edited by M. BARANGER and E. VOGT, Vol. **6** (New York, N. Y., 1973).
[27] E. R. FLYNN: private communication.
[28] W. A. LANDFORD and J. MCGORY: *Phys. Lett.*, **54** B, 238 (1973); W. A. LANDFORD: private communication.
[29] R. A. BROGLIA and C. RIEDEL: *Nucl. Phys.*, **92** A, 145 (1967).
[30] R. A. BROGLIA, C. RIEDEL, B. SØRENSEN and T. UDAGAWA: *Nucl. Phys.*, **115** A, 273 (1968).
[31] R. A. BROGLIA: *Symposium on Two-Nucleon Transfer and Pairing Excitations*, Argonne National Laboratory, March 20-21, 1972, Report PHY-1972 H, p. 113.
[32] A. J. LEGGETT: *Rev. Mod. Phys.*, **47**, 331 (1975).
[33] J. W. WEATLY: *Rev. Mod. Phys.*, **47**, 415 (1975).
[34] J. H. BJERREGAARD, O. HANSEN, O. NATHAN and S. HINDS: *Nucl. Phys.*, **89**, 145 (1966).
[35] G. IGO, P. D. BARNES and E. R. FLYNN: *Ann. of Phys.*, **66**, 60 (1971).
[36] D. R. BÉS and R. A. BROGLIA: *Phys. Rev. C*, **3**, 2349 (1971).
[37] R. A. BROGLIA, D. R. BÉS and B. NILSSON: *Phys. Lett.*, **50** B, 213 (1974).
[38] I. RAGNARSSON and R. A. BROGLIA: *Nucl. Phys.*, **263** A, 315 (1976).
[39] I. HAMAMOTO: this volume, p. 234 and 252.

[40] R. A. BROGLIA, R. J. LIOTTA and B. NILSSON: to be published.
[41] J. V. MAHER, J. R. ERSKINE, A. M. FRIEDMAN, J. P. SCHIFFER and R. H. SIEMSSEN: *Phys. Rev. Lett.*, **25**, 302 (1970).
[42] R. A. BROGLIA and P. F. BORTIGNON: *Phys. Lett.* **65** B, 221 (1976).
[43] R. M. DE VRIES: *Phys. Rev. Lett.*, **35**, 835 (1975).
[44] R. M. DE VRIES, D. SHAPIRA, M. R. CLONER, H. E. GOVE, G. SØRENSEN and G. GARRETT: *Phys. Lett.*, **67** B, 19 (1977).
[45] N. STEIN, C. WOODS and J. SAUNIER: contribution to the *European Conference on Nuclear Physics with Heavy Ions, Caen, 1976.*
[46] R. R. BETTS: *Proceedings of the Second International Conference on Clustering Phenomena in Nuclear Physics* (College Park, Md., 1974).
[47] D. R. BÉS, R. A. BROGLIA, O. HANSEN and O. NATHAN: *Phys. Rep.* (to be published).
[48] J. P. PARIKH: *Nucl. Phys.*, **63**, 214 (1965).
[49] G. G. DUSSEL, E. E. MAQUEDA and R. P. J. PERAZZO: *Nucl. Phys.*, **153** A, 469 (1970).
[50] A. BOHR: in *Nuclear Structure* (Vienna, 1968), p. 179.
[51] B. R. BAYMAN, D. R. BÉS and R. A. BROGLIA: *Phys. Rev. Lett.*, **23**, 299 (1969).
[52] D. R. BÉS: *Rev. Brasil. Fis.*, **2**, 255 (1972).
[53] L. LANDAU: *Journ. Phys. USSR*, **5**, 71 (1941).
[54] D. R. BÉS, G. G. DUSSEL, R. A. BROGLIA, R. LIOTTA and B. R. MOTTELSON: *Phys. Lett.*, **52** B, 253 (1974).
[55] R. A. BROGLIA, B. R. MOTTELSON, D. R. BÉS, R. LIOTTA and H. SOFIA: *Phys. Lett.*, **64** B, 29 (1976).
[56] D. R. BÉS, R. A. BROGLIA, G. G. DUSSEL, R. J. LIOTTA and H. M. SOFIA: *Nucl. Phys.*, **260** A, 1, 27 (1976); D. R. BÉS, R. A. BROGLIA, G. G. DUSSEL, R. J. LIOTTA and R. P. J. PERAZZO: *Nucl. Phys.*, **260** A, 77 (1976).
[57] P. F. BORTIGNON: this volume, p. 519.
[58] J. UNGRIN, R. M. DIAMOND, P. O. TJØM and B. ELBEK: *Mat. Fys. Medd. Dan. Vid. Selsk.*, **38**, No. 8 (1971).
[59] R. A. BROGLIA, J. S. LILLEY, R. PERAZZO and W. R. PHILLIPS: *Phys. Rev. C*, **1**, 1508 (1970).
[60] P. BARNES, E. ROMBERG, C. ELLEGAARD, R. CASTEN, O. HANSEN, J. MULLIGAN, R. A. BROGLIA and R. LIOTTA: *Nucl. Phys.*, **195** A, 1146 (1972).
[61] P. F. BORTIGNON, R. A. BROGLIA, D. R. BÉS and R. LIOTTA: *Phys. Rep.*, **30** C, 305 (1977).
[62] B. R. MOTTELSON: private communication; I. HAMAMOTO: this volume, p. 234 and 252.
[63] B. WILDENTHAL, B. PREEDON, E. NEWMAN and M. CATES: *Phys. Rev. Lett.*, **19**, 960 (1967); C. ELLEGAARD and P. VEDELSBY: *Phys. Lett.*, **26** B, 155 (1968).

Reprinted From
Elementary Modes of Excitation in Nuclei
© 1977, LXIX Corso
Soc. Italiana di Fisica - Bologna - Italy